

**Monitoring Reduced Emissions from Deforestation and
Forest Degradation (REDD+): Capabilities of High-
Resolution Active Remote Sensing**

Dissertation

Zur Erlangung der Würde des
Doktors der Naturwissenschaften

des Fachbereiches Biologie, der Fakultät für Mathematik, Informatik und
Naturwissenschaften
der Universität Hamburg

vorgelegt von
Thomas Baldauf
aus Stuttgart

Hamburg 2013

Genehmigt vom Fachbereich Biologie
der Fakultät für Mathematik, Informatik und Naturwissenschaften
an der Universität Hamburg
auf Antrag von Professor Dr. M. KÖHL
Weiterer Gutachter der Dissertation:
Professor Dr. S. KUNTZ
Tag der Disputation: 22. April 2013

Hamburg, den 08. April 2013

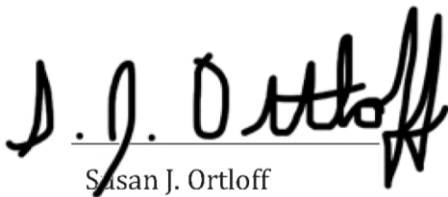


Professor Dr. C. Lohr
Vorsitzender des
Fach-Promotionsausschusses Biologie

I certify that the English of the dissertation „Monitoring Reduced Emissions from Deforestation and Forest Degradation (REDD+): Capabilities of High- Resolution Active Remote Sensing“ written by Thomas Baldauf from the Thünen Institute for World Forestry was reviewed and is correct.

The dissertation was reviewed by Susan J. Ortloff (US citizen)

- currently working as a freelance translator and editor
- sample of previously translated or edited works:
 - Prof. Dr. F.H. Schweingruber, Trees and Wood in Dendrochronology, Springer Verlag
 - Prof. Dr. F.H. Schweingruber, Tree Rings and the Environment, Springer Verlag, WSL
 - Dr. G. Kenk, New Perspectives of Oak Silviculture in Germany, FVA
 - Dr. E.E. Hildebrand, The Heterogeneous Distribution of Mobil Ions in the Rhizosphere of Acid Forest Soils, Entry in the Journal of Environmental Science and Health, FVA
 - Dr. G. Kattenborn, Atmospheric Correction of Landsat/TM Data over Mountainous Terrain, Entry in the Proceedings of the XVII ISPRS Congress



Susan J. Ortloff

January 28, 2013

Acknowledgements

This doctoral thesis completes several years of research at the Thünen Institute for World Forestry and at the University of Hamburg's cluster of excellence, CliSAP. My grateful thanks extend to everyone in the group for providing their encouragement, sharing their experience and lending their support.

Foremost, I would like to thank my primary supervisor, Prof. Dr. Michael Köhl. His expertise and constructive guidance were of great importance to this thesis and my entire work. Over the past years, he provided me with the opportunity to work in a number of rewarding research projects and to cooperate with national and international research partners. Just as much, I would like to thank my co-supervisor, Prof. Dr. Steffen Kuntz. The cooperation with Infoterra/Astrium GmbH has been an important stimulus for my study. I greatly value working with Steffen and all the Infoterra staff.

A supporting and motivating environment is essential for conducting research and producing results. Thus, I am also very grateful for my fellow colleagues at the Institute for World Forestry. Their support and frankness formed a creative atmosphere which proved invaluable during many phases of my doctoral thesis. Special thanks go to Dr. Daniel Plugge, Dr. Thomas Schneider and Dr. Wolf-Ulrich Kriebitzsch for their inspiring discussions and valuable inputs during my work. Dr. Raul Köhler was of great help in the Python world, and Konstantin Olschofsky did so in the RADAR world. Likewise, I would like to specially thank Manuel Haas, Florian Herzog and Dr. Reinhold Glauner, who generously supported me during the field work of my thesis. The staff of the scientific information center of the Thünen Institute always provided a helping hand. The work for this study was generously supported by financial contributions of the Thünen Institute, CliSAP and the German Ministry of Food, Agriculture and Consumer Protection (BMELV).

Special thanks go to Susan J. Ortloff for the final English review.

Finally, I would like to express my deepest gratitude to my wife Silke. I am fully aware that the time I spent devoted to my thesis was surely not the most amusing period of your life, but your steady encouragement and generous emotional support extended far beyond the basic prerequisite for accomplishing the thesis. Thank you.

Table of contents

Acknowledgements	I
Table of contents	II
List of Acronyms	V
List of Equations	VIII
List of Figures.....	IX
List of Tables.....	XIV
1 Abstract	1
2 Introduction.....	2
2.1 Role of forests in climate change	2
2.2 REDD+.....	4
2.3 The scope of the present study.....	10
3 Background.....	12
3.1 The phenomenon “forest degradation”	13
3.2 Estimation of forest biomass.....	20
3.3 Monitoring of forest degradation	21
3.3.1 Direct and in-direct methods	23
3.3.2 Remote sensing as an additional data source for monitoring forest degradation	24
3.3.3 Error and uncertainty considerations.....	27
3.4 Methodological developments	35
3.4.1 Change detection	35
3.4.2 Context and object based image analysis	37
3.4.3 Remote sensing sensor concepts	44
3.5 Error analysis strategies for change detection.....	50
4 Data and methods	54
4.1 Caracará forest project.....	54
4.2 Data from in-situ assessment.....	57

4.3	Data from remote sensing.....	59
4.4	Methods to detect forest degradation using RADAR.....	63
4.4.1	Pre-processing stages.....	63
4.4.2	Bi-temporal segmentation.....	65
4.4.3	Image understanding and object-level change detection.....	66
4.5	Methods to analyze the accuracy of the object-level change detection.....	74
4.6	Methods to identify influences of stand characteristics on the reliability of the detection of forest degradation.....	75
4.6.1	Tree biomass.....	75
4.6.2	Tree crown area.....	76
4.6.3	Social position and dominance.....	78
4.7	Methods to quantify influences of stand characteristics on the reliability of the detection of forest degradation.....	81
5	Results.....	83
5.1	Results of the developed methods to detect forest degradation using RADAR.....	83
5.1.1	Pre-processing stages.....	83
5.1.2	Bi-temporal segmentation.....	84
5.1.3	Image understanding and object-level change detection.....	86
5.2	Results of the accuracy analysis of the object-level change detection.....	93
5.3	Results of the identification of influences of stand characteristics on the reliability of the detection of forest degradation.....	95
5.3.1	Tree biomass.....	95
5.3.2	Tree Crown Area.....	96
5.3.3	Social position and dominance.....	96
5.4	Results of the quantification of the influences of stand characteristics on the reliability of the detection of forest degradation.....	98
5.4.1	Tree biomass.....	99
5.4.2	Tree crown area.....	100
5.4.3	Social position and dominance.....	101

6	Discussion	104
6.1	In-situ assessment	104
6.2	Detection of patterns of forest degradation using RADAR	106
6.2.1	Data pre-processing	106
6.2.2	Segmentation	106
6.2.3	Classification.....	107
6.3	Results and accuracies of the object-level change detection	109
6.4	Identification and quantification of the influences of stand characteristics on the reliability of the detection of forest degradation.....	110
6.4.1	Tree biomass	111
6.4.2	Tree crown area.....	112
6.4.3	Social position and dominance.....	113
6.5	Reporting on forest degradation within the scope of REDD+	115
7	Conclusions.....	119
8	References.....	122
9	Annex	147
9.1	Processes of the four objectives to verify the hypothesis	148
9.2	Metadata for „TerraSAR-X 2008“	149
9.3	Metadata for „TerraSAR-X 2009“	149
9.4	Script for social position and dominance	149
9.5	Class hierarchy, class descriptions and membership functions of the applied object-level change detection.....	150
9.6	Stepwise description of settings for the classification rule set	151
9.7	Results for all extracted trees for the estimation of aboveground biomass, the crown area, and the social position and dominance.....	152

List of Acronyms

ABG	Above ground biomass
AD	Activity data
AFOLU	Agriculture, Forestry and Other Land Uses
AWG-LCA	Ad-Hoc Working Group on Long-term Cooperative Action under the Convention
BEF	Biomass expansion factors
Bit	Binary digit
BMELV	Bundesministerium für Ernährung, Landwirtschaft und Verbraucherschutz;
CliSAP	Integrated Climate System Analysis and Prediction
cm	Centimeter
CO ₂	Carbon dioxide
COBIA	Context and object based image analysis
COP	Conference of the Parties
dbh	Diameter at breast height (at 1.30m)
DEM	Digital elevation model
EF	Emission factors
FAO	Food and Agriculture Organization of the United Nations
FMU	Forest Management Units
FRA	Global Forest Resource Assessment
GB	Giga byte; 10 ⁹ byte
GCP	Ground-control point
GHG	Greenhouse gas
GIS	Geographic information systems
GLAS	Geoscience Laser Altimeter System
GLC2000	Global Land Cover 2000; Result of the Global Land Cover Project of European Commission
GPG	Good Practice Guidance
GPS	Global positioning system

ha	Hectare
ICESat	Ice, Cloud, and land Elevation
IPCC	Intergovernmental Panel on Climate Change
IUFRO	International Union of Forest Research Organisations
LC	Land-cover
LiDAR	Light Detection And Ranging
LULUCF	Land Use, Land-Use Change and Forestry
m	Meter
mA	Minimum area
MAD	Multivariate Alteration Detection
mCC	Minimum crown cover
MMU	Minimum mapping unit
MODIS	Moderate Resolution Imaging Spectroradiometer
MRV	Measuring, reporting and verification
mTH	Minimum tree height
NDVI	Normalized Difference Vegetation Index
NFMS	National forest monitoring system
OLCD	Object-level change detection
PDOP	Positional dilution of precision
RADAR	Radio Detection and Ranging
RAM	Random-Access Memory
REDD	Reduction of Emissions from Deforestation and forest Degradation
RGB	Additive color model based on the colors Red, Green and Blue
SAD	South American Datum
SAR	Synthetic Aperture RADAR
SBSTA	Subsidiary Body for Scientific and Technological Advice
SFM	Sustainable forest management

TB	Terra byte; 10^{12} byte
TI	Thünen Institute; Federal Research Institute for Rural Areas, Forestry and Fisheries
UN	United Nations
UNFCCC	United Nations Framework Convention on Climate Change
UTM	Universal Transverse Mercator
WCC	World Climate Conference

List of Equations

Eq. (1)	52
Eq. (2)	52
Eq. (3)	52
Eq. (4)	68
Eq. (5)	68
Eq. (6)	69
Eq. (7)	69
Eq. (8)	75
Eq. (9)	77

List of Figures

- Figure 1: Map of land cover classification from the MODIS instrument aboard the satellite Terra. Forests (green) cover 30% of the Earth's land; from Simmon (2011). 2
- Figure 2: This figure shows an illustration of the differentiation of deforestation and forest degradation. In the left column IPCC definitions (forest, open forest and no forest) are used as land-cover ("LC") classes, in the right column "Status" is classified in "undisturbed", "disturbed" and "removed". The graph on the right shows various single processes of deforestation, i.e. changes from forest to no forest, and of degradation, i.e. forest to forest/open forest over time; from Baldauf et al. (2009). 16
- Figure 3: The different land-use types and forest conditions in a schematized tropical landscape (cf. ITTO (2002)). The forest conditions in the third row can also be seen as stages in the deforestation and forest degradation process, i.e. Primary forest to Secondary forest to Degraded forest land to Permanent Agriculture. 18
- Figure 4: Deforestation patterns in the federal state of Rondônia in western Brazil; from NASA (2009). 22
- Figure 5: Fire is commonly used to clear forested land in the tropics. An astronaut aboard the International Space Station captured this photograph of burning in Brazil on August 14, 2010; from NASA (2010). 23
- Figure 6: Different states of forest and forest degradation in terms of their biomass stocks, and the potential of detection by optical remote sensing techniques (left = undisturbed, middle = stealthy degradation, right = detectable degradation); from Baldauf et al. (2009). 27
- Figure 7: The composition of errors types and the total survey error; from Köhl et al. (2009). 28
- Figure 8: Theoretical examples for the concept of accuracy and precision of an estimator; from Köhl et al. (2006). 29
- Figure 9: Total error is plotted against its corresponding quantification of change; The red lines indicate decision boundaries for priority areas of action due to the classes High and Low, for both errors and quantification of change; This results in priority areas of action: High Error / Low Change = Medium Update Priority; High Error / High Change = High Update Priority; Low Error / Low Change = Low Update Priority; Low Error / High Change = Medium Update Priority; adapted from Jones et al. (2004). 32

- Figure 10: Error sources in a multi-date change detection analysis using remote sensing techniques; from Congalton and Green (2007)..... 33
- Figure 11: Exemplary workflow of a COBIA based method; adapted from Schiewe et al. (2001). ... 38
- Figure 12: Example of a membership function dialog in eCognition®; the numbered red frames are: (1) name of the feature, (2) available types of membership functions, (3) used type of membership function, (4) left and (5) right thresholds..... 43
- Figure 13: LiDAR pulse (here called Lidar beam) recording multiple returns as various surfaces of a forest canopy and soil are hit; from Lillesand et al. (2004). 45
- Figure 14: Spectral characteristics of common RADAR systems used in remote sensing; the systems are grouped regarding their respective wave bands L (23.5cm wavelength), S (12cm wavelength), C (5.7cm wavelength), and X (3.1cm wavelength); adapted from Richards (2009)..... 46
- Figure 15: Conceptual differences of remote sensing technologies and their respective penetration depths into the forest canopy; from Lefsky and Cohen (2003). 47
- Figure 16: Example for an error matrix; from (Czaplewski, 2003). 51
- Figure 17: The map shows the federal state Roraima in Brazil. The capital Boa Vista and the municipal Caracaraí, where the project area (red outline) is located, are indicated on the map. In the background a Landsat7 ETM+ scene from 2004 is shown in false color. Green areas show forest lands, pink areas show deforested spots. 55
- Figure 18: Map of the Caracaraí forest project; the red outline shows the coarse project area of about 30,000ha; the grey lines indicate the planned Forest Management Units (FMU). The FMUs 5 (light blue) and 6 (light red) have been used in this study. In the background a Landsat7 ETM+ scene from 2004 is shown in false color. Green areas show forest lands, pink areas show deforestation spots. In the upper left corner the Caracaraí forest project directly adjoins the stream Rio Branco (dark blue)..... 56
- Figure 19: Photo of an example for the durable unique identification on a tree bole for the tree number “002838” 57
- Figure 20: Design of the inventory system; (a) a systematic grid of 50m by 50m was constructed along a horizontal “Base line”. The resulting rows and columns form the grid cells that can be seen in the above figure. The grid cells were named due to their rows and columns in numerical order; (b) shows the localization of an exemplary tree in respect to the dot grid point (circle, ○) of the respective grid cell. 58

- Figure 21: Map showing the distribution of trees (green) inside the squares (grey) next to the Base line (dashed red line) within the project area; exemplary the referencing of a tree (Tree_ID= 26235) in respect to the dot grid point (15m east, 19m north) of the Square 74/1 is illustrated. 59
- Figure 22: Map showing the obtained QuickBird-2 image in the west; the red outline shows the coarse project area. 60
- Figure 23: Data set (ii); TerraSAR-X data from 2008, TerraSAR-X 2008..... 62
- Figure 24: Data set (iii); TerraSAR-X data from 2009, TerraSAR-X 2009:..... 62
- Figure 25: Example of the bi-temporal stack of the TerraSAR-X scenes: TerraSAR-X 2008 and TerraSAR-X 2009; The stack is displayed as RGB (Red = TerraSAR-X 2008, Green = TerraSAR-X 2009, Blue = TerraSAR-X 2009); from Baldauf and Köhl (2009). 65
- Figure 26: Classification rule set for object-level change detection. In this example, the class hierarchy consists of the two classes "Scale-level 1" and "Scale-level 2". Each class is defined by the class description that consists of one-dimensional membership functions. This example returns the interim results "Result 1" and "Result 2" that can be deduced by each class on the respective scale. 73
- Figure 27: Classes for the evaluation of tree-specific social position and dominance; based on Kraft (1884)..... 79
- Figure 28: This diagram is used as a template for the illustration of the quantification of the influences of each of the three stand characteristics; In the red box labeled with "1" the producer's accuracy summed for all classes is shown. In the red box labeled with "2" the number of extracted trees summed for all classes is presented. As both the numbers for "1" and "2" correspond for all three stand characteristics they are the same in all respective diagrams. In the red box "3" the producer's accuracies of each sub-class are listed for the results "not detected" and "detected" of the event "Change". The correct detection of the event "Change" is represented as "detected" (blue) and the incorrect detection of the event "Change" as "not detected" (red). In the red box "4" the number of the extracted trees in each sub-class is shown. 82
- Figure 29: Image objects of the scale levels L25 and L50 derived through multi-resolution segmentation; black outlines signifies image objects of level L50, blue lines show image objects of level L25 that further subdivides the image objects of L50, in the background

- the bi-temporal stack of the TerraSAR-X scenes is displayed; The stack is displayed as RGB (Red = TerraSAR-X 2008, Green = TerraSAR-X 2009, Blue = TerraSAR-X 2009). 85
- Figure 30: The classification rule set for object-level change detection shows the processing steps incorporating the class hierarchy, the class descriptions with its membership functions, the interim results and the final result. 87
- Figure 31: Screenshots exemplary showing three maps of the same location. In (a) „TerraSAR-X 2008“, in (b) “TerraSAR-X 2009” is displayed. Differences between (a) and (b) in terms of areas of dissimilar patterns are changes between April 20, 2008 and August 18, 2009, and originate from the extraction of trees in this time periode. These differences have been detected by the change detection algorithm and are displayed in (c). In (c) the background shows “TerraSAR-X 2009”. Polygons with lined patterns are areas of change detected in the multi-temporal TerraSAR-X data. The specific colors of the lined areas correspond to the change detection in respective scale levels, i.e. “L50”, “L25”, and their particular classes and sub-classes, i.e. “change_L50” and “change_L25” 90
- Figure 32: Screenshots showing map results of the object-level change detection for three examples, i.e., (a), (b), and (c). The legend is valid for all three maps. The background shows the optical remote sensing data that is used for visualisation. Polygons with lined patterns are areas of change detected by the classification of the multi-temporal TerraSAR-X data. According to the legend, the specific colors of the lined areas correspond to the change detection in respective scale levels. Taken from the in-situ data, the dark green triangles correspond to tree locations, light green circles to locations of extracted trees. 92
- Figure 33: The diagram shows the influence of the attribute “aboveground tree biomass” on the reliability of the detection of forest degradation in quintiles. For each quintile the specific producer’s accuracy values for “not detected” (red) and for “detected” (blue), and the number of trees are depicted. The rightmost column shows the respective sum of values for all quintiles. 99
- Figure 34: The diagram shows the influence of the attribute “tree crown area” on the reliability of the detection of forest degradation in five classes. For each class the specific producer’s accuracy values “not detected” (red) and “detected” (blue), and the number of trees are depicted. The rightmost column shows the respective sum of values for all classes. ... 100
- Figure 35: The diagram shows the influence of the attribute “social position and dominance” based on the evaluation rule set “Kraft” on the reliability of the detection of forest degradation in three classes. For each class the specific producer’s accuracy values “not detected”

- (red) and “detected” (blue), and the number of trees are depicted. The rightmost column shows the respective sum of values for all classes. 102
- Figure 36: The diagram shows the influence of the attribute “social position and dominance” based on the evaluation rule set “Leibundgut” on the reliability of the detection of forest degradation in three classes. For each class the specific producer’s accuracy values “not detected” (red) and “detected” (blue), and the number of trees are depicted. The rightmost column shows the respective sum of values for all classes. 103
- Figure 37: A simplified equation for a future REDD+ mechanism. REDD+ will only work sustainably on the ground, if the costs for the three components on the left (CP1, CP2, and CP3) are less than the benefit from the incentives component (CP4) on the right; adapted from (Baldauf and Köhl, 2012)..... 116
- Figure 38: Map of Madagascar showing forest areas (green) and a possible systematic sample grid. The rectangular boxes show grid points, which intersect with forest areas, the crosses indicate grid points that do not contain forest areas. 118
- Figure 39: A flowchart shows the single processes of the four objectives to verify the hypothesis. 148
- Figure 40: Screenshot showing the “Class Hierarchy” of the used classification. 150
- Figure 41: Screenshots showing the “Class Description” for (a) the class "change_L50" in scale “L50” and (b) the class "change_L25" in scale “L25”. 150
- Figure 42: Screenshots exemplary showing the “Membership Functions” for (a) the feature "Area" in scale “L50”, and for (b) the feature "ratio_08/ratio_09" in scale “L25”. 151

List of Tables

Table 1:	Land cover classes derived from the GLC2000, average AGB (tons ha ⁻¹) derived from the two approaches "direct remote sensing" (DR) and "combine and assign" (CA). The column labeled Δ indicates the difference between approaches (CA-DR); (adapted from Goetz et al. (2009)).	31
Table 2:	Metadata on panchromatic Quickbird-2 data; Metadata is roughly describing significant facts about the QuickBird-2 satellite scene delivered by DigitalGlobe®.	60
Table 3:	Metadata on the two TerraSAR-X datasets; Metadata is roughly describing significant facts about the TerraSAR-X satellite scenes delivered by Infoterra/Astrium GmbH.....	61
Table 4:	The four theoretical cases for differences between the two scenes TerraSAR-X 2008 and TerraSAR-X 2009 in the image stack as RGB (Red = TerraSAR-X 2008, Green = TerraSAR-X 2009, Blue = TerraSAR-X 2009).	67
Table 5:	Possible values for the features of equation (6) show the influence on the threshold "x". This value of "x" can be further used for the classification into the four theoretical cases introduced in Table 4.	70
Table 6:	Possible values for the features of equation (7) show the influence on the threshold "y". This value of "y" can be further used for the classification into the four theoretical cases introduced in Table 4.	71
Table 7:	Model summary and parameter estimates. Dependent variable is Shape_Area, which is based on the areas of the tree crowns in square meters and originated from the delineation of 10% of the total tree crowns in the project area.	77
Table 8:	Classification of tree crown area estimates into five classes.	78
Table 9:	Evaluation rule set "Kraft" with a description of the respective classes of Kraft (1884). 80	80
Table 10:	Evaluation rule set "Leibundgut" with a description of the respective classes of Leibundgut (1956).	80
Table 11:	Results of the pre-processing stages are depicted for ten exemplary datasets.....	84
Table 12:	Parameters for the multi-resolution segmentation on pixel level of the used data into two "scale levels", i.e. L25 and L50.	85
Table 13:	Error matrix showing the comparison of reference data and classification data. The reference data is based on the in-situ data. The classification data contains all locations of change and no change detected by the developed object-level change detection.....	93

Table 14:	Estimated accuracies for the classification results.	94
Table 15:	The categorization of the tree biomass estimation into quintiles results in the following minimum and maximum values of tree biomass for each class.	96
Table 16:	Results for ten exemplary datasets are depicted for tree specific estimation of aboveground tree biomass, tree crown area, and social position and dominance; The field Tree_No shows the unique identification for the individual trees, Chave_moist_2 lists the appropriate values for the single aboveground tree biomass values in kg, in Chave_moist_2_class these biomass data are categorized into respective quintiles. As in the field est_Crown _Area the results for the estimated tree crown area in square meters are given, these results are classified in CrownAreaClass. Lastly the fields Kraft and Leibundgut show the particular results for the social position and dominance for each depicted tree.	97
Table 17:	Estimates of data costs for a national approach. Figures on land area and forest area in 2010 are based on data of FAO's Global Forest Resource Assessment 2010 (FAO, 2010a). With a size of 5000ha per TerraSAR-X scene the amount of scenes and the respective data costs are estimated.	116

1 Abstract

REDD+ is a climate change mitigation mechanism for tropical forests presently being negotiated under the UNFCCC. It aims to attribute economic value to the carbon stored in forests, and thereby integrates forest protection into economic and political decision making processes. REDD+ embraces five activities that show a mitigating effect on climate change. One of these activities is reducing emissions from forest degradation.

Although forest degradation is an intrinsic part of REDD+, only rough estimates are available for the total of emissions from forest degradation. Nevertheless, these estimates show the importance of grappling with forest degradation in REDD+, if significant emission reductions are envisaged. Currently, however, REDD+ lacks access to scientifically sound, applicable and cost-efficient methods for reporting on forest degradation on a large scale.

The present case study analyzed high-resolution active remote sensing data to determine its suitability for reporting on forest degradation within the scope of REDD+. In the process it developed a method involving TerraSAR-X data to detect patterns of selective logging. Then, based on an accuracy assessment, it identified and quantified the influences of three stand characteristics, i.e. aboveground tree biomass, tree crown area, and social position and dominance, on the reliability of the developed method. Finally, the study demonstrates how the developed method could be implemented into the setup of an operational, robust, and transparent MRV-system.

The study proved that space-born RADAR can be used for monitoring patterns of forest degradation in tropical moist forests. Combined with appropriate methods, it enables the collection of unbiased activity data and thereby serves as a suitable tool for reporting on forest degradation within the scope of REDD+.

2 Introduction

“The United Nations Framework Convention on Climate Change and the Kyoto Protocol explicitly recognize the important role of forests in global climate change and, therefore, commit all Parties to protect them and manage them sustainably.” (FAO, 2007)

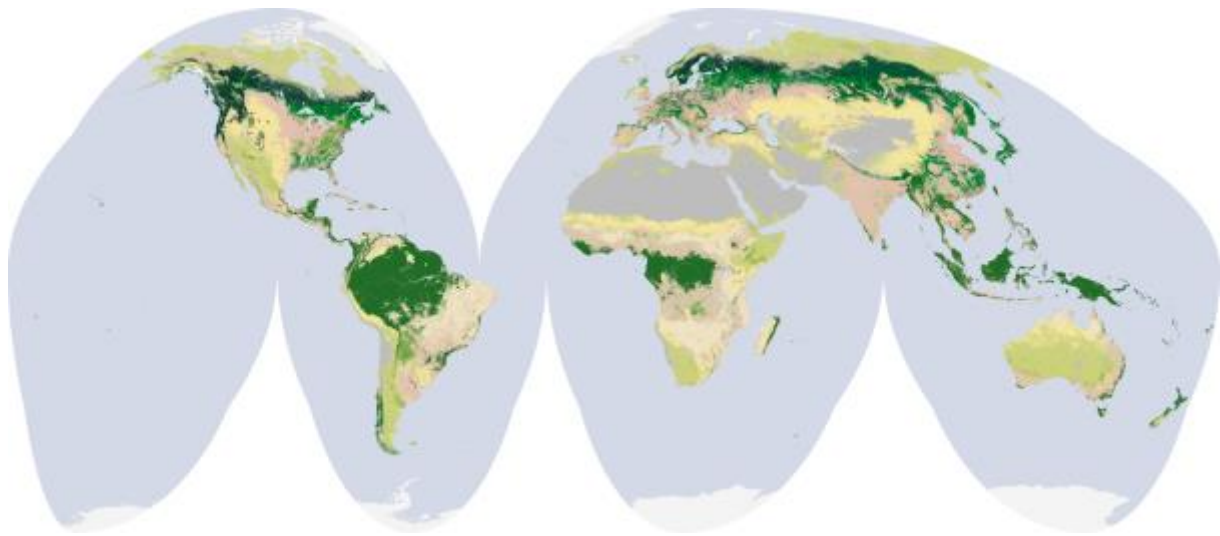


Figure 1: Map of land cover classification from the MODIS instrument aboard the satellite *Terra*. Forests (green) cover 30% of the Earth's land; from Simmon (2011).

2.1 Role of forests in climate change

Forests, in particular tropical forests, play a critical role in climate change as it emerges to be perhaps the greatest environmental challenge of the twenty-first century (FAO, 2012a). The exchange of carbon dioxide (CO₂) as a key greenhouse gas (GHG) in the global carbon cycle between the atmosphere and terrestrial ecosystems occurs through processes of photosynthesis, respiration, decomposition and changes in land use and land cover. Since the beginning of the last century, human-induced emissions from fossil fuel use and large-scale land use have greatly increased the concentration of CO₂ in the atmosphere (Schimel, 1995).

This widely accepted increase of evidence for a link between atmospheric GHGs and climate change, promotes the importance of the reduction of anthropogenic emissions of GHGs, in order to cope with internationally negotiated climate change goals. The economic aspects of climate change were intensively examined by Stern (2007), thus depicting four ways of contributing to the mitigation of climate change. One concentrates on non-energy emissions and highlights the cost-effectiveness of curbing deforestation as a way of reducing greenhouse gas emissions “if the right policies and institutional structures are put in place.” (cf. Stern (2007))

The world’s forests store a vast amount of carbon, 289 gigatonnes (Gt), in their biomass alone, i.e. more than one tenth of the total carbon of the Earth’s terrestrial ecosystems (FAO, 2010b; UNEP-WCMC, 2008). The Food and Agriculture Organization of the United Nations (FAO) estimates that the human-induced overuse of the global forests results in the release of about one-sixth of the anthropogenic global carbon emissions (FAO, 2012b). A significant impact on the increased release of GHGs in the atmosphere can be attributed to the occurring process of deforestation, i.e. the unsustainable management of forests and, as such, the permanent conversion of forested to non-forested lands, in tropical forests (Achard et al., 2002; Fearnside and Laurance, 2003, 2004; Houghton, 1991, 2003; UNFF, 2009).

Despite many endeavors to reduce this trend’s alarmingly high momentum, by slowing or even halting the deforestation rate for example through programs set up by the international community in the negotiations on forest and environmental policy, as of yet any success in combating the destruction of tropical forests has been limited. A key message from FAO’s Global Forest Resource Assessment (FRA) in 2010 was that, “the rate of deforestation and loss of forest from natural causes was still alarmingly high” from 2000-2010 (cf. FAO (2011b)). FAO (2011b) furthermore states that the net decrease of global forest area had only slowed down from estimated 16 million hectares per year in the 1990s to around 13 million hectares per year in the last decade.

The first World Climate Conference (WCC) was held in 1979 (WMO, 1979). Until the Stern Report in 2007, the economic dependencies of climate change had never been confirmed in such a holistic view, however, the global debate on climate change and the discussion on the role of sustainable management of the world's forests began in the early 1990s (UN, 1997). Since 1992, international negotiations on mitigating climate change under the United Nations Framework Convention on Climate Change (UNFCCC) have taken place. In 1995, the first session of the Conference of the Parties (COP) was held in Berlin. While the Kyoto Protocol, adopted in 1997 and entered into force 2005, "sets binding emission reduction targets for 37 industrialized countries and the European community in its first commitment period" (cf. UNFCCC (2011a)), it was only in Montreal in 2005 when the submission of the governments of Papua New Guinea and Costa Rica and eight other Parties requested that the UNFCCC secretariat adds an item entitled "Reducing emissions from deforestation in developing countries: approaches to stimulate action" to the provisional agenda (UNFCCC, 2005). In doing so, they augmented the climate change negotiations by including an appropriate path for the important field of tropical forests.

2.2 REDD+

Since the climate change conference in Bali 2007, the Reduction of Emissions from Deforestation and forest Degradation (REDD) has been officially negotiated as a climate change mitigation mechanism for tropical forests under the Ad-Hoc Working Group on Long-term Cooperative Action under the Convention (AWG-LCA) and Subsidiary Body for Scientific and Technological Advice (SBSTA).

Although, REDD has yet to have much impact on either the scientific community or international negotiations, its potential influence on climate change mitigation is undeniable and particularly impressive given its relative simplicity as a concept. Basically it aims to attribute economic value to the carbon stored in forests, and thereby integrating forest protection into economic and political decision making processes.

Regarding international negotiations the following four key decisions are of importance in describing the progress of REDD under the UNFCCC:

- Decision 1/CP.13 (Bali Action Plan),
- Decision 2/CP.13, both from COP13 in Bali (UNFCCC, 2008),
- Decision 4/CP.15 from COP15 in Copenhagen (UNFCCC, 2010), and
- Decision 1/CP.16 from COP16 in Cancun (UNFCCC, 2011b)

While at the beginning a process to “avoid deforestation” was discussed, nowadays a global mechanism is negotiated that embraces the five national activities: (i) reducing emissions from deforestation, (ii) reducing emissions from forest degradation, (iii) sustainable management of forest, (iv) conservation of forest carbon stocks, and (v) enhancement of forest carbon stocks; and holds a multitude of social, ecological and governmental safeguards, that have to be respected. All this is subsumed in the term REDD+. Mostly, the implementation of REDD+ is outlined in a phased approach, moving in a step-wise fashion from pilot activities to full, results-based REDD+ implementation (Meridian Institute, 2009; UNFCCC, 2011b).

Facing the fact that politicians see the red(d) light regarding the role of tropical forests in climate change, not only the above mentioned political negotiations are necessary, but also the existence of suitable methods for REDD+ or their development by the scientific community are essential. Fuller (2006) even relates these methods for REDD+ to a new era of transparency in forest governance.

Given the present state of the negotiations on REDD+, countries aspiring to generate benefits herein need to consider several components. They must implement, among other things, sound systems for measuring, reporting and verification (MRV) of carbon stocks and carbon stock changes (UNFCCC, 2012a). These systems must allow for the identification of all processes leading to deforestation and forest degradation and for the sensible quantification of emissions hereof. In addition to the MRV-system an efficient implementation of the potential REDD+ mechanism requires, a system for identifying and quantifying local and regional drivers of deforestation and forest degradation, and

adapting incentive schemes to manage with these drivers. Both preceding components allow for the definition of a forest reference (emission) level, against which the reduced emissions can be measured and benefits can be considered. Finally, an incentive scheme has to be set up offering different regionally or locally adapted options that en masse sustainably contribute on a national scale to the set of five REDD+ activities. Experiences from holistic, national REDD+ pilots show the interdependencies of these components (Baldauf et al., 2010) and give an idea of future workloads for national and regional REDD+ programs (BMZ, 2012; GIZ, 2011).

Official guidelines for MRV within the scope of REDD+ are yet to be established (UNFCCC, 2012b). The revisions of the Guidelines for National Greenhouse Gas Inventories (IPCC, 1996, 2006) and the revisions of the Good Practice Guidance (GPG) (IPCC, 2000, 2003b) of the Intergovernmental Panel on Climate Change (IPCC) provide a summary of methodologies that can form the basis for how developing countries¹ can estimate and monitor emission reductions from deforestation and forest degradation, and changes in forest carbon stocks. Already, various additional guiding reports and guidelines for Annex I Parties², identifying methods for the quantification of activities in the Land Use, Land-Use Change and Forestry (LULUCF) sector leading to emissions, have been published (Patenaude et al., 2005; Rosenqvist et al., 2003). Especially for the process of deforestation IPCC methods can be adapted or redeveloped in order to suit for REDD+ MRV-systems' requirements.

IPCC defines two target variables, (i) changes in forest area over time (activity data, AD), and (ii) changes in the average carbon stock per unit area over time (emission factors, EF) (IPCC, 2000, 2003b, 2006). IPCC advises that both AD and EFs have to be estimated in a statistically sound manner. To ensure the quality on all steps of the inventory design, IPCC proposes following the five principles: consistency, comparability, completeness, accuracy and transparency (cf. IPCC (2006)).

¹ In this context developing countries are Non-Annex I Parties; See UNFCCC (2012c)

² See UNFCCC (2012d)

The 2006 IPCC Guidelines provide guidance on estimation methods "at three levels of detail", i.e. tier 1 to tier 3 (cf. IPCC (2006)). As such, a tier represents a level of methodological complexity. The IPCC (2006) provides a framework of tier structure for the methods of the sector of Agriculture, Forestry and Other Land Uses (AFOLU):

- The simplest to use alternative is offered by tier 1. It utilizes globally-available activity data (e.g. on deforestation rates), and makes use of equations and default values (e.g. emission and stock change factors) that are directly provided by IPCC. FAO shows, that there are about 50-70% uncertainties associated with tier 1 estimates (UNFCCC, 2009).
- Tier 2 utilizes country- or region-specific data for the most important land-use categories. Emission factors and activity data show a higher temporal and spatial resolution than those used for Tier 1.
- Tier 3 uses high order methods including models and inventory measurement systems that are tailored for the country specific circumstances.

(cf. IPCC (2006))

Generally spoken, if the estimation methods are applied appropriately, firstly all tiers provide unbiased estimates, and secondly accuracy and precision improves for higher tiers. Designing an inventory of the different tiers facilitates the utilization of methods consistent with the available resources and capacities of the respective country. Furthermore, those categories of emissions and removals with the most significant contribution to national emission totals and trends can be brought to focus (IPCC, 2006). Taking note of these national circumstances, which include the availability of required data, capacities and in the end nationally available, finite financial resources, aims at ensuring a most effective inventory design, and anticipates that the inventory results can be reported and verified in a transparent manner (IPCC, 2006).

In the "Tropical Forestry Handbook" edited by Pancel (1993), Köhl (1993) provides in-depth insight into methods of forest inventories, how to gather data and obtain information on tropical forests in a statistically sound and reliable manner. In respect of forest inventories, as the "data supplier" for the

MRV component, these methods could qualify for a full implementation of all MRV requirements. Though, Holmgren and Thuresson (1998) stated that pure terrestrial based methods of forest inventories are expensive, cost-effectiveness, as already specified by Stern (2007) and van der Werf et al. (2009), is an important issue both in any of the above named REDD+ components and in REDD+ as an international mechanism. Accordingly, Wertz-Kanounnikoff and Verchot (2008) identified a trade-off between costs and accuracy for potential MRV-systems, and thus sees “the quest for cost-effective solutions [...] at the centre of the MRV debate”.

In a further work, Köhl et al. (2006) additionally discusses contemporary data sources, i.e. data from remote sensing and geographic information systems (GIS), and their appropriate incorporation into so called “integrated forest inventory systems”. For this present study, these integrated approaches differ from combined forest inventory approaches, the latter being further described in Mandallaz (1993). On the whole, integrated forest inventory approaches have the potential to provide higher cost-efficiency than pure terrestrial inventories alone (Achard et al., 2002; Bowden et al., 1979; Scott and Köhl, 1994), a fact that is especially valid for remote and hard to access areas (Plugge et al., 2010).

It has been shown that cost of inventory systems can play a crucial role in the realization of the potential REDD+ mechanism (Köhl et al., 2009). Murdiyarso et al. (2008) saw the cost of such systems highly dependent on national circumstances. Moreover, Böttcher et al. (2009) discussed the subject of opportunity costs that “represent the highest alternative land-use of the area under deforestation threat, including net revenue from the conversion itself”. As a consequence, Plugge et al. (2012) elaborated on country specific breakeven-points that define the optimal setting of a forest inventory in relation to its costs. Moreover, Köhl et al. (2011) stated that different sampling designs have direct implications on the expected cost, and hence may provide enormous financial advantages. As a result they maintained, “if expensive remote sensing alternatives are suggested”, a suitable MRV-system can be justified “as an investment that aims to generate financial benefits” (cf. Köhl et al. (2011)).

Therefore, when commencing considerations on a REDD+ MRV-system, the careful planning of forest inventory options for all its particular stages is needed, to find an optimal design under the specific national conditions. This circumstance has implications on the advice of IPCC concerning the estimation of AD and EFs. While the derivation of respective national EFs for all five major carbon pools, i.e. (i) aboveground biomass, (ii) belowground biomass, (iii) dead wood, (iv) litter, and (v) soil organic matter, needs intensive terrestrial investigations for higher tiers (GOFC-GOLD, 2011), terrestrial inventory based estimation of country-specific AD can be complemented with the use of appropriate remote sensing techniques in order to improve the cost-efficiency of the respective inventory (Achard et al., 2008; Baldauf et al., 2009; DeFries et al., 2007; Herold and Johns, 2007).

In 2003, two significant studies enlightened the role of remote sensing in the monitoring of tropical forest environments, i.e. Foody (2003) and Rosenqvist et al. (2003). The first concluded that to realize the potential of remote sensing technologies “developments in mapping and monitoring land cover change [...] are [...] required” (cf. Foody (2003)). The second reviewed existing remote sensing technologies and stated that “techniques for detecting and spatially quantifying types of deforestation [...] activities [...] are reasonably well established” (cf. Rosenqvist et al. (2003)). However, purely estimating deforestation, or in other words changes in forest area over time, and thereby neglecting the menace from forest degradation is not sufficient for REDD+.

Even though forest degradation is seen by Simula and Mansur (2011) as “one of the major sources of greenhouse gas (GHG) emissions”, there is a tremendous lack of information regarding its significance and quantification on a global scale. With a slightly different definition of forest degradation than it is generally understood in the REDD+ context, ITTO (2002) used various sources to compile an estimation of the extent of degraded and secondary forests worldwide: 850 million hectares. This value equals the total area of Brazil or twice the area of all current 27 member states of the European Union, and thereby explains the significance of the subject. Other sources, like e.g. Gaston et al. (1998), specify the estimates of carbon emissions from forest degradation in tropical Africa to be more than twice as much than those from deforestation

On the whole, this shows the urgent need for methods that are scientifically sound, applicable in praxis, and cost-efficient, to report on forest degradation on large scales within the scope of REDD+.

2.3 The scope of the present study

Since 2007 REDD has been on the international agenda as a potential mechanism to mitigate climate change, and since 2010 UN-parties have been in negotiations on the five activities of REDD+, one being “reducing emissions from forest degradation”. The significance of forest degradation as an environmental, social and economical problem cannot be overestimated. Hitherto, scientifically sound, applicable and cost-efficient methods to report on forest degradation on large scale have not been at hand.

Forest degradation can be seen as an action that results in no change of forest area as such, but as a change in quality of the forest’s condition (Lanly, 2003). Respective attributes to measure this change can be more general such as health and vitality, the production capacity of market or non-market goods and services, or more specified such as the species composition, distribution of diameter at breast height (dbh, 1.30m), tree height, standing volume, biomass, or mortality. Any method to report on forest degradation needs to approach the question, how to quantify this change in quality of the forest’s condition. The change can be assessed at different spatial scales for different purposes. While the aggregation of small scale effects to national values and significances is an appropriate path, the other way round is impossible. Monitoring changes in forest quality on small scales, however, has proven to be very costly. In other fields, remote sensing technologies have provided valuable cost-efficiency for large scale monitoring. Thus, it has to be investigated, if the use of remote sensing data would provide capabilities for reporting on forest degradation. If so, an approach needs to be developed that can be embedded in national MRV-systems thereby making it possible to overcome the hitherto existing obstacles to reporting on forest degradation within the scope of REDD+.

The present study is intended to provide contributions to the development of scientifically sound and operational methods for reporting on forest degradation within the scope of REDD+, and thus focuses on the following hypothesis:

High-resolution active remote sensing data is a suitable tool to report on forest degradation within the scope of REDD+.

The present study investigates four objectives to verify this hypothesis³:

- Objective (A) Different remote sensing techniques are reviewed to compile a method to report on forest degradation within the scope of REDD+.
- Objective (B) Develop an approach to detect forest degradation in tropical moist forests using high-resolution Radio Detection and Ranging (RADAR) data.
- Objective (C) Quantify influences of stand characteristics on the reliability of the developed approach.
- Objective (D) Quantify the accuracy of this approach.

³ Figure 39 on page 148 shows a flowchart identifying the single processes of the four objectives to verify this hypothesis

3 Background

At the United Nations Conference on Sustainable Development in Rio de Janeiro, Brazil, on June 21st, 2012 Christiana Figueres, the Executive Secretary of the UNFCCC, re-confirmed that “Under the UNFCCC, they [Governments] have set the goal of a maximum 2 degrees Celsius temperature rise, with a view to considering 1.5 degrees Celsius.”. She continued with “There is no doubt that the scope and speed of action urgently needs to be stepped up, and that holds true for all three Conventions.” (cf. UN (2012))

This two degrees Celsius global warming goal is nothing really new. To avert the worst consequences of global warming, the leaders of the Group of the eight wealthiest nations (G8) reaffirmed in L’Aquila on July 8th, 2009 the work of IPCC and principally agreed to limit global warming to two degrees Celsius, among other ways, by cutting their greenhouse gas emissions (cf. G8 (2009)). At the COP15 in Copenhagen in 2009 the Parties recognized “the scientific view that the increase in global temperature should be below 2 degrees Celsius”, to achieve the essential objective of the Convention (cf. UNFCCC (2010)).

The role of REDD+ in reaching this goal was addressed by Angelsen (2008), who added that REDD “must be included in the next global climate regime”, if the efforts to combat climate change and the goal are taken serious.

Accordingly, at its 36th session, SBSTA continued its work inter alia on methodological guidance relating to modalities for MRV, and a possible draft decision on these matters is expected to be finalized “for consideration and adoption by the Conference of the Parties at its nineteenth session” (cf. UNFCCC (2012b)). The above cited statement by Christina Figueres leaves no doubt that apart from political will and effort, the scientific community is asked to make its contribution. So, additional developments of inter alia modalities for measuring, reporting and verifying anthropogenic forest-related emissions need the particular attention of the scientific community. Particularly, the scientific community is expected to work on methods to MRV the implementation of

the five activities of REDD+, one being “Reducing emissions from forest degradation” (cf. UNFCCC (2011b)).

As stated in the Introduction, scientifically sound, applicable and cost-efficient methods are necessary for reporting on forest degradation over large scales within the scope of REDD+. Herein integrated forest inventories play an important role in finding an optimal path that combines the three characteristics above. In chapter 0, different techniques are reviewed that can be used in a compilation process to develop a method that enables reporting on forest degradation within the scope of REDD+.

3.1 The phenomenon “forest degradation”

There is a multitude of studies regarding the process of defining the term ‘forest’. Lund (1999) identified no fewer than 133 different definitions of ‘forest’, eight based on administrative units, 66 on land cover and 59 on land use. All of which define the status of an area. Köhl et al. (2000) questioned whether the harmonization or standardization of the term forest is a “mission impossible”. Most often a forest is defined according to FAO as:

“Land with tree crown cover (or equivalent stocking level) of more than 10 percent and area of more than 0.5 hectares (ha). The trees should be able to reach a minimum height of 5 meters (m) at maturity in situ.” (cf. FAO (1998))

Even more complex are definitions of processes like, e.g. afforestation, reforestation, or deforestation, as illustrated by Lund (1999). The International Union of Forest Research Organisations (IUFRO) tried to get involved in the debate with the question: “How to Get Society to Understand Forest Terminology?” (IUFRO, 2000). Moreover, when comparing definitions of processes or development stages, it must be understood that many definitions are “esoteric and, from a resource inventory stand point, difficult to classify in the field” (cf. IUFRO (2000)).

Definitions of 'forest degradation' can be found in a huge number of publications (Achard et al., 2007; Achard et al., 2002; Avitabile et al., 2011; Baldauf et al., 2009; FAO, 2007; Grainger, 1993; Guariguata et al., 2009; IPCC, 2003a; ITTO, 2002; Lanly, 2003; Lund, 1999; Simula, 2009; Simula and Mansur, 2011; UNFCCC, 2006).

For instance, Grainger (1993) finds appropriate the definition: "a degraded forest may be defined as the temporary or permanent reduction in the density, structure, species composition or productivity of vegetation cover" (cf. Grainger (1993)). However, due to their reduced productivity this definition would classify old-growth forests as degraded forests (IUFRO, 2000), a fact, which certainly is hard to get society and even foresters to understand.

Simula and Mansur (2011) see the general problem herein as the fact that "one person's degraded forest is another person's livelihood" (cf. Simula and Mansur (2011)). In other words, forest degradation has to be seen as a relative concept linked with the respective objectives.

In consequence, it is important, not only from a scientific point of view, that a specific definition of 'forest degradation' be developed as part of the activities to be considered under REDD+ (UNFCCC, 2010). Especially since, as Achard et al. (2007) point out, "forest degradation can also be a precursor to deforestation". (cf. Achard et al. (2007))

Distinguishing forest degradation from other processes like deforestation is straightforward. Deforestation can be defined as the conversion from forest land to other land uses, i.e. a decrease in the area covered by forest (FAO, 2003). Consequently, forest degradation could be seen as "a process within forests that leads to a significant reduction in either tree density or proportion of forest cover" (cf. Achard et al. (2002)). Although, the concepts of these approaches were formulated before any REDD+ negotiations took place, some ideas could still be used for REDD+.

Originally compiled for use in the context of the Kyoto Protocol, IPCC (2003a) stated that 'forest degradation' relates to direct human-induced changes in carbon stocks and thus a particular definition "should at least include carbon stock changes in all relevant pools" (cf. IPCC (2003a))

Furthermore, several possible definitions of ‘forest degradation’ and respective methodological implications were presented (cf. IPCC (2003a)). Moreover, the following definition was agreed upon that still provides room for national adaptation in terms of three variables:

‘A direct, human-induced, long-term loss (persisting for X years or more) of at least Y% of forest carbon stocks [and forest values] since time T and not qualifying as deforestation’⁴.

(cf. IPCC (2003a))

In addition, FAO has initiated a particular study to define issues related to REDD+ and to identify the elements of ‘forest degradation’ as well as the best practices for their assessment (FAO, 2007). In this context, Simula (2009) provided a review of the existing international and national definitions for ‘forest degradation’ and analyzed their elements and parameters. He concludes that as an option for further action one should consider expanding “efforts to measure and assess forest degradation” (cf. Simula (2009)).

Regarding REDD+, UNFCCC organized a workshop on reducing emissions from deforestation in developing countries⁵ where pertinent definitions based on decisions of UNFCCC and on reports by IPCC are assembled:

- Forest = $\left\{ \begin{array}{l} \text{minimum crown cover (mCC) } 10 - 30\% \\ \text{minimum tree height (mTH) } 2 - 5\text{m} \\ \text{minimum area (mA) } 0.05 - 1\text{ha} \end{array} \right\}$
- Deforestation =
{a measurable sustained decrease in crown cover from greater than the mCC to less than the mCC }
- Forest degradation =
{a measurable sustained decrease in crown cover with crown cover remaining greater than mCC }

(cf. UNFCCC (2006))

Following the above definitions, the process of ‘forest degradation’ appears as a more complex change in land cover than deforestation. This circumstance was recognized by Baldauf et al. (2009)

⁴ Where X, Y and T are undefined

⁵ Held in Rome, Italy on August 30th to September 1st, 2006

The role of forest degradation in climate change

Although, Simula and Mansur (2011) see forest degradation as “one of the major sources of greenhouse gas (GHG) emissions”, in 2003 IPCC (2003a) identified that none of the existing international reporting instruments incorporate “activities similar to those described as forest degradation” (cf. IPCC (2003a)).

In addition to ITTO’s compilation of an estimation of the worldwide extent of degraded and secondary forests, i.e. 850 million hectares (cf. ITTO (2002)), Houghton (2005) and Bucki et al. (2012) collected data sources on estimates of carbon emissions from forest degradation in addition to the emissions from deforestation:

- Humid tropics, +5%, (Achard et al., 2004)
- Brazilian Amazon, Peruvian region, +25–47%, (Asner et al., 2005)
- Tropical regions, +29%, (Houghton, 2003)
- Tropical Asia, +25–42%, (Flint and Richards J.F, 1994; Houghton and Hackler, 1999; Iverson et al., 1994)
- Tropical Africa, +132%, (Gaston et al., 1998)

While these data sources explicitly show the importance of forest degradation and its resulting emissions of carbon, their range, i.e. from 5% to 132%, shows the uncertainty attached to their quantification. The latter circumstance underlines the need for respective monitoring methods.

Causes of forest degradation

As can be concluded by the careful distinction between deforestation and forest degradation in Figure 2, the underlying causes of these two processes can both be similar or divergent (Lanly, 2003). ITTO (2002), although having a different perspective and objective on forest degradation, identified one of the main common cause of deforestation and forest degradation, i.e. seek for agricultural land (see Figure 3).

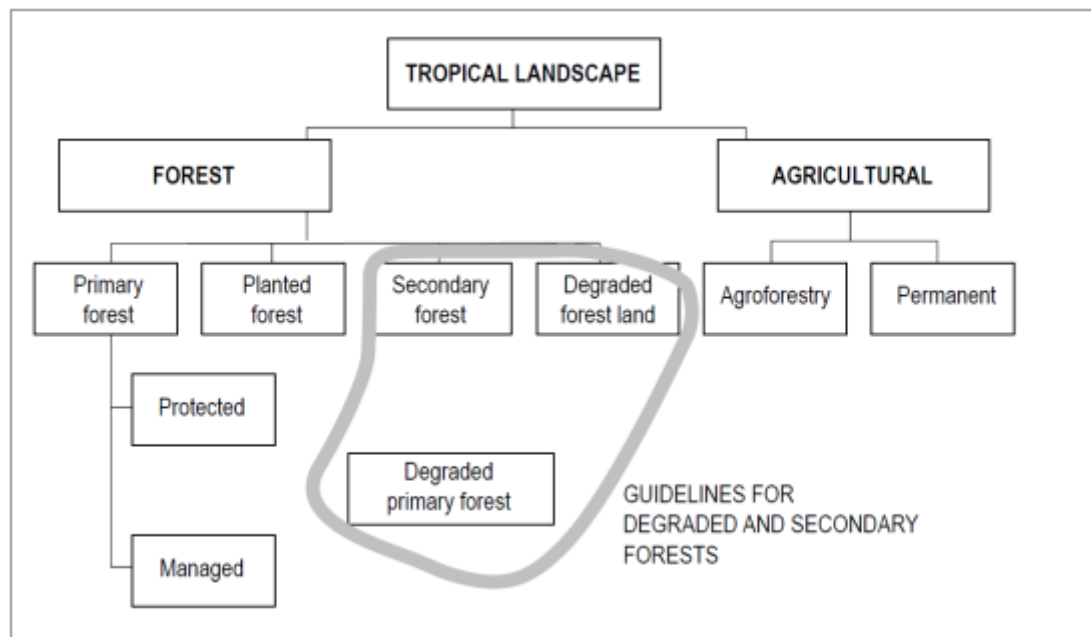


Figure 3: The different land-use types and forest conditions in a schematized tropical landscape (cf. ITTO (2002)). The forest conditions in the third row can also be seen as stages in the deforestation and forest degradation process, i.e. *Primary forest* to *Secondary forest* to *Degraded forest land* to *Permanent Agriculture*.

Already in 1995, the concerns regarding population pressures and their growing demand for agricultural land was omnipresent “in literature on deforestation, soil degradation, loss of biodiversity, threats to future peace and stability, food scarcities, global warming and underdevelopment” (cf. Agrawal (1995)).

Specific causes for forest degradation were presented by Lanly (2003) (i.e. selective felling, fuel wood, and grazing), Fearnside and Laurance (2004) (i.e. selective logging, surface fires, habitat fragmentation, and edge effects), Peres et al. (2006) (i.e. low-intensity timber harvesting, fuel wood collection, small-scale mining, and understory thinning) and Wertz-Kanounnikoff and Verchot (2008) (i.e. selective logging, forest fires, over-exploitation of fuel wood, and mining). While this catalogue is far from being complete, it is obvious that, in terms of occurrence, selective logging plays an important role as a cause of forest degradation.

Linke et al. (2007) investigated forest disturbances in ecosystem management and described the impact of anthropogenic and natural processes on landscape- and stand-level forest structures. They

also explained the spatial patterns of the above processes, whereas temporal and spatial scale, as well as disturbance severity and rate play an important role for their characterization. Applying the characterization by Linke et al. (2007) on the causes of forest degradation as listed above shows that, of them all, selective logging entails the least disturbance per unit of area and is thereby expected to be most difficult to monitor.

Remaining problems

Forest degradation does not implicate a reduction of the forest area, but rather a change of quality in the forest's condition (Lanly, 2003). Reporting on this change may be achieved by monitoring quite general attributes, such as health and vitality and the production capacity of market or non-market goods and services, or more specific attributes like species composition, distribution of dbh, tree height, standing volume, biomass, or mortality. Within the scope of REDD+, where emissions from forest degradation are to be estimated, biomass and its respective change over time is of main interest. The estimation of forest biomass is further investigated in chapter 3.2.

In terrestrial inventories the changes in number of trees per hectare can give an indication of the degree of forest degradation, whereas in remote sensing based investigations, spatial patterns of changes in crown cover can be used for this purpose (Culvenor, 2003; Healey et al., 2007; Hudak et al., 2007). The monitoring of forest degradation is investigated more in detail in chapter 3.3.

In this regard a problem remains since anthropogenic processes, forest degradation and sustainable forest management (SFM) all share the process of selective logging. While SFM embraces methodological and planned management of forest resources, forest degradation, as stated in chapter 3.1, comprises unmanaged forms of forest resource utilization that can be considered non-sustainable, uncontrolled and unplanned. In respect to climate change matters, the sustainable use of forest resources entails a positive mitigation effect, as on the one hand remaining forests still fulfill multiple functions, and on the other hand the extracted timber can substitute a variety of non-wood products, e.g. for building purposes, and as part of a cascading use system substitute fossil fuels. On

the contrary, forest degradation leads to reasonable amounts of carbon emissions⁶. A further issue is the threshold of a forest's resilience. Due to its unsustainable nature, areas of forest degradation reach a point at which they are unable to return to an original stable state earlier than areas of sustainable forest management.

The spatial pattern of selective logging within forest degradation, however, corresponds to the spatial pattern of selective logging within sustainable forest management (Coops et al., 2007). The distinction between forest degradation and SFM in remote sensing alone can only be undertaken within in-direct methods with the use of proxies⁷. This approach is based on labor-intensive manual interpretations and thus a successful large-scale application is highly questionable.

3.2 Estimation of forest biomass

As reflected in the proposed definition of forest degradation by IPCC (2003a), the estimation of the extent of the sources and sinks of carbon dioxide through changes in the cover, use, and management of forests, requires reliable estimates of the biomass of forest lands. Examples of human activities that change the forest biomass density are silviculture, harvesting, and forest degradation. This field has been intensively studied in the past decades. Negative changes in forest biomass indisputably lead to emissions of carbon. Nevertheless, direct methods to monitor the emissions from forest degradation can fall short when addressing the issue of cost-efficiency, an issue that, as stated above, is very important for the successful implementation of REDD+.

The direct measurement of biomass of forests can only be accomplished by destructive sampling (Houghton, 1991). This procedure, however, is based on intensive tree felling and is therefore unquestionably time-consuming, and thus nearly impossible on large scale. Consequently, the quantification of biomass in forests is realized by the estimation of aboveground biomass based on direct measurements such as tree diameter and height, in combination with the use (i) of models converting diameter to biomass by means of biomass expansion factors (BEF) (Brown and Lugo,

⁶ See chapter 2.1 on page 2

⁷ See chapter 3.3.1 on page 23

1992; Schroeder et al., 1997) or (ii) of allometric equations from individual tree measurements (Brown, 1997; Segura and Kanninen, 2005).

Most notably, Brown (1997) supplied a relevant base in a primer for the estimation of tree biomass and respective changes for tropical forests. Brown (1997) not only compiles a list of species specific wood densities for all tropical forests, but also develops biomass regression equations for estimating the biomass of tropical trees for the three climatic zones “dry”, “moist” and “wet”. Further work, e.g. by Chave et al. (2005), used the same categories, due to the fact that for tropical forests species specific regression models can be viewed as inapplicable. However, Segura and Kanninen (2005) and Vieilledent et al. (2011) stated that universal equations by broad ecological zones may not accurately reflect the tree biomass in a specific area or region, further work is needed in the development of biomass regression equations on regional and national scale.

A promising approach for further development was described by Hildebrandt and Iost (2012). They use a terrestrial laser system for automated high-resolution tree volume estimation. Accordingly, this method has potential to improve the estimation of forest biomass in temperate forests and possibly in tropical forests, as well.

3.3 Monitoring of forest degradation

The identification of causes of deforestation and forest degradation, both direct causes and underlying causes, are of importance for all components of REDD+. Direct implications exist for definition of a forest reference (emission) level, and for development of an incentive scheme. However, indirect implications for the MRV-system arise, as well. Both Peres et al. (2006) and Wertz-Kanounnikoff and Verchot (2008) confirmed an impact of causes of forest degradation on monitoring feasibility. This means that for each cause of forest degradation, a suitable method for monitoring the specific AD and EF must be available, in order to estimate the total emissions from forest degradation within the scope of REDD+. Figure 4 and Figure 5 show two prominent causes of deforestation, i.e. seek for agricultural land and fire. While both these processes embody patterns of

deforestation that can be classified as “highly detectable” by present remote sensing devices, Peres et al. (2006) render, e.g. selective logging “marginally detectable” and understory forest practices “almost undetectable”. Moreover, they consider the detectability of the different causes classified as “marginally detectable” “expensive, technically challenging to implement and available only for limited or specific areas” (cf. Peres et al. (2006)). Herold et al. (2011) proactively proposed focusing present efforts on monitoring forest degradation based on the main causes that provoke the degradation of forest lands, i.e. selective logging, forest fires, over-exploitation of fuel wood, and mining.

The subsequent chapters of the present study focus on forest degradation patterns of selective logging within the scope of REDD+.

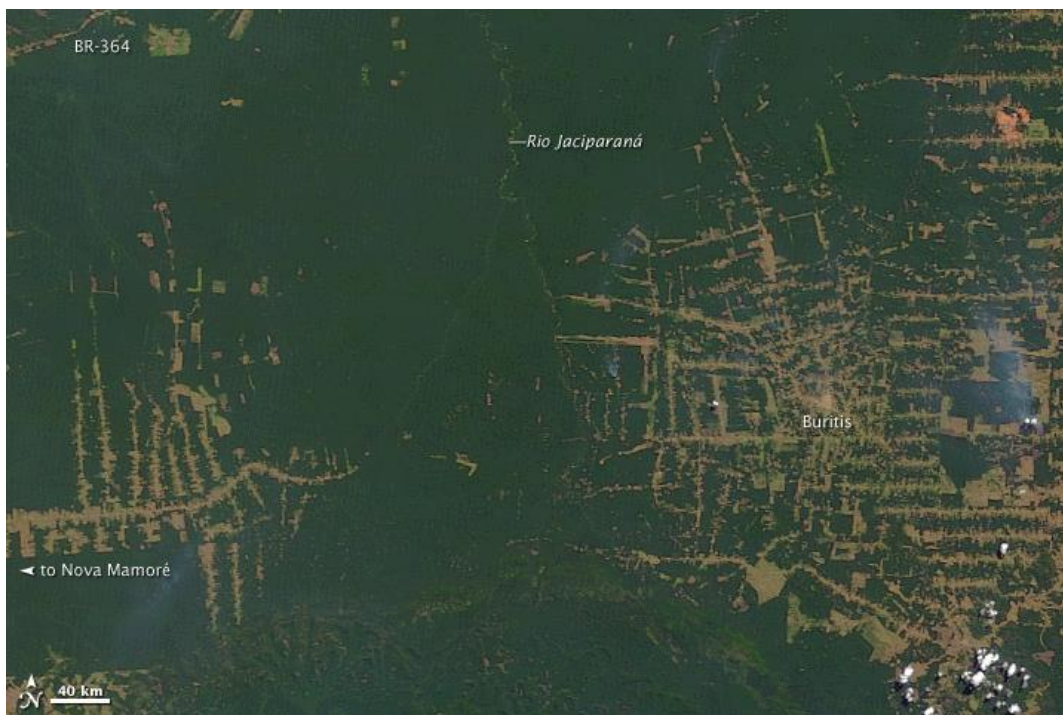


Figure 4: Deforestation patterns in the federal state of Rondônia in western Brazil; from NASA (2009).



Figure 5: Fire is commonly used to clear forested land in the tropics. An astronaut aboard the International Space Station captured this photograph of burning in Brazil on August 14, 2010; from NASA (2010).

3.3.1 Direct and in-direct methods

Methods that have been proposed to specifically monitor the emissions from forest degradation can be grouped into (i) direct and (ii) in-direct methods (Bucki et al., 2012; Gibbs et al., 2007; Goetz et al., 2009; Mollicone et al., 2007; Wertz-Kanounnikoff and Verchot, 2008). While (i) make use of directly addressing specific causes, (ii) use proxies like, e.g. proximity of settlements or roads (Bucki et al., 2012; GOF-C-GOLD, 2011), or stratification of forest lands into, e.g. intact and non-intact (Laestadius et al., 2011; Mollicone et al., 2007). Both groups, i.e. (i) and (ii), allow for the estimation of areas of forest degradation, however, the direct quantification of emissions from forest degradation can only be estimated using (i). The application of a stratification matrix allows for derived quantification of emissions from forest degradation (Bucki et al., 2012; Gibbs et al., 2007; Mollicone et al., 2007). Regarding the above described tiered approach of IPCC⁸ in-direct methods can deliver information for tier 1 and partly for tier 2, while a country applying for tier 3, without doubt, needs to implement

⁸ See 2.2 on page 4

direct methods (IPCC, 2003b, 2006). Groups (i) and (ii) can generally be complemented with the use of remote sensing data. In this respect, a multitude of hitherto existing experiences exist, some of which address the issue of forest degradation.

3.3.2 Remote sensing as an additional data source for monitoring forest degradation

Since the 1950s, remote sensing data has been acquired by a variety of airborne and space-borne sensors (Rosenqvist et al., 2003). Available remote sensing sensors can be classified into active and passive sensors. The latter are sometimes also called optical sensors.

For the fields of forestry Malingreau (1993) considered remote sensing applicable in the identification and analysis of forest lands, i.e. their location and size, and the level of human pressure visible through deforestation, fires and agroforestry.

Regarding the role of forests in climate change Rosenqvist et al. (2003) identified four key fields where remote sensing data could make significant contributions:

- Provision of systematic observations of relevant land cover;
- Support to the establishment of carbon stock baselines;
- Detection and spatial quantification of change in land cover;
- Quantification of aboveground vegetation biomass stocks and associated changes therein.

(cf. Rosenqvist et al. (2003))

In contrast to these positive views on the role of remote sensing within the scope of forestry in general, the perception of its role in operational applications for monitoring forest degradation is less enthusiastic. For the most part, the prevailing opinion published in literature on methods to monitor deforestation and forest degradation highlights that deforestation patterns are much more straightforward to detect than those of forest degradation (Achard et al., 2007; Achard et al., 2002; DeFries et al., 2007; Eliasch, 2008; Gibbs et al., 2007; Herold et al., 2011; Houghton, 2005; Köhl et al., 2009; Lambin, 1999; Lanly, 2003; Rosenqvist et al., 2003).

In 2003, Rosenqvist et al. (2003) provided a general review of remote sensing technology in support of the Kyoto Protocol, and gave insight into adequate remote sensing techniques. They evaluated forest degradation as generally more difficult to detect by remote sensing than deforestation, and expressed the need for longer time series of remote sensing data in this respect. Furthermore, Rosenqvist et al. (2003) highlighted the requirement for in situ data, meaning an integration of remote sensing technology in terrestrial inventory methods.

More specifically on forest degradation Houghton (2005) addressed that carbon stocks in forests may change without a change in forest area. Optical remote sensing data was assumed to rather detect changes in forest area and, however, fall short when “more subtle shifts in carbon stocks, especially after canopy closure” occur (cf. Houghton (2005)). DeFries et al. (2007) found that in some cases visual interpretation of high-resolution data can detect small-scale canopy damage. Furthermore, they recognized that for assessing the dynamics associated with forest degradation “annual monitoring may be needed” (cf. DeFries et al. (2007)). Similarly, Herold et al. (2011) saw this frequency of observations as a limiting factor, if methods for monitoring forest degradation use direct methods based on optical sensors.

In addition, Gibbs et al. (2007) considered unlikely for current optical sensors to detect all types of forest degradation without the application of innovative methods and ground-based observations. More specifically, Eliasch (2008) averred that “some types of degradation do not create gaps in the canopy”, e.g. activities in the understory vegetation layers. For this, he saw that “further research should be undertaken” (cf. Eliasch (2008)).

The quality of data from optical sensors depends on their spatial, spectral, radiometric and temporal resolutions. The wide set of optical remote sensing sensors and their specific characteristics have been classified by DeFries et al. (2007) for the particular needs of REDD. But the use of this classification is rather limited more to monitoring applications for deforestation than forest degradation.

Meneses-Tovar (2011) reported on positive results in a large-scale approach that used the Normalized Difference Vegetation Index (NDVI) as an indicator of forest degradation. However, NDVI being based on phenological analysis requires huge data bases and careful selection of remote sensing data.

Already in 2003 Rosenqvist et al. (2003) pointed out that space-borne Synthetic Aperture RADAR (SAR) data could be of use for detecting land cover change and quantifying canopy closure. Regarding such active remote sensing data, DeFries et al. (2007) saw opportunities in the use of RADAR data, as they “can potentially detect degradation”. Likewise, Saatchi et al. (2011) considered active sensors such as LiDAR (Light Detection And Ranging) and RADAR (Radio Detection And Ranging) suitable to estimate biomass at different spatial scales. Whereas Herold et al. (2011) rendered processes that affect only the forest understory undetectable through optical remote sensing, Baldauf et al. (2009) clarified the conceptual differences of passive and active remote sensing sensors. After this, passive sensors record reflections rather of the objects surface, the X- and C- Band of RADAR is sensitive to small twigs and leaves, and the L-Band with its long wavelength is reflected by larger structures. This circumstance allows RADAR- and LiDAR-data to show remote sensed information about the structures even beneath the forest canopy⁹. Further details on the technologies of RADAR and LiDAR are given in chapter 3.4.3¹⁰.

When reviewing practical experiences in using remote sensing as an additional data source for monitoring forest degradation, the detectability of forest degradation by remote sensing data has to be seen as a critical issue. Regarding the cost-efficiency of approaches including high temporal frequency, like annual monitoring, the cost for data procurement, image analysis and classification accuracies with respect to spectral, geometric and spatial image corrections can be obstacles for practical applications in national MRV-systems. Especially in natural forest stands in the tropics and subtropics, mostly characterized by contiguous canopy covers and heterogenic vertical stand

⁹ see Figure 15 on page 47

¹⁰ See 3.4.3, LiDAR and RADAR, on the pages 44ff

structures, the detection of forest degradation by optical remote sensing sensors can only be made operational, if the formerly closed canopy cover is dissolved (see Figure 6).

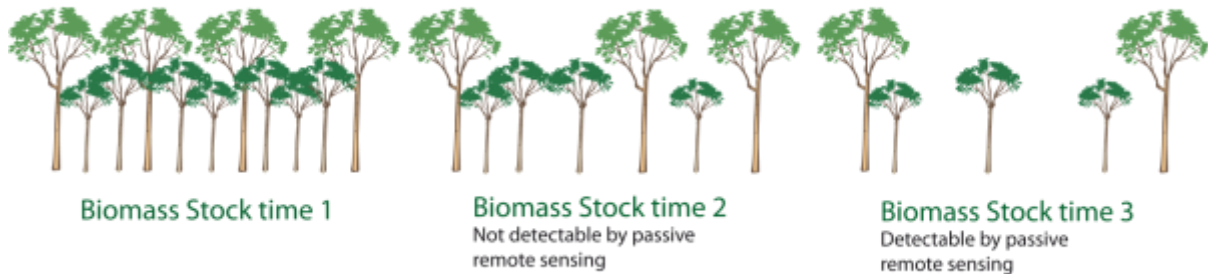


Figure 6: Different states of forest and forest degradation in terms of their biomass stocks, and the potential of detection by optical remote sensing techniques (left = undisturbed, middle = stealthy degradation, right = detectable degradation); from Baldauf et al. (2009).

In spite of the obstacles in monitoring forest degradation as described above, FAO (2011a) emphasized the need of policy makers and forest managers “to know where forest degradation is taking place, what causes it and how serious the impacts are” (cf. FAO (2011a)). All these issues are necessary to prioritize the allocation of finite human and financial resources used to counteract the process of forest degradation. Additionally, Bucki et al. (2012) identified the problematic issue that, if a country only monitors and reports on deforestation, harvesting patterns are adapted from clear-cutting towards unmonitored and unreported forest degradation. This however would have a dangerous influence on reaching the anticipated emissions reduction targets.

3.3.3 Error and uncertainty considerations

As already agreed upon by the Parties at the COP15 in Copenhagen in 2009, monitoring systems, that have to be established for REDD+ purposes, are to “Provide estimates that are transparent, consistent, as far as possible accurate, and that reduce uncertainties, taking into account national capabilities and capacities” (cf. Decision 4/CP.15, 1. (d) (ii) in UNFCCC (2010)).

Clear definitions of the above terms are specified in IPCC’s Good Practice Guidance of 2000 (IPCC, 2000) and IPCC’s Good Practice Guidelines of 2003 (IPCC, 2003b). In summary, transparency aims at facilitating replication and assessment of inventories, consistency refers to the use of equivalent

methodologies over a period of years. Accuracy is a measure employed to guarantee that results do not systematically neither over- nor underestimate true values. Uncertainty is a parameter associated with the results of measurements that comprises the dispersion of respective values originating from errors in inventory components.

Regarding these errors, estimation of AD and EF involve two major error types: sampling errors and non-sampling errors. Both of which can be summarized in a total survey error. Köhl et al. (2009) provided a valuable illustration on the theoretical composition of errors for a set of input data in respective surveys (see Figure 7).

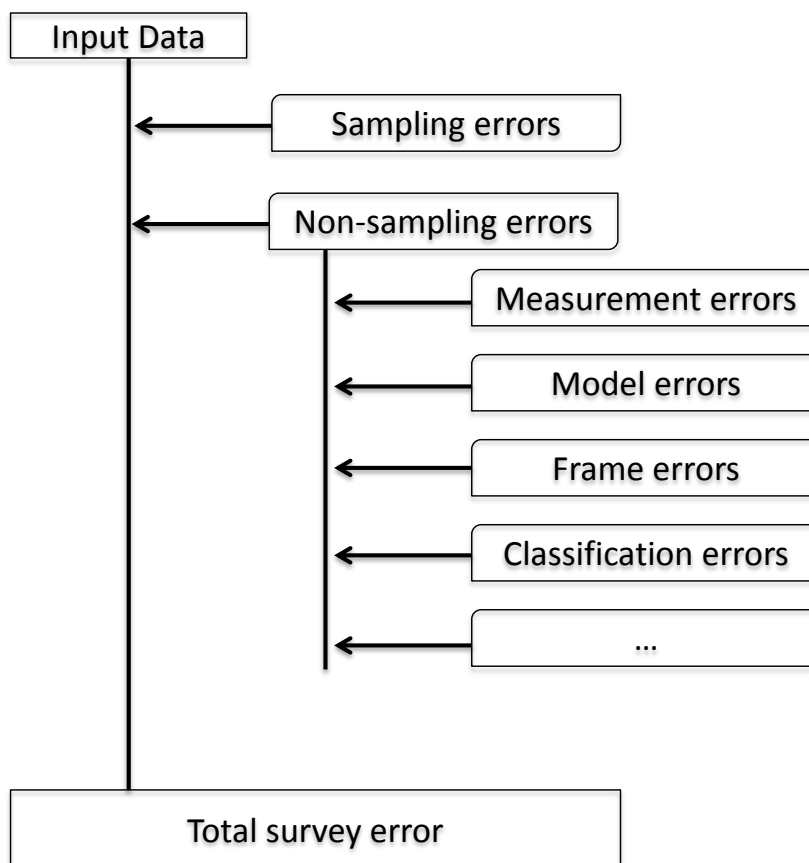


Figure 7: The composition of errors types and the total survey error; from Köhl et al. (2009).

Accordingly, Köhl et al. (2006) clarified that sampling errors arise from the circumstance that only a subset from a whole population is examined and the samples “may deviate from true population values” (cf. Köhl et al. (2006)). Both the sample size and the survey design can be used to control the size of sampling errors. Non-sampling errors embody all other sources of errors involved in a survey,

like, e.g. “faulty application of definitions, classification errors, measurement errors, errors arising from the application of functions and models, calculation errors, or frame errors” (cf. Köhl et al. (2009)). Köhl et al. (2006) concluded that the quantification of different types of errors can be realized by means of precision, accuracy, and bias. In this context, the difference of accuracy and precision is of further use and was most easily explained by Vanclay (2001) and adapted by Köhl et al. (2006).

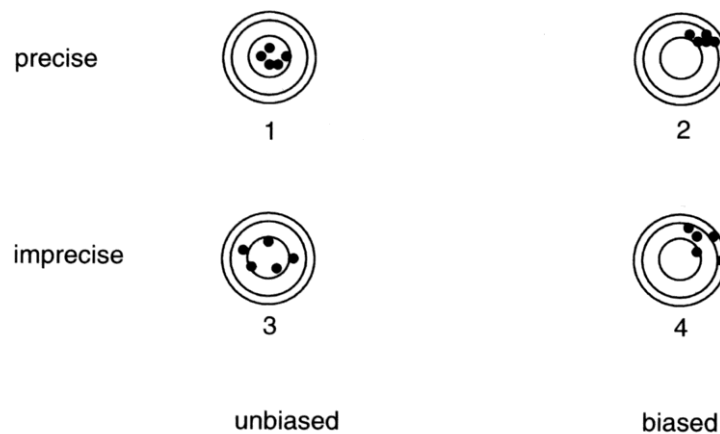


Figure 8: Theoretical examples for the concept of accuracy and precision of an estimator; from Köhl et al. (2006).

As a last definition of terms in these fields, bias is directly related to the accuracy of an estimate and refers to systematic errors that affect any sample with the same constant error.

From a statistic point of view these error and uncertainty considerations are “business-as-usual” (Congalton, 1991; Czaplewski, 2003; Köhl et al., 2006; Scott and Köhl, 1993) and their application within forest inventories and monitoring studies is beyond question. Henceforth, Patenaude et al. (2005) stated that cost in forest inventory is always related to meet specific requirements. Stehman and Czaplewski (1998) highlighted the design and analysis of accuracy assessment as “Fundamental Principles”. All three, Achard et al. (2007), Jones et al. (2004), and Eliasch (2008), emphasized the importance of accurate and precise estimates in forest inventories or specifically in greenhouse gas related forest assessments. However, in fields of climate change negotiations and REDD+ awareness for such sensitivities are not always guaranteed.

In an extensive pan-tropical study on monitoring of deforestation Achard et al. (2007) found that a main necessity in large-scale monitoring of deforestation is verification, i.e. that used methods are “reproducible, provide consistent results when applied at different times, and meet standards for assessment of accuracy” (cf. Achard et al. (2007)). As shown by Köhl et al. (2009) and also by Plugge et al. (2011) even small assessment errors are able to outweigh successful efforts to reduce deforestation and forest degradation. Thus, monitoring cost render important, as an MRV-system might be seen as an investment that aims to generate financial benefits (Köhl et al., 2011). Stern (2007), Wertz-Kanounnikoff and Verchot (2008), and van der Werf et al. (2009) together identified cost-effectiveness as an important issue in REDD+. Wertz-Kanounnikoff and Verchot (2008) even see “the quest for cost-effective solutions [...] at the centre of the MRV debate”.

Generally, methodological considerations on monitoring forest degradation involve a compromise between certainty and investment (Köhl et al., 2011). This circumstance adds further limitations in reporting on forest degradation to those obstacles of pure technical capacity to sense and record the qualitative change of forests as described in chapter 3.3.2.

Gibbs et al. (2007) listed benefits and limitations of different methods that are available to estimate national-level forest carbon stocks. More concrete, Goetz et al. (2009) realized a comparison of two methods for estimation of biomass densities by land cover types, and thereby estimated the impact of respective differences (see Table 1). For forest land cover types these differences show relative values between -79% and 81%. The huge differences between different methods that were used show the necessity of accuracy and error considerations.

Table 1: Land cover classes derived from the GLC2000¹¹, average AGB (tons ha⁻¹) derived from the two approaches "direct remote sensing" (DR) and "combine and assign" (CA). The column labeled Δ indicates the difference between approaches (CA-DR); (adapted from Goetz et al. (2009)).

Land cover types	DR [t/ha]	CA [t/ha]	Δ [t/ha]	Δ [%]
Closed evergreen lowland forest	216	274	57.2	21%
Degraded evergreen lowland forest	121	172	50.3	29%
Submontane forest (900 – 1500 m)	238	187	-51.4	-27%
Montane forest (>1500 m)	170	94.6	-75	-79%
Swamp forest	251	347	96.2	28%
Mangrove	48.3	101	52.6	52%
Mosaic Forest/Croplands	91.5	96.6	5.1	5%
Mosaic Forest/Savanna	77.4	91.9	14.5	16%
Closed deciduous forest	84.9	81.8	-3.1	-4%
Deciduous woodland	35.2	89.4	54.2	61%
Deciduous shrubland with sparse trees	11.5	61	49.5	81%
Open deciduous shrubland	12.8	61.6	48.8	79%

Murdiyarsa et al. (2008) addresses the high dependency of the cost of MRV-systems on national circumstances. Within a study on deforestation rates, Jones et al. (2004) plotted the total error against its corresponding quantification of change (see Figure 9). Decision lines in the graph give respective information on spatially explicit priority areas of actions. Furthermore, Böttcher et al. (2009) discussed the subject of opportunity costs that represent the most profitable "alternative land-use of the area under deforestation threat, including net revenue from the conversion itself" (cf. Böttcher et al. (2009)). In consequence Plugge et al. (2012) elaborated on country specific breakeven-points that define the optimal setting in terms of minimum error requirements of a forest inventory in relation to its specific costs.

¹¹ GLC2000 is a result from the Global Land Cover 2000 Project of the European Commission; for further details see JRC (2010)

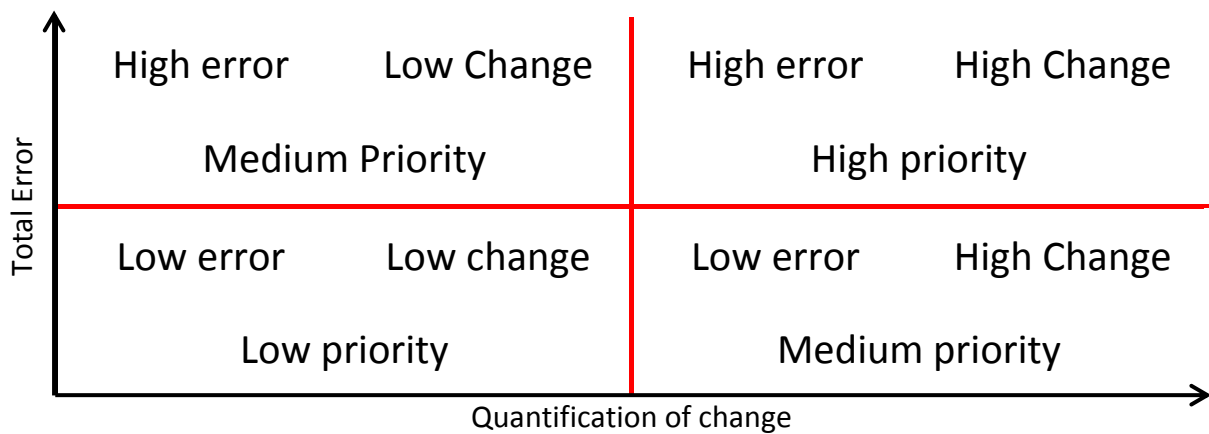


Figure 9: Total error is plotted against its corresponding quantification of change; The red lines indicate decision boundaries for priority areas of action due to the classes *High* and *Low*, for both errors and quantification of change; This results in priority areas of action: High Error / Low Change = Medium Update Priority; High Error / High Change = High Update Priority; Low Error / Low Change = Low Update Priority; Low Error / High Change = Medium Update Priority; adapted from Jones et al. (2004).

Grassi et al. (2008) proposed the use of the principle of conservativeness in order to "address the potential incompleteness and high uncertainties of REDD estimates" (cf. Grassi et al. (2008)) and sees both, uncertainties and incompleteness, obligatory for quantifying carbon stock changes in a REDD regime including the monitoring of forest degradation.

Already in 2003, the IPCC suggested in its GPG the use of the Reliable Minimum Estimate (RME) to address uncertainties (IPCC, 2003b). Introduced by Dawkins (1957) the RME is the minimum quantity to be expected with a given probability thus serving as a substitute for the lower bound of a confidence interval. Köhl et al. (2009) explained that the expansion of the principle of RME from an ordinary sampling error perspective to a concept of total survey errors would render possible the transfer to assessing forest carbon stock changes, and thus be used in reporting on forest degradation.

The involvement of remote sensing techniques requires special attention on uncertainties embedded in estimating changes between two points in time. Influences by map accuracies at both occasions

and the degree of changes exist. Fuller et al. (2003) presented a statistical approach providing quantification of the reliability of change estimates. Results of their study suggested that a sensitive detection of area changes by multi-temporal analysis of remote sensing data is rather unfeasible. On the contrary, Congalton and Green (2007) stated that present scientific methods and technical requirements exist that provide change detection approaches incorporating remote sensing technologies. Obviously, they propose to identify and quantify the sources of errors involved, and presented a respective theoretical example that seems rather complex (see Figure 10).

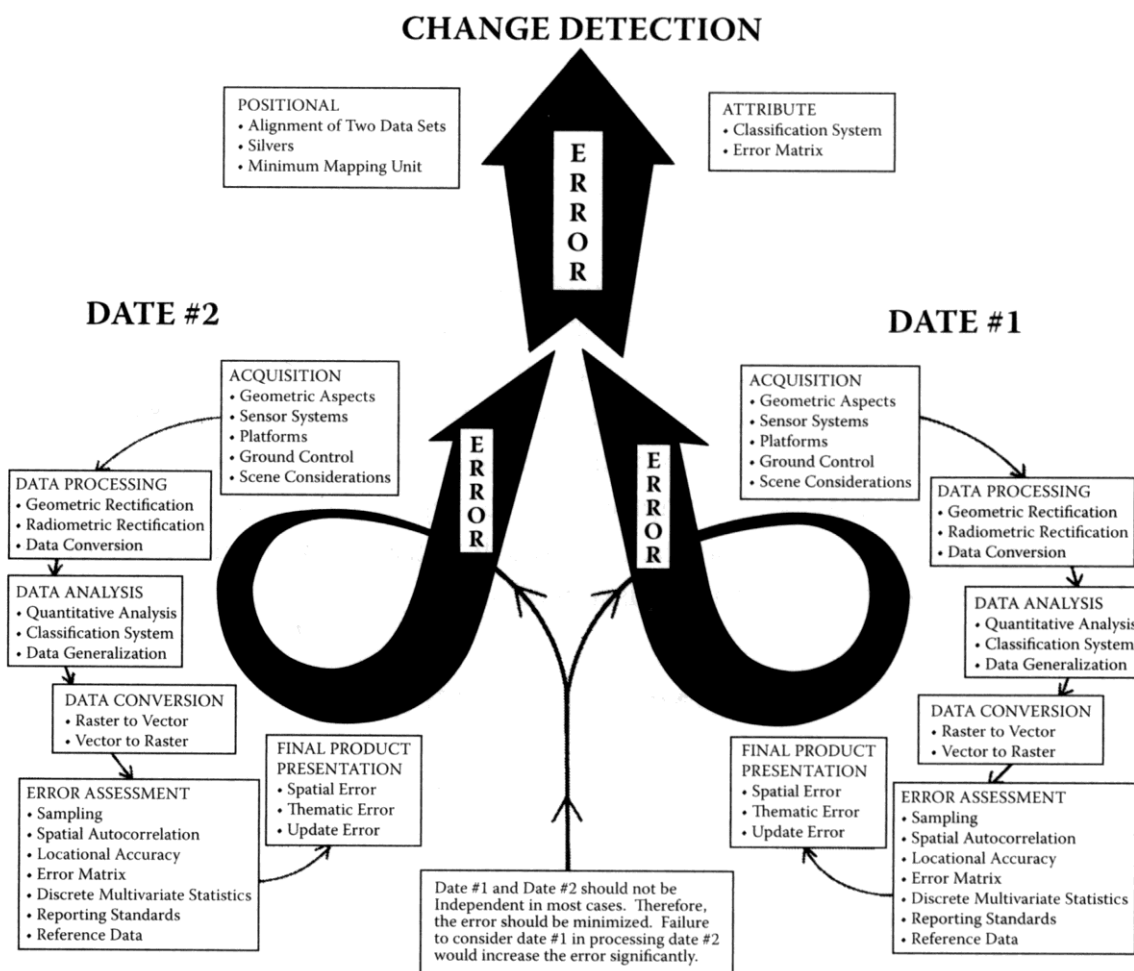


Figure 10: Error sources in a multi-date change detection analysis using remote sensing techniques; from Congalton and Green (2007).

Plugge et al. (2010) proposed a methodology that uses a top-down approach for the assessment of REDD activities and employs a bottom-up approach for aggregation of the emissions from deforestation and forest degradation including respective errors. The results of this integrated method showed that capabilities of producing reliable results on a national level exist.

Nevertheless, Köhl et al. (2011) observed the importance to include cost-efficiency aspects in the selection of the remote sensing alternatives to be used and concludes that special justification is needed “if expensive remote sensing alternatives are suggested” (cf. Köhl et al. (2011)).

To minimize error impacts, FAO (2011a) highlighted the need of further work on identification and description of appropriate criteria and indicators for measuring forest degradation (cf. FAO (2011a)). As such, Penman (2008) emphasized that further work on the proposed definition on forest degradation, i.e. the thresholds X years and Y% change and time T, “could take ages” (cf. Penman (2008)). In this respect, Plugge and Köhl (2012) explained the implication of uncertainties for both corresponding area and forest degradation intensities, i.e. Y% change.

As Köhl and Baldauf (2012) assured, methodological developments in active remote sensing technologies and in innovative change detection methods promise to overcome many deficiencies of former remote sensing systems, to open new perspectives for operational application, and to provide approaches for overcoming hitherto existing obstacles in monitoring forest degradation. Hence, further reviews of these methodological developments and of their application are shown in chapter 3.4.

3.4 Methodological developments

The following sub-chapters show important methodological developments in the three areas “change detection”, “object-based image analysis”, and “remote sensing sensor concepts”. All three form the basis of the present study, and are therefore reviewed with special emphasis.

3.4.1 Change detection

Detection of changes in remote sensing has a long history and is sometimes seen as one of its most successful applications (Anderson, 1977; Carmel et al., 2001; Singh, 1989). It involves the use of multi-temporal data sets to discriminate areas of change (Lillesand et al., 2004) or to identify differences in the state of an object or phenomenon (Singh, 1989) between dates of imaging. For both processes a variety of portfolios of methods exist (Canty, 2010; Coppin et al., 2004; Kennedy et al., 2009; Lu et al., 2004; Mas, 1999). Most of which can be grouped into algebraic methods, post-classification comparisons, principal components analyses, decision thresholds and unsupervised classifications of changes.

However, it must be clearly stated that all methods are subject to certain errors (Foody and Boyd, 1999). Carmel et al. (2001) identify two major sources of error, i.e. location error and classification error, with the used types of spatial data sets. Hence, van Oort (2007) proposes the use of the common error matrix for change detection, which has been refined by Congalton and Green (2007). This subject is covered in more detail in chapter 3.5.

For the field of forestry, Hame (1988) presented ways to interpret “forest changes from satellite scanner imagery”. In 2001, operational methods for tropical deforestation mapping were implemented (Achard et al., 2001; Hayes and Sader, 2001). The detection methods for vegetation or forest land cover changes, working with various vegetation indices, have been widely used for coarse to medium resolution data, e.g. for Moderate Resolution Imaging Spectroradiometer (MODIS) or SPOT 4’s VEGETATION sensor (Borak, 2000; Bucha and Stibig, 2008; Stibig and Bucha, 2005; Zhan et al., 2002), or for Landsat products (Hilker et al., 2009; Leckie et al., 2002; Sader et al., 2003; Santos et

al., 2008). Occurring disadvantages have been solved by specific model based approaches (Berberoglu and Akin, 2009; Chen et al., 2008; Im et al., 2007; Kennedy et al., 2009; Mayaux et al., 2005; Morisette et al., 1999).

Despite these achievements, not only the developments in the fields of sensor technologies, making available higher resolution remote sensing data¹² (Lillesand et al., 2004; Wulder and Franklin, 2003; Wulder et al., 2008), but also the request for further, medium to fine scale applications, as shown by Wulder and Franklin (2007), demanded different, more advanced digital change detection techniques that utilize, e.g., multivariate statistical approaches. These could also overcome past deficiencies, that were identified by, e.g., Fuller et al. (2003) when stating that the “measurement of small to medium scale changes over large areas requires levels of precision in mapping which are near impossible to achieve with satellite image classification alone” (cf. Fuller et al. (2003)). One of these promising approaches is Multivariate Alteration Detection (MAD). MAD is based on canonical correlation analysis¹³, which itself “measures the relationships between the observed values of two sets of variables” (cf. Clark (1975)). Canonical correlation analysis uses cross-covariance matrices for two sets of variables to find linear combinations of these sets, which have maximum correlation with each other. Clark (1975) detected that “canonical correlation analysis has received comparatively little attention” (cf. Clark (1975)) and listed relevant geographical studies using canonical correlation analysis. However, the concept was further improved and MAD was presented by Nielsen et al. (1998) in 1998 within the scope of change detection studies. Additional developments were realized by Coppin et al. (2004). At this time, MAD uses two sets of multivariate observations, e.g. digital image data assessed at two different points in time, and transforms them into a difference between linear combinations of the original variables.

GOFC-GOLD (2011) concludes that due to its superior features for land-cover change detection MAD deserves more attention in the future.

¹² The subjects of spatial resolution and scale level are further discussed in chapter 3.4.2.

¹³ Originally presented before the American Mathematical Society and the Institute of Mathematical Statisticians at September 12th, 1935 and published as “Relations between two sets of variates” (cf. Hotelling (1936))

3.4.2 Context and object based image analysis

Another important development is the use of methods involving context and object based image analysis (COBIA) for change detections. Fisher (1997) states that most traditional pixel-by-pixel image analysis and classification methods assume that real land cover can be perfectly represented by a number of quadratic pixels and furthermore these pixels form a homogeneous land surface.

In general, these methods examine the values of single pixels only in an isolated way disregarding the spatial neighborhood of each pixel. However, in the majority of cases a decision on the membership of a pixel to a class bears a consideration of the individual adjacencies. This applies to high resolution images in particular. As within these the desired data objects, like e.g. tree crowns, are composed of a number of pixels shaping separate sub-objects, and according to Guindon (1997) therefore require the consideration of their individual neighborhood. In this respect pure pixel based methods are limited. As a result of the above described problems conventional classification methods applied to high resolution data often leads to dispersed and isolated objects within the classification results. Stuckens et al. (2000) describes these pixels being differently classified than their neighbors with the term "Salt-and-Pepper effect". This effect can be attenuated by filters, but cannot be entirely avoided.

Bähr and Vögtle (2005) conclude that the considerable difference between conventional classification methods and object oriented ones is the work either with pixels or with object primitives, i.e. spectral homogenous regions, in order to define significant objects, which thereby play an important role in COBIA. Thus, methods using COBIA do not examine pixels in an isolated mode, but use the environment and observe the spatial neighborhood.

Figure 11 illustrates an exemplary workflow of a COBIA based method. Apart from processing steps, which are usually used in remote sensing approaches, Guindon (1997) additionally identifies two steps for COBIA based methods:

- Analysis of objects instead of isolated pixels through segmentation, i.e., segregating an image into spectral homogenous regions, and
- Image understanding, i.e., information about the inherent structural properties of real objects and their expected relationships.

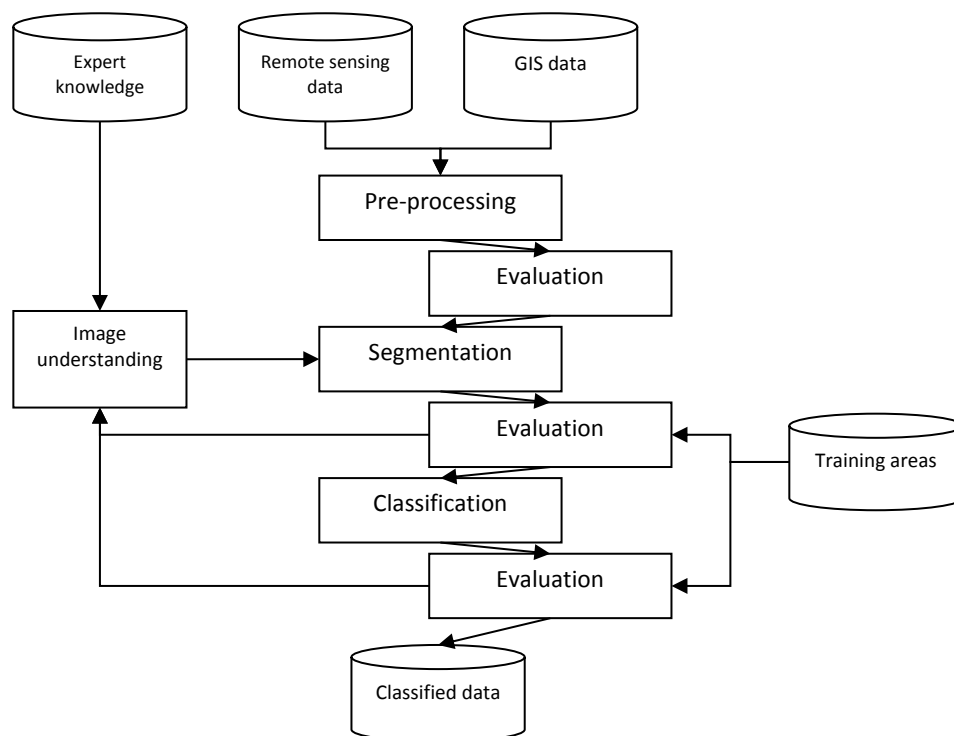


Figure 11: Exemplary workflow of a COBIA based method; adapted from Schiewe et al. (2001).

Blaschke (2010) delivers insight into a multitude of COBIA based studies on environmental monitoring from 2000 to the present. Object-level change detection (OLCD) instead of the traditional pixel-based algorithms was first introduced by Coppin et al. (2004) and Desclée et al. (2004). Nackaerts et al. (2005) presented an OLCD approach for forestry and Desclée et al. (2006) finds OLCD “to be very efficient to identify forest land cover changes” in temperate forests (cf. Desclée et al. (2006)). Bontemps et al. (2008) successfully applied OLCD with a multi-temporal segmentation

technique for the short period of only 3 years in combination with SPOT data in a tropical forest in Brazil based on findings of INPE (2006).

There exist several “ready to use” software solutions for COBIA purposes, e.g. ENVI FX’s Feature Extraction Tool, ERDAS’s IMAGINE Objective or Trimble’s eCognition®. The software eCognition® can be understood as a system containing a combination of the COBIA methods described above and providing a platform for among other things the development of OLCD-approaches. eCognition® which was used for this study.

Spatial resolution and scale level

Research, e.g. from Marceau and Hay (1999), typically showed that changes in spatial resolution of remote sensing data and scale directly influence the classification quality. In this context it is important to establish the term minimum mapping unit (MMU). It represents the smallest entity in an image that can be displayed as a discrete object and can be calculated by the squared length of the resolution of a data source. According to the sensor characteristics for Landsat Thematic Mapper 7¹⁴, this is 0.09 ha for QuickBird-2¹⁵ about 6m² for multispectral, and 0.4 m² for panchromatic data. In this regard, Herold (2011) sees a marked difference between the technically possible and the reality based upon the methods and techniques. This difference generally enlarges the MMUs. Different scales can considerably change the displayed land cover. Saura (2002) reveals that the larger the MMU, the more fragmented or sparsely distributed objects are repelled, and the more connected classes of a large area become dominant. This means that selecting a specific MMU directly influences the degree of detail of a classification and the complexity of an image. The verification of a correlation between scale and spatial variance of pixels was already shown by Woodcock and Strahler (1987) by contrasting the spatial resolution with the local variance in multiple tests. Thereby they were able to notify the highest possible level of information. As an example, the composition of a tree is represented by fewer pixels if the MMU is increased. At the same time, the probability that

¹⁴ Satellite with optical sensors with a highest multi-spectral spatial resolution of 30m. For further details see NASA (2012).

¹⁵ Satellite with optical sensors with a highest multi-spectral spatial resolution of 2.44m and a maximum panchromatic spatial resolution of about 0.6m. For further details see chapter 4.3.

these pixels bear a resemblance with adjacent ones decreases. According to Woodcock and Strahler (1987), this results in an enlargement of the variance.

As a conclusion, relevant objects for analysis can change dependent on the thematic background used to examine the data and the purpose of the data. However, objects being important for a research can be examined on different scales, at the same time. This could then be identified with the term “multi-scale approach”.

Segmentation

As briefly introduced above, segmentation processes images into homogenous regions, or so called image objects. Information on these image objects are mostly collected in a database. This information can be evaluated in the subsequent classification process, either rule based or through a statistical classifier. For this, the user employs semantic information, in order to improve image analysis. This information is characterized by meaningful image objects and their mutual relations. The process of segmenting can be realized by different approaches. Haralick and Shapiro (1985) differentiate six groups of segmentation methods:

- Measurement space guided spatial clustering:
Similar to an unsupervised classification or clustering method
- Single linkage region growing schemes:
Compares pixels with their neighbors, whereas similar ones are connected, i.e., region growing algorithm; Similarity is defined through the difference between two single pixels
- Hybrid linkage region growing schemes:
Compares pixels with their neighbors, whereas similar ones are connected, i.e. region growing algorithm; Similarity is defined through the difference between a number of pixels defining a vector of properties for each pixel
- Centroid linkage region growing schemes:
Region growing method that scans the image from starting points on, and compares pixel values with mean values of regions

- Spatial clustering:

Both histogram- and region growing methods are used to recognize peak values in the feature space, compare them with the nearest lower values, and possibly merge them to regions

- Split and merge schemes or Quadtree-method:

These split and merge schemes use the entire image as initial segment, which is then divided by the difference of pixel values; this process is repeated until only homogenous regions most of diverse sizes exist. Well-known is the Quadtree-method, which produces four segments per pass

Segmentation starts with pixel sized segments. The method fuses the segments through the appliance of criteria of homogeneity. This process is repeated until the heterogeneity of the segments is minimized, which is a condition that is defined through thresholds and parameters of tolerance at the beginning of segmentation through the user. The distribution of the starting points and the synchronized growing of the segments assure objects of comparable sizes. The formerly mentioned thresholds and parameters in the segmentation process define size and shape of desired objects by calculating the heterogeneity between adjacent pixels, where “Scale” is one main input parameter. In this respect, the “Scale” parameter is a theoretical, abstract term that controls the maximum allowed heterogeneity for the resulting image objects. This means that for rather heterogeneous data, the resulting image objects for a given scale parameter tend to be smaller than in more homogeneous data. Modifying the “Scale” parameter controls the size of the image objects. In addition to the “Shape” factor, which distinguishes the ratio between color and shape, and spatial properties, and which can be discriminated by the “Compactness” ratio, further variables are used to define homogeneity of object primitives.

Segmentation can also be used to derive meaningful image objects on different scale levels; in this case it is called multi-resolution segmentation. Multi-resolution segmentations are used, if subsequent classifications on various scales, like, e.g. change detection of forest degradation processes, need to be performed. The results of a multi-resolution segmentation are summarized in a

hierarchical network of inter-connected image objects. The image objects are made available through segmentation of different resolutions and characterize information on various scale levels. The modification of the value of tolerance alters the respective object primitives in the scale level. The connection of the image objects permits each object to recognize its neighbor, and its sub- and super- objects, i.e., the lower and higher scale level. Topology of the network guarantees that the borders are consistent, i.e., edges of image objects and their relevant sub- or super- objects correspond. A new level can be constructed on its sub- or super-objects, which are then fused or split based on the threshold for tolerance and on the criteria of homogeneity. An object database is created through the segmentation that consists of spectral characteristics.

Image understanding

The process of “Image understanding” generates information about the inherent structural properties of real objects and their expected relationships. In contrast to pure pixel based methods, information on size, shape, perimeter, and texture of each object are summarized in object databases. Furthermore, topology attributes and other spatial information, like, e.g., relationships to neighboring and relevant sub- or super- objects, can be included.

Information on image objects are generally applied to generate a body of rules defining object classes and are used in subsequent classification processes. As already shown in Figure 11¹⁶ this information is based on expert knowledge. The user describes and expresses this information through combinations of characteristics or even functions of characteristics. These expressions are developed either from one-dimensional membership-functions or from a minimum-distance classification of the nearest neighbor.

The first approach uses thresholds for memberships in the classification. Figure 12 shows a membership function, which generally spoken is showing the probability of an object belonging to a

¹⁶ See page 38

class. In other words: If the condition is fulfilled for an image object, it is assigned to the respective class. Functions can be associated among each other to improve the results of classifications.

The second approach renders a free definable, multi-dimensional feature space, being composed of object characteristics, and is used to describe and define object classes.

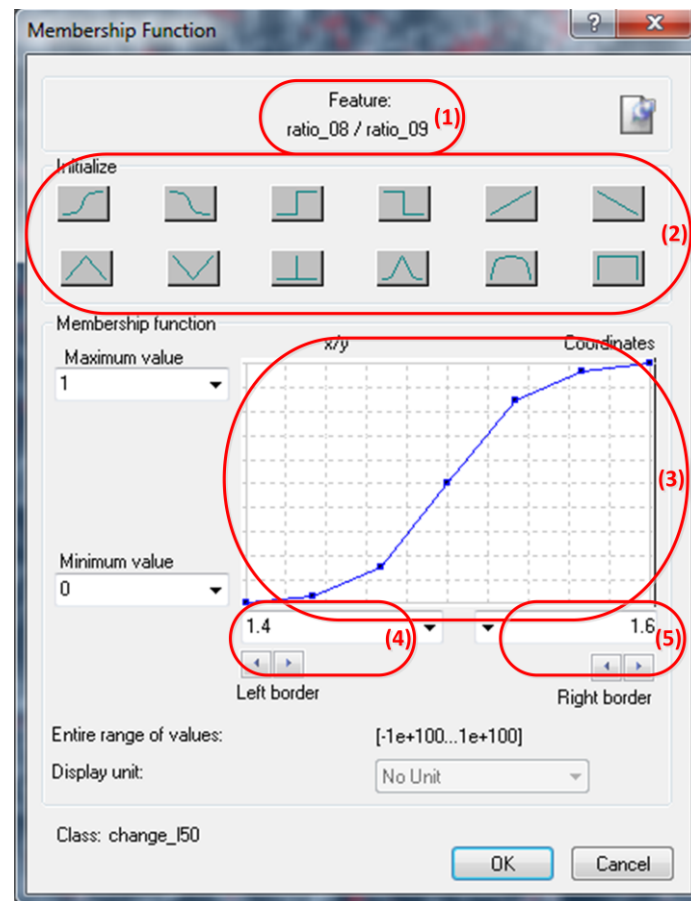


Figure 12: Example of a membership function dialog in eCognition®; the numbered red frames are: (1) name of the feature, (2) available types of membership functions, (3) used type of membership function, (4) left and (5) right thresholds.

In order to increase semantic flexibility in complex land cover categories, according to Binaghi et al. (1999), an exact definition and classification of objects to classes proves to be a hindrance. Another approach would be the technique of fuzzy-logic, where image objects can be classified with certain likelihood to a class. In order to distinguish the opposite of a class, e.g. “no change”, a method can be used, which is called “masking technique”. This technique assigns the likelihood of the class “change” using one or several certain thresholds, whereas the class “no change” can be defined by the

inverted function. A subsequent ranking process reassigns definite classes based on the aforementioned likelihood to particular objects for export of the classification results.

In conclusion, context and object based image analysis could provide image objects, which furthermore are used in an enhanced land-cover change detection approach based on multivariate alteration detection.

3.4.3 Remote sensing sensor concepts

A final field of essential methodological developments in the last two decades has lately gained increasing attention, i.e., different sensor concepts, in particularly those of active remote sensing systems. Active remote sensing systems utilize instruments that send a pulse of energy to the Earth's surface. Materials such as leaves, branches, stems and soil, reflect the energy pulse and this energy is received and recorded by the instrument. For the fields of forest applications, RADAR and LiDAR techniques have been described. LiDAR, also called laser scanning or laser altimeter, uses pulses of laser light while RADAR uses electromagnetic waves of different wavelengths. Aspired forest attributes are calculated from these data mainly by means of regression estimates.

LiDAR

The use of LiDAR has proven to be a valuable method for deriving forest stand characteristics relevant to forest management (see Figure 13). Particularly for estimating tree and canopy height for both forest stands and individual trees a reliable suite of techniques exist (Parker et al., 2004; Saatchi et al., 2011; Simard et al., 2008; St-Onge et al., 2008; Zhang and et al., 2008). Different studies report successful synergies of LiDAR and RADAR data to estimate forest biomass (Clark et al., 2011; Hyde et al., 2007; Næsset et al., 2011; Sun et al., 2011). However disadvantageous for operational applications of LiDAR remote sensing is, the fact that most LiDAR systems studied in the context of forest assessments are not space-borne, but instead flown at low altitudes. The Geoscience Laser Altimeter System (GLAS) instrument was once stationed aboard the Ice, Cloud, and land Elevation

(ICESat) satellite¹⁷, yet after seven years in orbit, ICESat's science mission ended due to the failure of its primary instrument (NSIDC, 2013), leaving its suitability for the detection of forest degradation unproven. On the whole, LiDAR data are costly for frequent data acquisition, and thus the suitability of airborne LiDAR systems for extensive areas is highly limited (Parker et al., 2004).

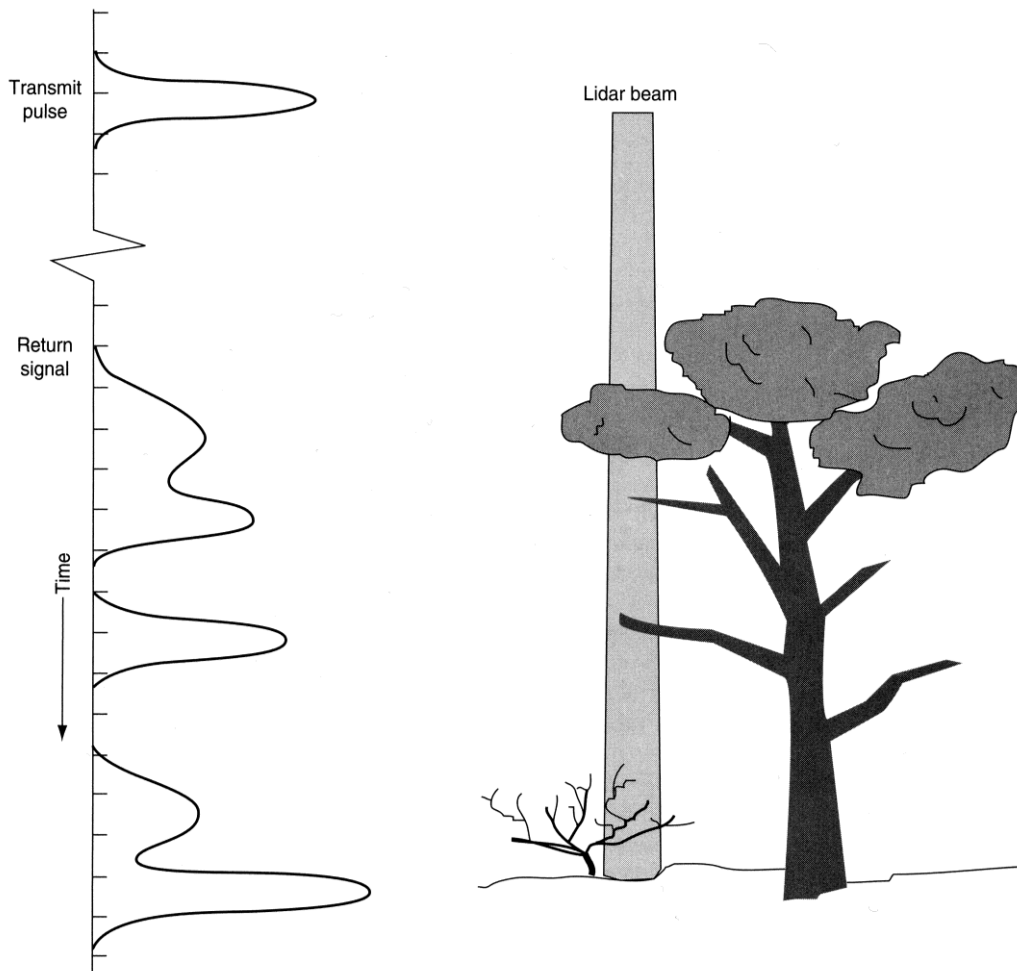


Figure 13: LiDAR pulse (here called Lidar beam) recording multiple returns as various surfaces of a forest canopy and soil are hit; from Lillesand et al. (2004).

RADAR

The potentials of imaging RADAR in ecological applications have already been reviewed by Kasischke et al. (1997). The wavelengths used with RADAR are about four to five orders of magnitude longer than those used in optical remote sensing (see Figure 14).

¹⁷ The ICESat satellite was launched by NASA (National Aeronautics and Space Administration) on January, 12th, 2003.

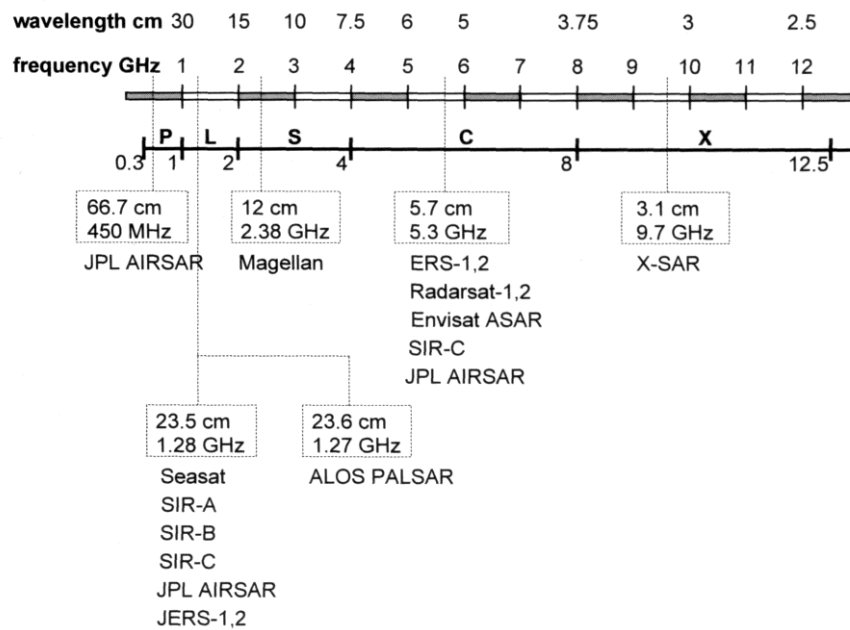


Figure 14: Spectral characteristics of common RADAR systems used in remote sensing; the systems are grouped regarding their respective wave bands L (23.5cm wavelength), S (12cm wavelength), C (5.7cm wavelength), and X (3.1cm wavelength); adapted from Richards (2009).

In contrast to optical sensors, which record reflections of the objects' surface, RADAR is sensitive to small twigs and leaves (X-and C-Band), and its long wavelength (L-Band) is only reflected by larger structures (see Figure 15). These conditions theoretically allow RADAR-data to provide information about structures beneath the forest canopy (Sun et al., 1991; Wulder and Franklin, 2003). Kasischke et al. (1997) showed that polarization of RADAR signals in a vertical (V) or a horizontal (H) direction, i.e., VV, VH, HV, or HH, is an additional feature of these sensors that can be used for accentuating the backscatter from objects with particular orientations, such as tree boles in recent clear-cuts. Furthermore, Luckman et al. (1998) describes the advantages of RADAR systems and their frequent application in the tropics and mountainous regions. Since the platforms carry their own active energy source and only few atmospheric constituents, i.e., no clouds or other air-borne particles, interfere with detection at the wavelengths used for RADAR remote sensing, they can be used at any time of day and under nearly any weather condition.

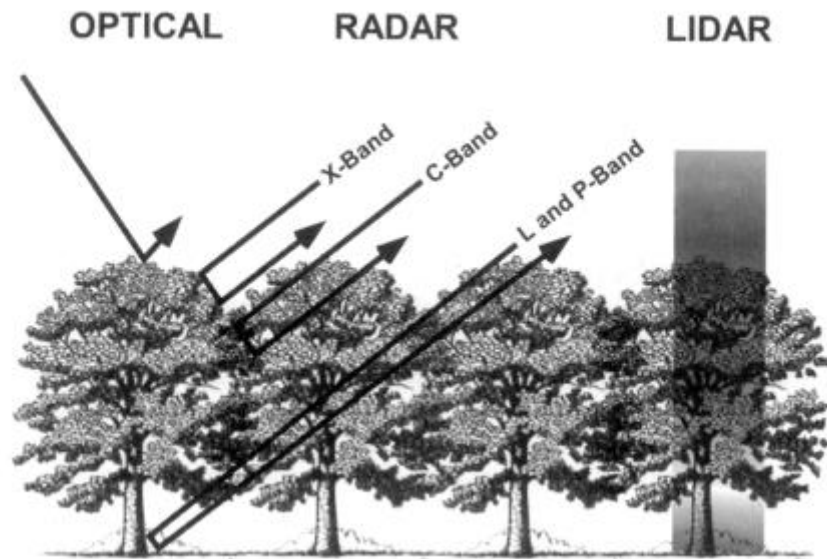


Figure 15: Conceptual differences of remote sensing technologies and their respective penetration depths into the forest canopy; from Lefsky and Cohen (2003).

Recent forest inventory experiments with profiling radar have shown to provide valuable data for stand-level forest inventories (Carleer and Wolff, 2004; Coops, 2002; Hyypä et al., 2000; Kugler et al., 2006; Wang and Dong, 1997). Neeff et al. (2003) provided a convincing basis for the monitoring of forest structure over huge areas at low cost using RADAR data.

SAR P-, L-, C-band and AGB

In addition to the above described RADAR characteristics, like e.g. the polarization, synthetic aperture RADAR (SAR) as a specific RADAR system parameter plays an important role in RADAR-based forest applications. In contrast to other imaging RADAR systems, Henderson and Lewis (1998) clarify that SAR "...preserves the inter-pulse phase structure of the received signals", which allows the parameterization for specific purposes. One of these is the ability to directly estimate and model forest biomass, which was shown in many studies in the 1990s that report the proportionality of the intensity in SAR images of the P-, L- and C-bands to the aboveground biomass of forest stands (Beaudoin et al., 1994; Bergen and Dobson, 1999; Foody et al., 1997; Kasischke et al., 1994; Le Toan et al., 1992; Luckman et al., 1998; Luckman et al., 1997; Ranson et al., 1997; Wang et al., 1995). This proportionality could be found by further studies in tropical forests, as well (Castel and et al., 2002;

Kuplich et al., 2000; Kuplich et al., 2005; Mitchard et al., 2009; Pulliainen et al., 2003; Romshoo and Shimada, 2001; Santos et al., 2003; Santos et al., 2006). Le Toan et al. (2004) and Neeff et al. (2005) used C- and L-Band of various SAR sensors, in order to model forest carbon budgets. In an interesting study Mitchard et al. (2011) tried to measure biomass changes due to deforestation in central Africa using multi-temporal L-band radar backscatter from ALOS¹⁸.

Biomass saturation level in RADAR data

In 1995, Imhoff (1995b) described the occurrence of the effect of saturation within RADAR data and stated “...the predictive capability of the relationships are not useful past certain biomass levels”, although the correlation coefficients were acceptable (cf. Imhoff (1995b)). He subsequently estimated the biomass saturation levels for the forest data of SAR C-band (20 tons/ha), L-band (40 tons/ha), and P-band (100 tons/ha) (cf. Imhoff (1995b)). Most of the aforementioned studies in this chapter perceived the same effect, but partly valued different absolute levels. On the whole, this effect negatively affects the application of the direct estimation of forest biomass for three out of five IPCC’s ecological zones of the tropical domain, i.e., dry, moist and rain forests, where on all four continents between 100 to 680 tons of dry matter per hectare aboveground biomass would be expected (IPCC, 2006).

A recent study showed that, among other things, the effect of saturation within RADAR data limits the use for direct forest biomass estimation within the scope of REDD+. The authors “believe it is at best unhelpful, [...] to suggest that radar intensity provides a direct measurement of forest aboveground biomass” (cf. Woodhouse et al. (2012)).

TerraSAR-X

In June 2007 the German radar satellite TerraSAR-X was launched to provide very high resolution X-band synthetic aperture radar data in three imaging modes for scientific and commercial purposes (DLR, 2005). Further details on TerraSAR-X are given in the Basic Product Specification Document by

¹⁸ Advanced Land Observing Satellite “Daichi” (ALOS) is a Japanese Earth observation satellite that carries an array type L-band SAR. For further details see JAXA (2012)

DLR (2010), and on its specific design in Pitz and Miller (2010). While initial studies concentrated on urban areas (Eineder et al., 2009; Esch et al., 2005; Roth et al., 2005), Baghdadi et al. (2008) and Leyk et al. (2002) demonstrated the sensitivity of TerraSAR-X data in environmental and forestry studies. Kuntz (2010) highlighted the potential of space borne SAR for monitoring tropical environments. Furthermore, Enghart et al. (2011) used TerraSAR-X data for direct biomass estimation and biomass regression modeling. The respective findings show the limitation of this method evoked by the saturation effect of X-Band radar signals at biomass values higher than 80t/ha, whereas others give reason to expect lower relevant values (Imhoff, 1995b; Luckman et al., 1997).

Change detection with RADAR

Apart from direct biomass estimation, Rosenqvist et al. (2003) views space-borne SAR data as a useful tool, for detecting land cover changes. They affirm that textural changes, such as burn scars, provoked by fire and causing substantial change to the structure of a forest, can be detected from SAR for several years after the incident. Texture-analysis methods on various SAR data were used to successfully identify deforestation patterns, even in tropical forests (Huang, 2008; Mesquita Jr. et al., 2008). Thiel et al. (2006) utilized multi-image segmentation and object-based classification of L-band SAR data for detection of deforestation.

Using TerraSAR-X data Baldauf and Köhl (2009) were able to detect harvesting of individual trees in a vast tropical forest land and concluded that this approach could be used for monitoring forest degradation purposes in tropical forests.

3.5 Error analysis strategies for change detection

Lillesand et al. (2004) considers classifications in general “not complete until its accuracy is assessed” (cf. Lillesand et al. (2004)).

Typically, studies using remote sensing focus the error analysis strategies on the comparison between results and reference data. It would be an enormous, and thus expensive, method to compare the classification results at every pixel with the reference basis, and thus render them impracticable on a large scale. Hence, such data can be acquired from sample areas, which Lillesand et al. (2004) describe as intended to be “representative, uniform land cover” being “withheld for the postclassification accuracy assessment” and consequently not implemented in the classification process. In this context, sampling can again be defined as the process of achieving information on an entire population by choosing single observations, where different statistical methods can be discerned. A register of statistically sound sampling techniques can be found in Köhl et al. (2006).

In most cases, the aforementioned comparison is realized using error matrices, where a comparison of the relationship between reference data and equivalent classification results is carried out in a category-by-category manner. The correctly categorized classes are aligned in the upper left to lower right diagonal of the error matrix, as to be seen in Figure 16.

		Count of sample points				Mapped area (ha)	
Map Classifier	Reference Classifier				Total	Estimated (100 sampled points)	Exact (all Map Objects in the GIS)
	Forest	Old- growth forest	Non- forest				
Forest	43	1	4		48	480,000	409,346
Old- growth forest	2	6	0		8	80,000	41,634
Non- forest	14	3	27		44	440,000	549,020
Total	59	10	31		100		
Estimated true area (ha)	590,000	100,000	310,000		1,000,000	1,000,000	1,000,000
Estimated overall accuracy: $(43+6+27)/100=76\%$							
Kappa: $[100 \cdot (43+6+27) - (59 \cdot 48 + 10 \cdot 8 + 31 \cdot 44)] / [100^2 - (59 \cdot 48 + 10 \cdot 8 + 31 \cdot 44)] = 0.58$							
	Estimated producer's accuracy				Estimated user's accuracy		
Forest	43/59=	73%			43/48=	90%	
Old-growth forest	6/10=	60%			6/8=	75%	
Non-forest	27/31=	87%			27/44=	61%	

Figure 16: Example for an error matrix; from (Czaplewski, 2003).

The errors that occurred in the classification can be grouped to omissions and commissions. The first refer to those pixels or image objects that are incorrectly classified in one category and are shown in the column fields which do not belong to the above mentioned diagonal. In contrast, commission errors describe pixels or image objects, which are classified as one class, but according to the reference data belong to another, and can respectively be seen in the non-diagonal row fractions. In addition, overall accuracy and the accuracies of the single classes are normally shown in an error matrix, as well. The producer's accuracy specifies, how well training areas are classified, and the user's accuracy indicates the probability of the actual representation of a classified pixel or image object to a class in reality.

According to Congalton and Green (2007) these three accuracy parameters can be established as follows:

$$\text{Overall accuracy: } OA = \frac{\sum_{k=1}^N a_{kk}}{\sum_{i,k=1}^N a_{ik}} \quad \text{Eq. (1)}$$

$$\text{Producer's accuracy: } PA(class_i) = \frac{a_{ii}}{\sum_{i=1}^N a_{ki}} \quad \text{Eq. (2)}$$

$$\text{User's accuracy: } UA(class_i) = \frac{a_{ii}}{\sum_{i=1}^N a_{ik}} \quad \text{Eq. (3)}$$

Along with the analysis through the error matrix, there are examinations of classification results by the Kappa index of accuracy that is described by Campbell (2007) as a scalar statistic quantifying the agreement between the reference and map classifiers in a multivariate error matrix. Definitions and notations for these accuracy parameters are explained by Magnussen (2009). Considering the errors of omission and errors of commission mentioned above, Congalton and Green (2007) sees the Kappa value as a review of the information of the error matrix. It catches a value of 0 to 1, whereas 0 shows no conformity, and 1 stands for full conformity. Czaplewski (2003) sees values of Kappa larger than 0.6 as an indication for good consistency in forestry research. Within the scope of these so called "hard classifiers", problems of evaluations may arise as they are unable to correctly represent nature's indistinct transitions. Foody (2002) states that, if pixels are assigned to just one class, it will be assumed, that an image consists of just pure, unmixed pixels. This, however, will not occur in most cases in the natural world.

The statistical evaluation of classification methods is illustrated in the above schemes of error analysis. However, soft classifiers such as the fuzzy approach produce classification results, which can only be exercised within these conventional methods after performing some additional processing,

e.g. after transferring the results of soft classifiers into distinct classes. This process is known as defuzzification and, according to Binaghi et al. (1999), comprises a high loss of information. An alternative can be adapting the method of error analysis to the characteristics of the soft classification. Binaghi et al. (1999) tried to estimate the accuracy of corresponding memberships between classification and reference data. This is realized by modifying the ordinary method in such way as to compare the degree of membership to a certain class with the reference data, resulting in the degree of correlation. In contrast, Trimble (2011) makes it possible to directly use the degree of membership to a class as quantification of error. The higher an object's degree of membership, the higher the object's assured classification. Additionally, the minimal and the maximal degree of membership and the mean value and standard deviation are calculated. Comparing the best with the second best membership expresses the severability of classes.

4 Data and methods

The illustration of the Caracaraí forest project, where the present study was carried out, forms the first step of this chapter. In a second step, both the in-situ data and the data from remote sensing that have been used in the study are described. Subsequently, explanations of the used methods follow, i.e., methods to detect forest degradation using RADAR, methods to identify influences of stand characteristics on the detection of forest degradation, and methods to quantify the accuracy of the results.

4.1 Caracaraí forest project

The project site is located in northern Brazil in the federal state Roraima. Roraima's landscape is indicated as Northern Amazonia, whereas the north-east is marked by savannas, and the south and the west are characterized by high forest cover proportion (see Figure 17). Evident periods of rain and dry seasons exist. Vast areas of Roraima's soils are degraded through extensive stock farming and continuous slash and burn. However, the project site was a restricted and controlled area without these effects.

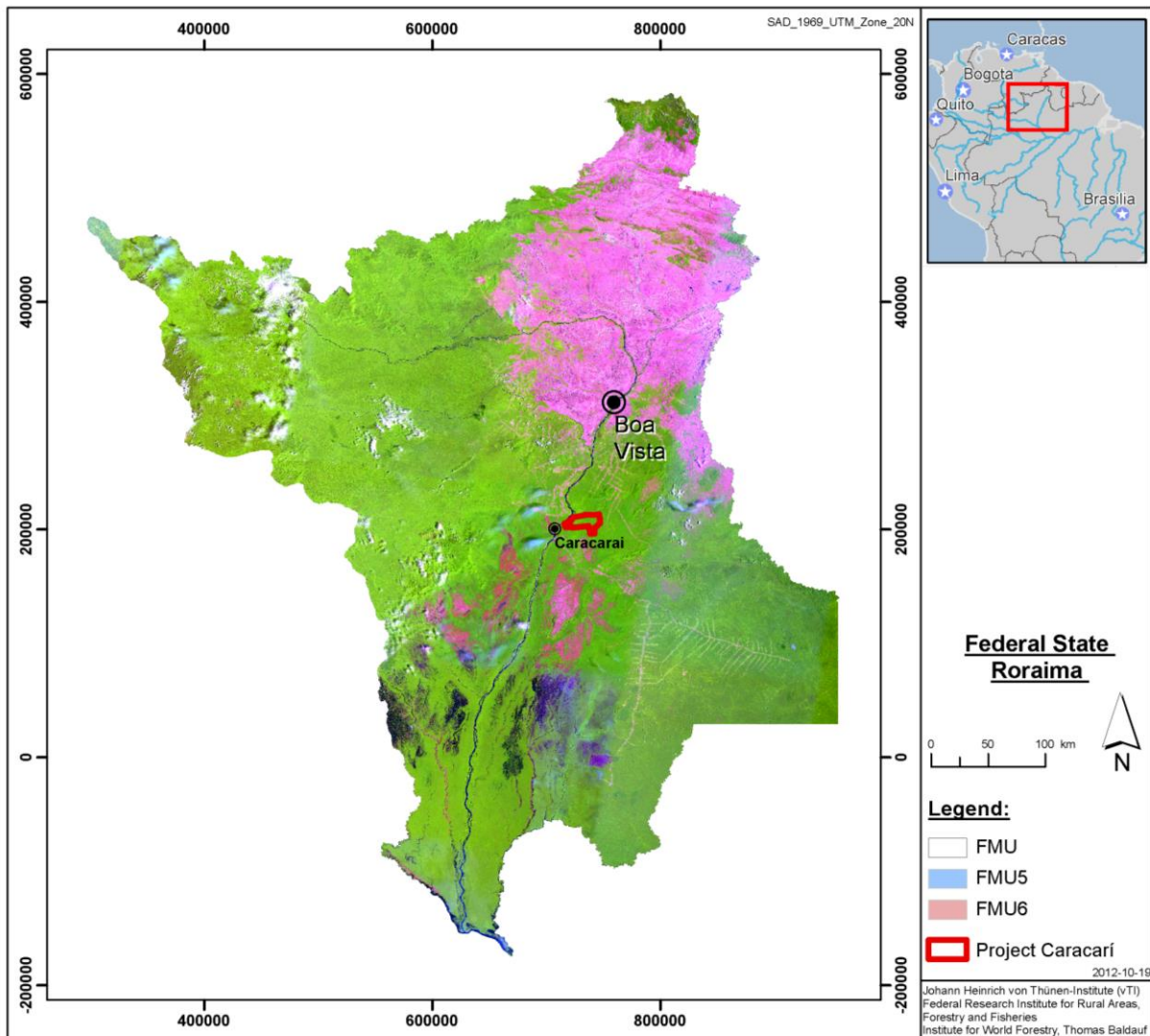


Figure 17: The map shows the federal state Roraima in Brazil. The capital Boa Vista and the municipal Caracará, where the project area (red outline) is located, are indicated on the map. In the background a Landsat7 ETM+ scene from 2004 is shown in false color. Green areas show forest lands, pink areas show deforested spots.

The project site, covered with approximately 30,000 ha of natural moist forests, is located about 130km to the south of Roraima’s capital Boa Vista near the city Caracará and is found on the Guyana Shield, an area that is part of a global biodiversity hotspot. Apart from some areas of clearing most of the project site is completely comprised of forests. Alongside streams the height above sea level is about 60m and ascends to 100m in the interior. Exceptions are some hills which hold an elevation of up to 280m. The vegetation can be denominated as “evergreen tropical lowland rainforest”, being a form of alternation between the rainforests of central Amazonia and the dry forests of northern

Roraima. Figure 18 shows the coarse outline of this forest area. There are no legal settlements within the boundaries of the project site.

The forest lands of the project are comprised in various Forest Management Units (FMU). The FMUs have been managed according to the principles of sustainable forest management, as defined by the Principles, Criteria, and Indicators for well-managed forests, developed by the Forest Stewardship Council (FSC, 2002) and holds the FSC certificate 'GFA-FM/COC-001250, 2008-01-18'. In this regard, Haas (2006) gives a detailed insight into past activities in the project area and the FMUs.

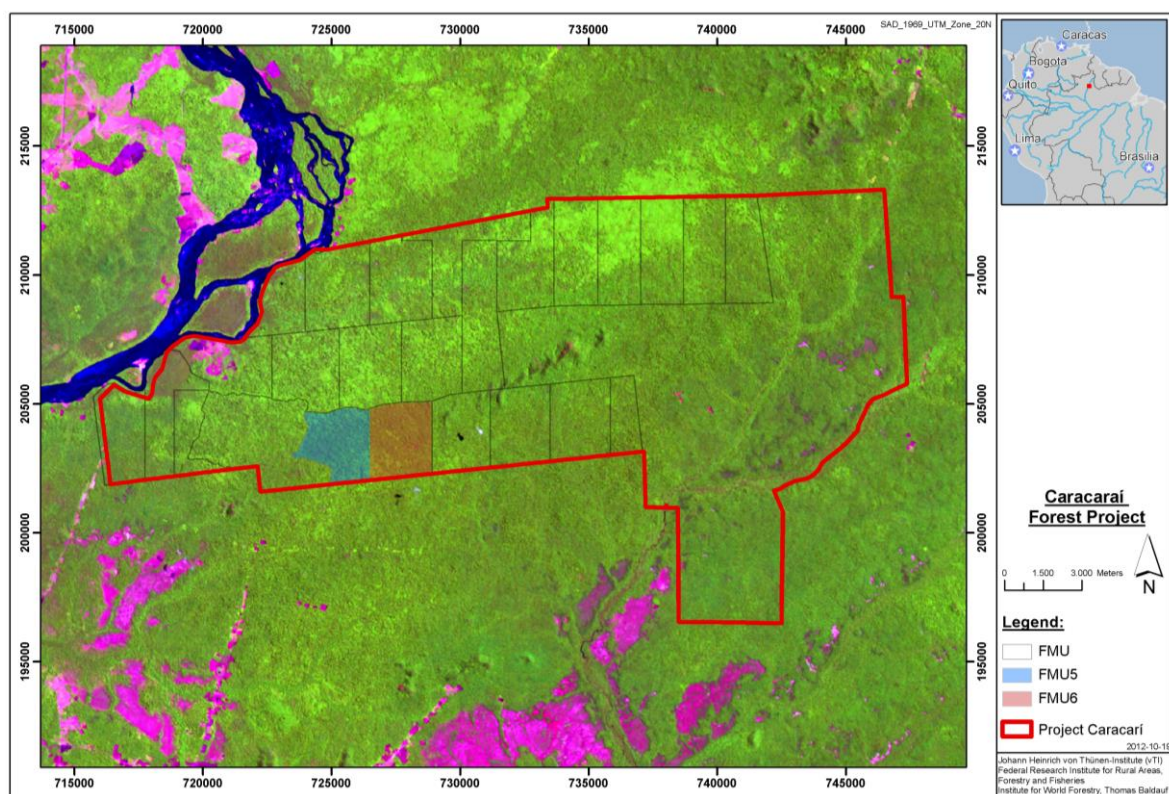


Figure 18: Map of the Caracará forest project; the red outline shows the coarse project area of about 30,000ha; the grey lines indicate the planned Forest Management Units (FMU). The FMUs 5 (light blue) and 6 (light red) have been used in this study. In the background a Landsat7 ETM+ scene from 2004 is shown in false color. Green areas show forest lands, pink areas show deforestation spots. In the upper left corner the Caracará forest project directly adjoins the stream *Rio Branco* (dark blue).

4.2 Data from in-situ assessment

In 2004 and 2005, Haas and Glauner (2005) conducted an initial, coarse forest inventory, identifying 334 tree species, belonging to 54 families and 135 genera. Ten compartments were established, covering an area of 17,303 ha. Starting in 2006 detailed inventories were made as a total tally of each of the compartments, and these were further compiled to annual operational plans, e.g. for the FMUs 5 and 6 in the season 2008 (Haas, 2009c). These plans show inventory data of the in-situ assessments that include tree specific spatial information, tree species, and dendrometric data, such as dbh, height and crown parameters. Furthermore, auxiliary data on the quality of the trees, and the structure and status of the forest and its topographic characteristics as well as on possible human induced impacts were collected.



Figure 19: Photo of an example for the durable unique identification on a tree bole for the tree number “002838”.

The inventory system was developed by Haas (2007) and consists of squares of 50m by 50m across the whole compartment, in which all trees, i.e., large emergent trees, medium sized trees and understory trees with a dbh of at least 35cm, are taken into account and are marked with a durable

unique identification (see Figure 19). The design of the inventory system as a total tally of the inventory area allows a geographic localization of each of the 48,141 trees in the FMUs 5 and 6. Figure 20 shows a map excerpt of the inventory system applied. Further specific details of the inventory methodology are described in Haas (2007).

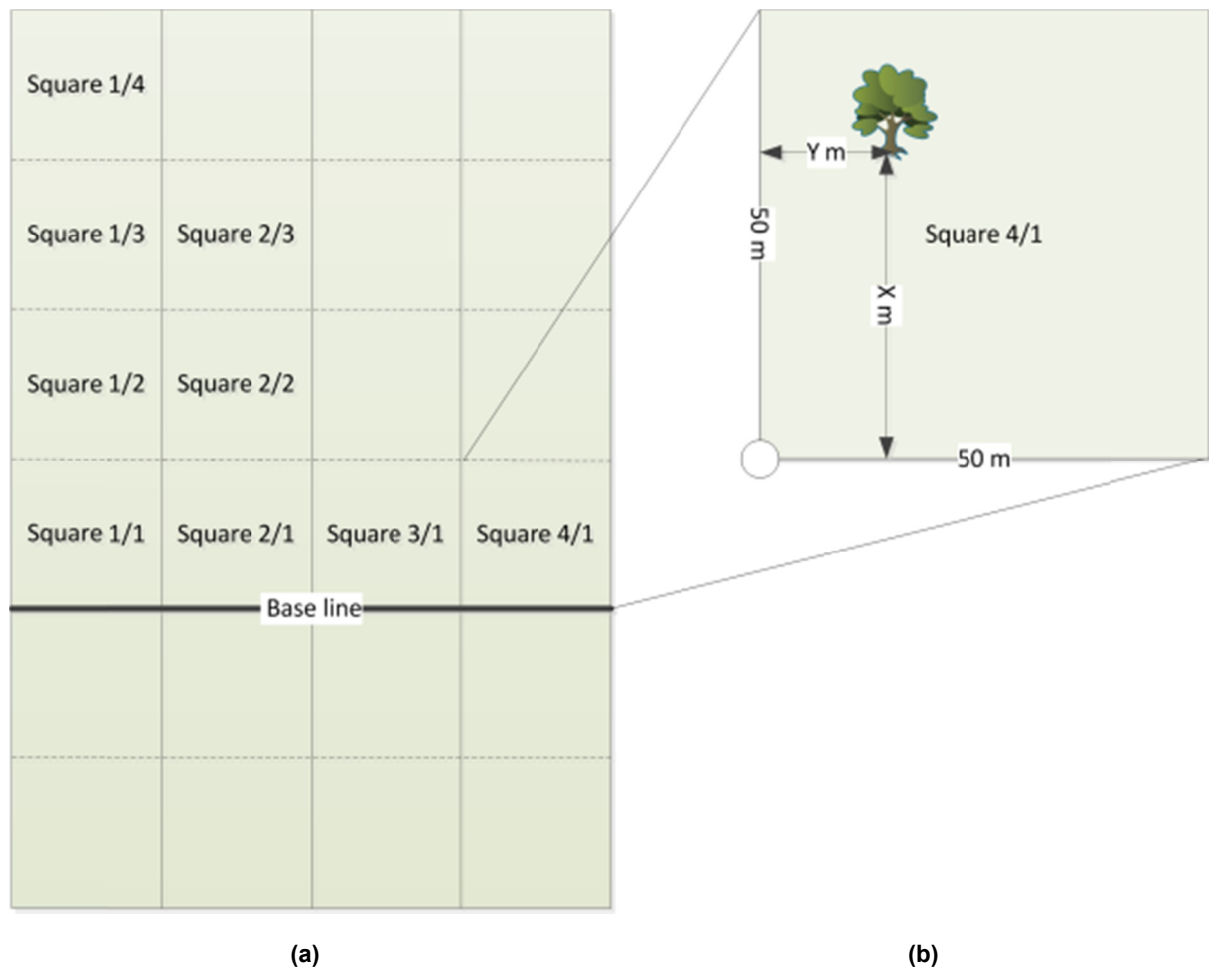


Figure 20: Design of the inventory system; (a) a systematic grid of 50m by 50m was constructed along a horizontal “Base line”. The resulting rows and columns form the grid cells that can be seen in the above figure. The grid cells were named due to their rows and columns in numerical order; (b) shows the localization of an exemplary tree in respect to the dot grid point (circle, ○) of the respective grid cell.

In 2006, a forest management plan for the project was assembled that specifies the planning for the sustainable forest management (Haas, 2006). In this manner, in parts of one of ten compartments reduced impact logging was realized between 2007 and 2008. This area has been used in this study. As a consequence of the logging a number of 5,663 trees were logged in an area of about 1,585ha in

the FMUs 5 and 6 (Haas, 2009a). Data on the chain of custody (Haas, 2009b) and the tree specific identifications, as shown in Figure 19, allowed for a detailed spatial planning and reconstruction of the locations of all the trees, i.e., 42,478 remaining trees and 5,663 harvested trees, in a Geographic Information System (GIS) (see Figure 21). During the logging process relevant parts of the tree, i.e., stump and all parts of the tree bole, were marked with the same identification as was done within the inventory (see Figure 19). This allowed cross-validation of the felled trees as they were being hauled away.

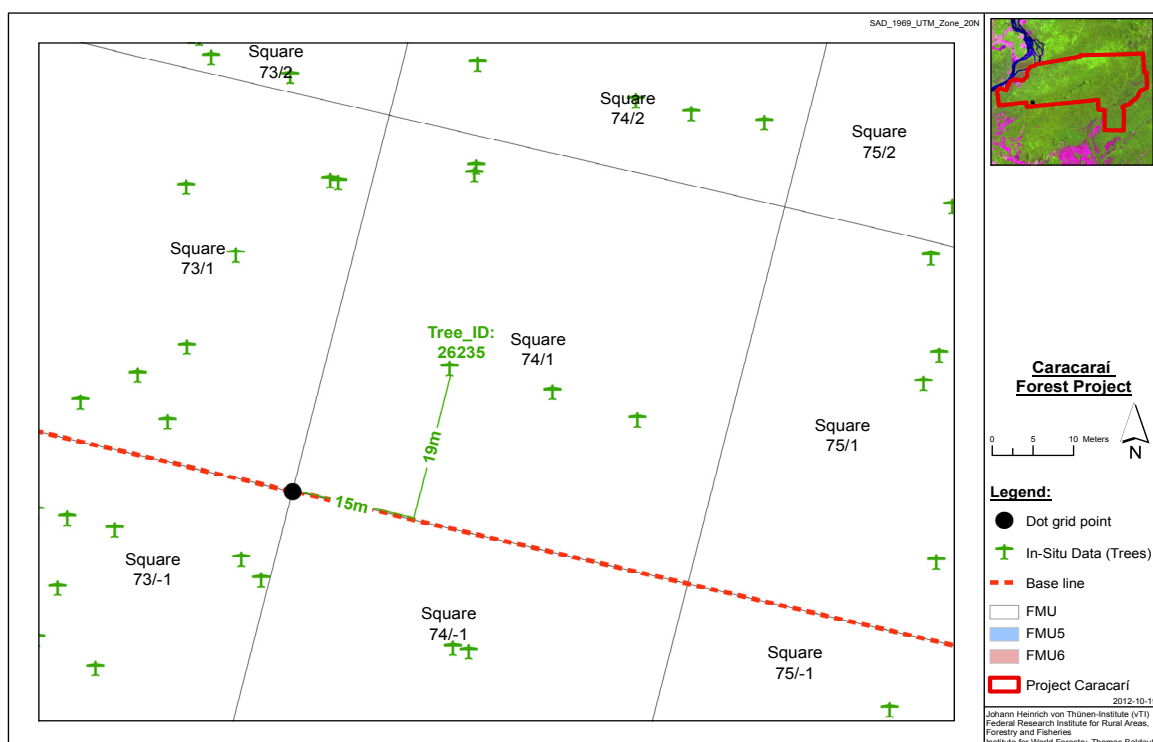


Figure 21: Map showing the distribution of trees (green) inside the squares (grey) next to the Base line (dashed red line) within the project area; exemplary the referencing of a tree (Tree_ID= 26235) in respect to the dot grid point (15m east, 19m north) of the Square 74/1 is illustrated.

4.3 Data from remote sensing

Various remote sensing datasets of the area of investigation were available in the project. In the study the following three remote sensing datasets have been used (i) panchromatic Quickbird-2 data from 2004 (see Table 2 and Figure 22), (ii) TerraSAR-X data from 2008 and (iii) TerraSAR-X data from 2009 (see Table 3, Figure 23 and Figure 24).

Metadata on Quickbird-2 data

Table 2: Metadata on panchromatic Quickbird-2 data; Metadata is roughly describing significant facts about the QuickBird-2 satellite scene delivered by DigitalGlobe®.

Dataset (i): Panchromatic Quickbird-2 data		
Acquisition date	18.03.2004	
Cloud cover	5%	
Catalog ID	1010010002CA8201	
Spatial resolution	0.64 meters	
Environmental quality	90 - Excellent	
OFF-NADIR	14 degrees	
Image Location		
Vertex	Latitude	Longitude
southwest	1,8036	-61,0709
northwest	1,9539	-61,0707
northeast	1,9517	-60,9108
southeast	1,8026	-60,9104
center	1.878	-60,9907



Figure 22: Map showing the obtained QuickBird-2 image in the west; the red outline shows the coarse project area.

Metadata on TerraSAR-X data

Table 3: Metadata on the two TerraSAR-X datasets; Metadata is roughly describing significant facts about the TerraSAR-X satellite scenes delivered by Infoterra/Astrium GmbH.

	Dataset (ii): „TerraSAR-X 2008“¹⁹		Dataset (iii): „TerraSAR-X 2009“²⁰	
Acquisition	20.04.2008 09:48:40		17.08.2009 09:48:51	
itemName	Level 1B Product		Level 1B Product	
missionInfo	mission: TSX-1 orbitDirection: DESCENDING		mission: TSX-1 orbitDirection: DESCENDING	
acquisitionInfo	sensor: SAR imagingMode: HS lookDirection: RIGHT antennaReceiveConfiguration: SRA polarisationMode: SINGLE polLayer: VV elevationBeamConfiguration: spot_064 imagingMode: spotLight		sensor: SAR imagingMode: HS lookDirection: RIGHT antennaReceiveConfiguration: SRA polarisationMode: SINGLE polLayer: VV elevationBeamConfiguration: spot_064 imagingMode: spotLight	
productVariantInfo	productType: EEC_SE_HS_S productVariant: EEC projection: MAP mapProjection: UTM resolutionVariant: SE radiometricCorrection: CALIBRATED		productType: EEC_SE_HS_S productVariant: EEC projection: MAP mapProjection: UTM resolutionVariant: SE radiometricCorrection: CALIBRATED	
imageDataInfo	imageDataDepth: 16		imageDataDepth: 16	
sceneInfo	sceneID: C29_N35_D_HS_spot_064_R_2008-04- 20T09:48:40.441944Z		sceneID: C73_N35_D_HS_spot_064_R_2009-08- 17T09:48:51.625996Z	
Image Location	sceneCoords		sceneCoords	
	Latitude	Longitude	Latitude	Longitude
southwest	1,853	-60,910	1,852	-60,912
northwest	1,872	-61,009	1,872	-61,010
northeast	1,825	-61,018	1,825	-61,019
southeast	1,806	-60,919	1,806	-60,921
center	1,839	-60,965	1,839	-60,966

¹⁹ See 9.2 on page 149 for further detail

²⁰ See 9.3 on page 149 for further detail

In the following, the dataset (ii) is named “*TerraSAR-X 2008*”, and the dataset (iii) is named “*TerraSAR-X 2009*”.

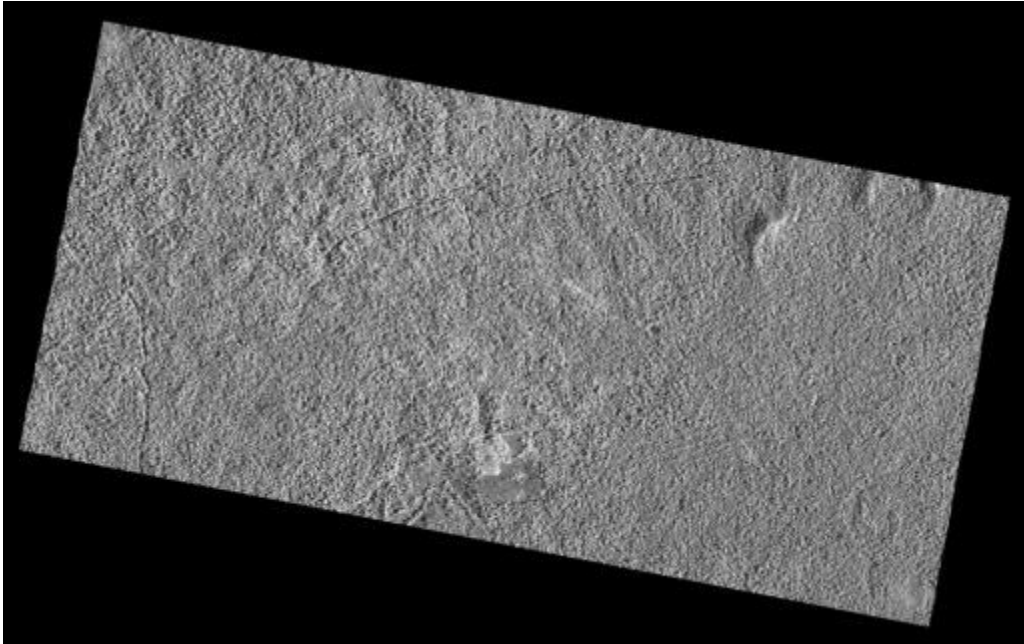


Figure 23: Data set (ii); TerraSAR-X data from 2008, *TerraSAR-X 2008*.

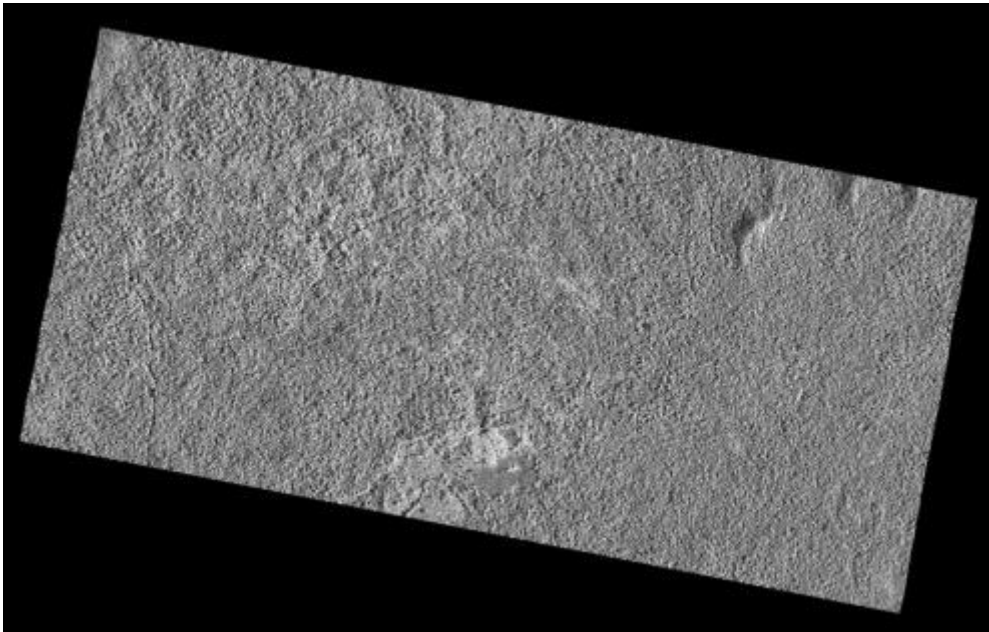


Figure 24: Data set (iii); TerraSAR-X data from 2009, *TerraSAR-X 2009*:

4.4 Methods to detect forest degradation using RADAR

In the present study contributions to scientifically sound and operational methods for reporting on forest degradation within the scope of REDD+ are developed. Chapter 3.1 identifies selective logging as a major cause of forest degradation. Simultaneously, selective logging entails the slightest disturbance per unit of area of all causes of forest degradation listed in chapter 3.1. Chapter 3.3 showed that some approaches for reporting on forest degradation exist; however, sound and operational methods incorporating the detection of spatial patterns of selective logging are non-existent, yet. Consequently, in chapter 4.4 methods are developed to detect spatial patterns of selective logging as forest degradation in tropical moist forests using high-resolution RADAR data. Figure 39 on page 148 shows a flowchart identifying the single methodological processes of the four objectives to verify the hypothesis of the present study.

4.4.1 Pre-processing stages

In April 2010 intense fieldwork was carried out, in order to co-register both the three sets of remote sensing data and the in-situ assessment data. It was possible to use the design of the inventory by Haas (2006), and perform a re-measurement of relevant identifiable spots within the inventory area. For this re-measurement a high-accuracy global positioning system (GPS), the Trimble GeoExplorer XH with an external Zephyr antenna, was used. This setting theoretically allows for a location accuracy of decimeters. However, in most cases this value cannot be achieved in tropical forests especially under tree crowns. Regarding the objective of the study, a location accuracy of less than two meters was seen as sufficient and could be reached for each ground-control point (GCP). Careful planning based on expected values of positional dilution of precision (PDOP) for each measurement session proved valuable. The PDOP value is a numerical measure for the theoretical, possible error in the accuracy of the GPS's position to specify the additional multiplicative effect of GPS satellites geometry (Pawlowicz, 2007). PDOP values from 1 to 5 theoretically may produce good results; higher values are of limited use only. In this manner, 16 GCPs, each with a PDOP value lower than 4, were used for an affine transformation process for co-registration of the above named four data sets, i.e.

the two TerraSAR-X scenes, the Quickbird2 scene and the in-situ data. As the RADAR data sets are syndetic co-registered, they could be taken as spatial registration basis.

Apart from these spatial corrections, atmospheric correction can be necessary (Kennedy et al., 2009; Tomppo et al., 2008; Vermote et al., 1994). Although according to inter-alia Song et al. (2001) optical remote sensing data can be affected by atmospheric effects, no respective correction was carried-out. This was due to the fact that the optical data was only used for visual interpretations, which could be performed without any limitation.

A bi-temporal stack of the above described TerraSAR-X scenes, i.e. *TerraSAR-X 2008* and *TerraSAR-X 2009*, was generated (see Figure 25). Thus, the two scenes *TerraSAR-X 2008* and *TerraSAR-X 2009* are incorporated in one image stack as two bands. This was accomplished in ERDAS IMAGINE and realized in order to facilitate the subsequent processes of the context based image analysis including the development of an object-level change detection method. These two processes were completed using the software eCognition²¹. This product can be understood as a system containing a combination of diverse methods, both iterative manual and automated ones, of image understanding. The software uses information implemented in semantics, in order to improve image analysis. Meaningful image objects and their mutual relations characterize this information. For each of these objects, information is collected in a database, and can be evaluated either rule based or through a statistical classifier.

²¹ The versions that were used are Definiens® eCognition® Developer 8, Definiens eCognition Developer 8.64, and Trimble eCognition Developer 8.7 64bit.

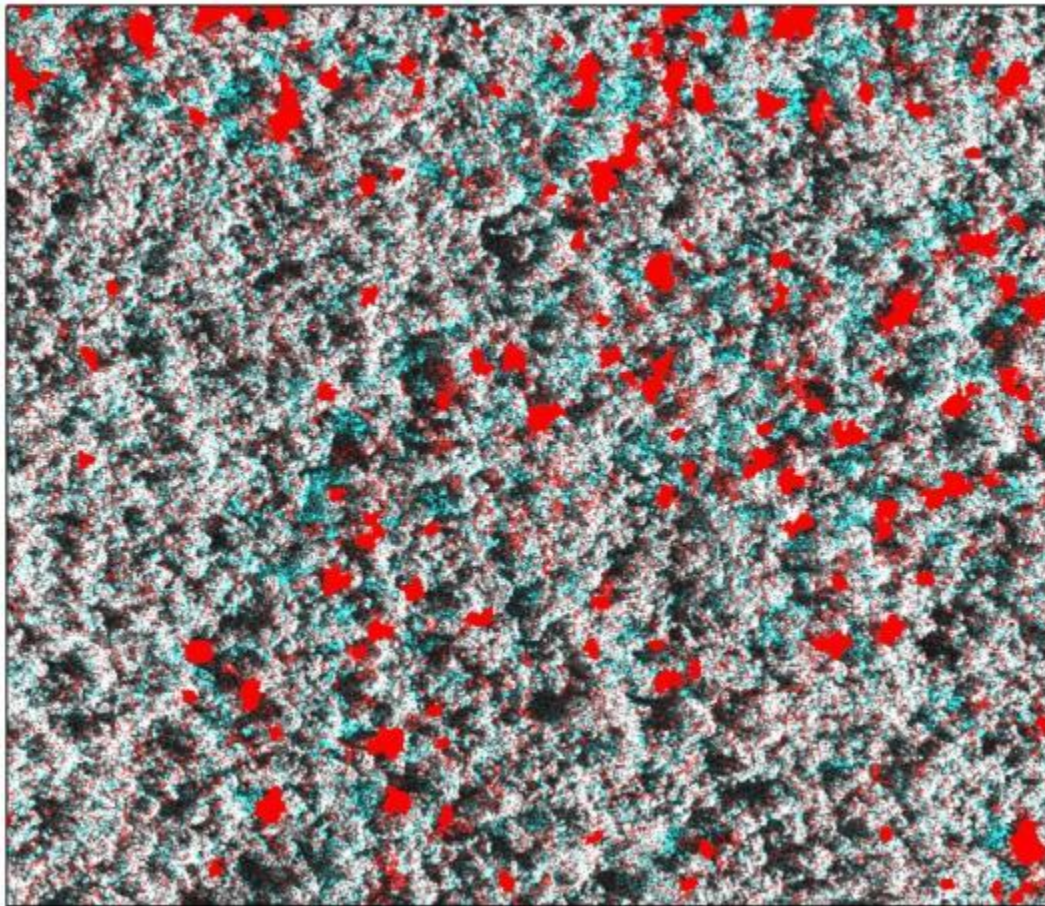


Figure 25: Example of the bi-temporal stack of the TerraSAR-X scenes: *TerraSAR-X 2008* and *TerraSAR-X 2009*; The stack is displayed as RGB (Red = *TerraSAR-X 2008*, Green = *TerraSAR-X 2009*, Blue = *TerraSAR-X 2009*); from Baldauf and Köhl (2009).

4.4.2 Bi-temporal segmentation

Common to methods using COBIA, prior to the actual classification a segmentation was carried out. It processes the used remote sensing data into meaningful, homogenous regions, also called image objects. The image objects contain a set of pixels. This set of pixels of an image object v is denoted as P_v .

This primer step is a significant and influential stage in COBIA, as all further processes use these image objects. In this study, the segmentation approach “centroid linkage region growing schemes” was used to segment the bi-temporal stack (*TerraSAR-X 2008* and *TerraSAR-X 2009*). This approach is named multi- or bi-temporal segmentation, and respects the subsequent change detection purposes.

Seeing that the automated possibilities of influencing parameters for segmentations are limited, they have to be empirically controlled. The main influencing parameter is the “Scale” parameter, a theoretical and abstract term that controls the maximum allowed heterogeneity for the resulting image objects. By modifying the “Scale” parameter the size of image objects is controlled. In the segmentation process two “scale levels” are generated to safeguard the detection of changes on various scales.

4.4.3 Image understanding and object-level change detection

Using the generated image objects of the segmentation process, the actual change detection is realized by the processes of image understanding and object-level change detection. Hereby, the image objects from the bi-temporal segmentation form the spatial basis for the change detection methods. The so called object-level change detection associates the segments of the image objects to the location of the trees in the project area. The alteration detection within these image objects is based on differences of spectral and structural characteristics between the image objects of the two points in time, i.e., 2008 and 2009. This chapter identifies the methods, how these differences are evaluated.

On the whole, image understanding guides the user through a multitude of intermediate results. These intermediate results must be verified and where appropriate the image objects must be improved until they correspond with the visual impression of objects in reality, i.e., in this study correspondence with trees and tree crowns.

Theoretical deduction and observations

Firstly, preliminary image understanding was achieved by theoretical deduction of observations in the bi-temporal stack in Figure 25: The stack shows differences of pixel values between the two points in time, represented in image bands by the scenes *TerraSAR-X 2008* and *TerraSAR-X 2009*, in the colors red and cyan. This circumstance results from the assignment of the three colors red, green and blue (RGB) to the two bands (Red = *TerraSAR-X 2008*, Green = *TerraSAR-X 2009*, Blue = *TerraSAR-*

X 2009). If in theory a tree was harvested between the two points in time, when the two TerraSAR-X scenes were recorded, the image stack shows the reflection of this tree in red (as the tree is existent at the recording time April 20, 2008) and does not show the respective reflection in green or blue (as the tree is not existent on August 17, 2009). This theoretical case results in a R-G-B assignation of 1-0-0. Thus, a red spot can be seen in this case. Reversely, cyan spots can be perceived, if a new tree grows into a formerly uncovered spot (a R-G-B assignation of 0-1-1). Table 4 shows all theoretical cases that are possible for RGB assignation of the used image stack.

Table 4: The four theoretical cases for differences between the two scenes *TerraSAR-X 2008* and *TerraSAR-X 2009* in the image stack²² as RGB (Red = *TerraSAR-X 2008*, Green = *TerraSAR-X 2009*, Blue = *TerraSAR-X 2009*).

Theoretical cases	<i>TerraSAR-X 2008</i>	<i>TerraSAR-X 2009</i>	Color in image stack
1 (no change)	Reflection	Reflection	White
2 (object extracted)	Reflection	No reflection	Red
3 (new object)	No reflection	Reflection	Cyan
4 (no object)	No reflection	No reflection	Black

Evaluating the image objects' characteristics

Secondly, further image understanding was accomplished by evaluating the image objects' spectral characteristics. Accordingly, the following two spectral characteristics²³, in OLCD also often named features, were calculated for all the image objects for both bands of the image stack (*TerraSAR-X 2008* and *TerraSAR-X 2009*):

²² See Figure 25 on page 65

²³ Based on Trimble (2011)

Firstly, the mean intensity of all pixels forming an image object (Mean):

$$\bar{c}_k(v) = \bar{c}_k(P_v) = \frac{1}{\#P_v} \sum_{(x,y,z,t) \in P_v} c_k(x, y, z, t) \quad \text{Eq. (4)}$$

Where:

- $\bar{c}_k(v)$ is the mean intensity of image layer k of an image object v
- P_v is the set of pixels of an image object v with $P_v = \{(x;y;z;t) : (x;y;z;t) \in v\}$
- $\#P_v$ is the total number of pixels contained in P_v
- $c_k(x, y, z, t)$ is the image layer intensity value at pixel $(x;y;z;t)$
- \bar{c}_k is the mean intensity of image layer k .

The two resulting features are:

$$\bar{c}_{TerraSAR-X 2008} = (\text{Mean of TerraSAR-X 2008})$$

$$\bar{c}_{TerraSAR-X 2009} = (\text{Mean of TerraSAR-X 2009})$$

Secondly, the amount that a given image layer contributes to the total brightness (Ratio):

$$r_k = \frac{\bar{c}_k(v)}{\sum_{k=1}^n \bar{c}_k(v)} \quad \text{Eq. (5)}$$

Only valid if $w_k^B = 1$ and $c(v) \neq 0$.

Where:

- r_k is the amount that a given image layer k contributes to the total brightness
- $\bar{c}_k(v)$ is the mean intensity of image layer k of an image object v
- $\bar{c}(v)$ is the brightness of an image object v
- w_k^B is the brightness weight of image layer k .

The two resulting features are:

$$r_{TerraSAR-X 2008} = (\text{Ratio of TerraSAR-X 2008})$$

$$r_{TerraSAR-X 2009} = (\text{Ratio of TerraSAR-X 2009})$$

The two features “Mean of *TerraSAR-X 2008*” and “Mean of *TerraSAR-X 2009*” can comprise values between 0 and 2,048²⁴, while the values of the two features “Ratio of *TerraSAR-X 2008*” and “Ratio of *TerraSAR-X 2009*” are between 0 and 1. Higher values in each of the four features show the existence of an object, speaking of forests, this means a tree.

Translation of the observations into object-level change detection

Thirdly, due to changes of the spatial patterns of crown cover in time, i.e. between the two recording times of “*TerraSAR-X 2008*” and “*TerraSAR-X 2009*”, the theoretical examples shown in Table 4 can be observed throughout the image stack generated in 4.4.1. This observation was translated into two object-level change detection equations using the features of Eq. (4) and Eq. (5):

Algebraic difference of the mean intensities for each of the image objects:

$$\begin{aligned} \bar{c}_{TerraSAR-X\ 2008} - \bar{c}_{TerraSAR-X\ 2009} > x \\ (\text{Mean of } TerraSAR-X\ 2008) - (\text{Mean of } TerraSAR-X\ 2009) > x \end{aligned} \quad \text{Eq. (6)}$$

Quotient of the ratios for each of the image objects:

$$\begin{aligned} \frac{\Gamma_{TerraSAR-X\ 2008}}{\Gamma_{TerraSAR-X\ 2009}} > y \\ (\text{Ratio of } TerraSAR-X\ 2008) / \text{Ratio of } TerraSAR-X\ 2009 > y \end{aligned} \quad \text{Eq. (7)}$$

Where x and y are thresholds for the latter change detection.

While no further limitations exist for Eq. (6), Eq. (7) is valid only for values of “Ratio of *TerraSAR-X 2009*” > 0. The two equations (6) and (7) for object-level change detection can be classified as Multivariate Alteration Detection (MAD)²⁵ based methods.

²⁴ The range of values originates from the image data depth of the original satellite data, i.e. 16bit (binary digit). One bit can have the value of either 1 or 0, thus 16bit equals $2^{16} = 65,536$ possible values. In spite this theoretical image depth, data of TerraSAR-X actually shows values of 0 to 2,048 (i.e. 11bit), only.

²⁵ See 3.4.1 on page 35

The development of an operational method for the detection of forest degradation in forms of patterns of selective logging using RADAR data, focuses on the detection of the theoretical case “2 (object extracted)”²⁶. However, an overestimation of such changes has to be limited, resulting in a careful control of misinterpretations of the theoretical cases 1, 3 and 4 (“no change”, “new object” and “no object”) of Table 4. These theoretical cases can be classified by defining the threshold for “x” or “y”. For a better understanding, Table 5 incorporates possible values for the features of Eq. (6) and Table 6 for Eq. (7). Additionally, for all exemplary values a classification of respective “*Theoretical cases*” is given in Table 5 and Table 6.

Table 5: Possible values for the features of equation (6) show the influence on the threshold “x”. This value of “x” can be further used for the classification into the four theoretical cases introduced in Table 4.

Possible value for „Mean of TerraSAR-X 2008”	Possible value for “Mean of TerraSAR-X 2009”	„x” in equation (6)	<i>Theoretical cases</i>
2000	2100	-100	1 (no change)
2000	200	1800	2 (object extracted)
500	1500	-1000	3 (new object)
150	200	-50	4 (no object)

²⁶ See Table 4 on page 67

Table 6: Possible values for the features of equation (7) show the influence on the threshold “y”. This value of “y” can be further used for the classification into the four theoretical cases introduced in Table 4.

Possible value for “Ratio of TerraSAR-X 2008”	Possible value for “Ratio of TerraSAR-X 2009”	„y” in equation (7)	<i>Theoretical cases</i>
0.90	0.95	0.95	1 (no change)
0.90	0.05	18	2 (object extracted)
0.10	0.90	0.11	3 (new object)
0.10	0.15	0.66	4 (no object)

The examples in Table 5 show that for image objects where an object, like a tree, was extracted (Theoretical case = “2 (object extracted)”), high values of the threshold “x” for Eq. (6) can be observed. The same holds true for high values of the threshold “y” in Table 6 for Eq. (7). However, it can be observed that within the range of above values only for threshold “y” a decisive break can be deduced, i.e. the value $y=1$. If $y \geq 1$ is valid for an image object, it can be classified as of *Theoretical cases* = “2 (object extracted)”. This general validity of Eq. (7) is supportive of the transferability of the applied approach. Consequently, Eq. (6) is not pursued in further stages of this study, but the classification algorithms are based on Eq. (7).

Classification rule set and OLCD classification

The classification rule set consists of three sections: “Class Hierarchy”, the “class descriptions” and interim results (see Figure 26). The first two sections can be subsumed as the actual classification process.

The use of two “scale levels” to improve the classification results safeguards the detection of changes on various scales. Thus, image objects of each “scale level” are assigned to separate classes. Or in other words, for each “scale level” of the segmentation a class with respective sub-classes is defined.

Figure 26 shows, how such classes can be grouped in a hierarchical structure, i.e., “Class Hierarchy”, allowing child classes to inherit attributes from parent classes. These parent classes are also called “super-objects”, the child classes “sub-objects”. The definition of the classes is realized in the “class description”, containing simplistic one-dimensional membership functions. Eventually, the application of a classification achieves interim results.

In this study, the one-dimensional membership functions are used to describe the classification threshold “ γ ”. Thereby, the classes for the two events, i.e., “*change*” and “*no change*”, are defined, which in the end, are expected to detect areas that show patterns of forest degradation in the study area.

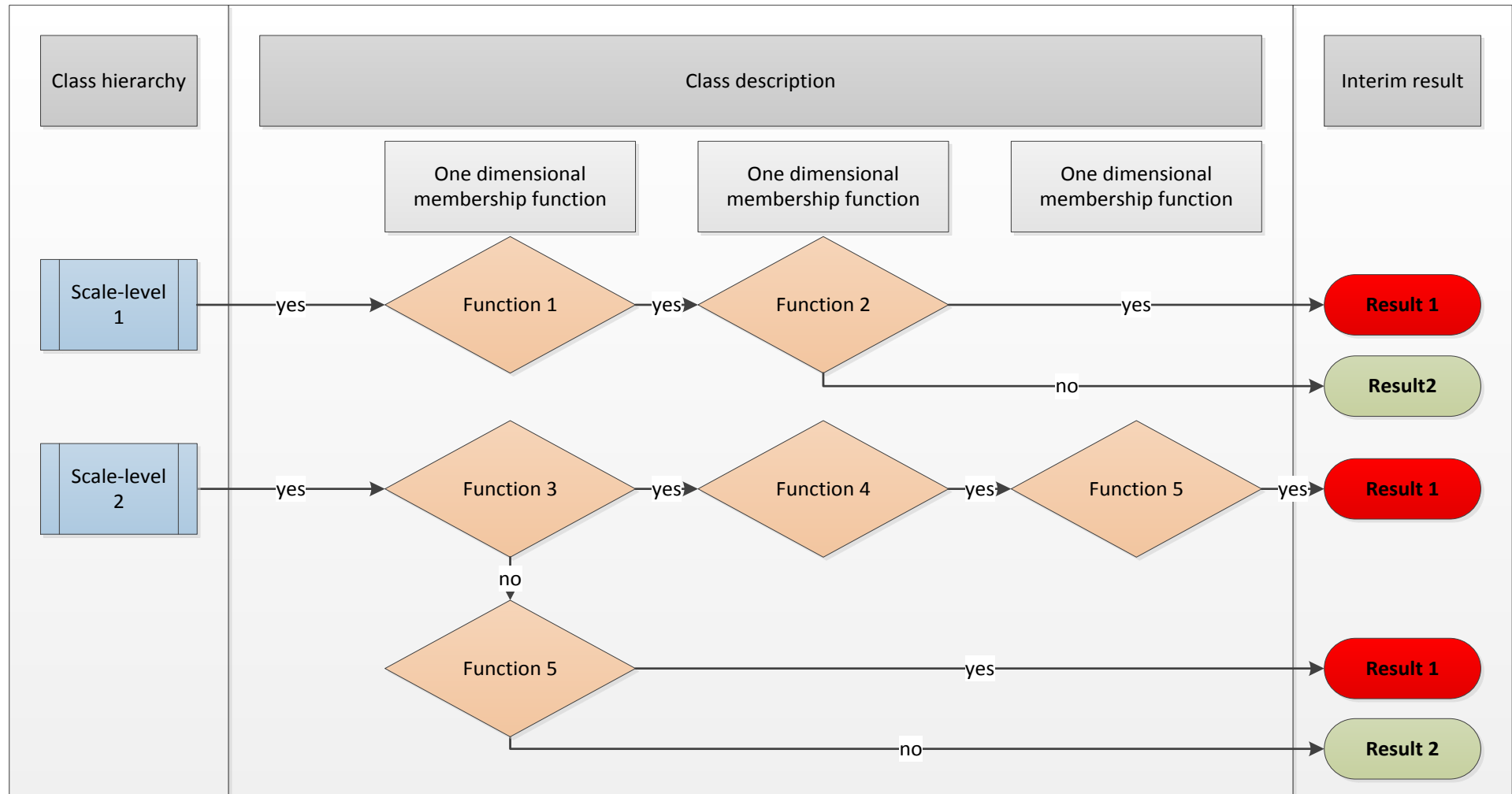


Figure 26: Classification rule set for object-level change detection. In this example, the class hierarchy consists of the two classes “Scale-level 1” and “Scale-level 2”. Each class is defined by the class description that consists of one-dimensional membership functions. This example returns the interim results “Result 1” and “Result 2” that can be deduced by each class on the respective scale.

4.5 Methods to analyze the accuracy of the object-level change detection

Following the approaches described in chapter 3.5, the accuracy of the object-level change detection is assessed. Hence, after the de-fuzzyfication of the classification results each class is quantified using tables comparing absolute and relative figures of the respective classes. Finally, an error matrix is assembled that shows the relationship between reference data and equivalent classification results for both events “change” and “no change”, and furthermore gives the following statistical measures introduced in chapter 3.5²⁷:

$$- \text{ Overall accuracy: } OA = \frac{\sum_{k=1}^N a_{kk}}{\sum_{i,k=1}^N a_{ik}} \quad (\text{see Eq. (1)})$$

$$- \text{ Producer's accuracy: } PA(class_i) = \frac{a_{ii}}{\sum_{i=1}^N a_{ki}} \quad (\text{see Eq. (2)})$$

$$- \text{ User's accuracy: } UA(class_i) = \frac{a_{ii}}{\sum_{i=1}^N a_{ik}} \quad (\text{see Eq. (3)})$$

²⁷ See Eq. (1), Eq. (2) and Eq. (3) on page 52

4.6 Methods to identify influences of stand characteristics on the reliability of the detection of forest degradation

In order to identify and quantify influences of stand characteristics on the reliability of detecting forest degradation in tropical moist forests using RADAR remote sensing techniques, the following three attributes are investigated:

- Tree biomass
- Tree crown area
- Social position and dominance

All three attributes are expected to have an influence on the detectability of the extraction of the single trees. This influence can be quantified by evaluating their respective role in the above described accuracy assessment of the classification process. In the end, for each of the three attributes, particular accuracy assessments are determined and analyzed. For this all three attributes are evaluated with individual methods and then accumulated in a geodatabase²⁸.

4.6.1 Tree biomass

In order to estimate the particular aboveground tree biomass, the use of the in-situ data described in 4.2 of all individual trees was used with the regression model of Chave et al. (2005):

$$\langle AGB \rangle_{est} = p * \exp \left(-1.499 + 2.148 \ln(dbh) + 0.207 (\ln(dbh))^2 - 0.0281 (\ln(dbh))^3 \right) \quad \text{Eq. (8)}$$

where

- AGB is the total aboveground biomass in kg
- p is the wood specific gravity in g/cm³; this study uses the default value of 0.5g/cm³
- dbh is the diameter at breast height in cm

²⁸ The used geodatabase is implemented in ArcSDE and was already used for importing the in-situ data. In addition, this environment allows for further interactions, e.g. by SQL-based queries, from all software programs used in this study, i.e. Trimble's eCognition, ESRI's ArcGIS and IBM's SPSS.

By means of Eq. (8) and the dbh measurements from the in-situ data the aboveground tree biomass can be estimated for all trees in the project area.

This general equation is applicable for moist forest stands and has been evaluated in relevant test-sites in Brazil (Chave et al., 2005). Chave et al. (2005) acknowledge that an overestimation of the tree biomass values for larger trees may occur. Although better equations may exist, e.g. using tree height as an additional predictive variable, resulting in more accurate estimations of the actual AGB, this common approach has been used with the intention of evaluating the influence of AGB of single trees in the detection of forest degradation patterns. For this, the exact tree biomass value is not of main importance.

4.6.2 Tree crown area

The in-situ data do not provide measurements of individual tree crown areas. However, the high-resolution panchromatic Quickbird scene allows for the visual detection of tree crowns, filling this gap. The delineation of tree crowns was performed for a subset of ten percent of the relevant trees using ESRI ArcGIS 10. Subsequently, the tree crown areas of these trees were calculated and saved as the variable *Shape_Area*.

In a further step, a model based on these digitized trees, i.e., the variable *Shape_Area*, and their respective dbh was developed in IBM SPSS Statistics 20 to estimate all tree crown areas. This approach has already been widely used in temperate forests (Bechtold, 2003, 2004; Hann, 1997) and tropical forests (Mugo et al., 2011). Table 7 shows possible models and their parameter estimates as interim results from the analysis in SPSS.

Table 7: Model summary and parameter estimates. Dependent variable is *Shape_Area*, which is based on the areas of the tree crowns in square meters and originated from the delineation of 10% of the total tree crowns in the project area.

Equation	Model Summary					Parameter Estimates			
	R ²	F	df1	df2	Sig.	Constant	b1	b2	b3
Linear	.531	635.263	1	561	.000	-21.145	1.383		
Logarithmic	.508	578.735	1	561	.000	-584.536	157.501		
Inverse	.383	348.533	1	561	.000	262.976	-11640.931		
Quadratic	.541	330.061	2	560	.000	-58.511	2.104	-.002	
Cubic	.542	220.203	3	559	.000	-42.478	1.667	.001	-6.534E-6
Compound	.374	335.587	1	561	.000	23.542	1.011		
Power	.406	382.835	1	561	.000	.159	1.380		
S	.346	296.440	1	561	.000	5.681	-108.397		
Growth	.374	335.587	1	561	.000	3.159	.011		
Exponential	.374	335.587	1	561	.000	23.542	.011		
Logistic	.374	335.587	1	561	.000	.042	.989		

As expected the R²-values of all of the models are rather low. This is due to the fact that the development of tree crowns is very complex and can only partially be described by the dbh alone. Since instead of the exact value of the tree crown area, it is the influence of this attribute of stand characteristics on the detectability of the respective tree that is of importance, these low values were accepted and the quadratic model (R² = 0.541) was used. Thus, the resulting crown area model used in this study is shown in Eq. (9):

$$eCA = -58.511 + 2.104 * dbh - 0.002 * dbh^2 \quad \text{Eq. (9)}$$

Where:

- eCA = estimated Crown Area in sqm
- dbh = diameter at breast height in cm

Using Eq. (9) and the dbh measurements from the in-situ data an estimation of the tree crown area for all trees in the project area can be implemented.

Furthermore, a classification of the estimated tree crown area values was implemented. This classification comprises of five classes due to their respective tree crown area in square meters (sqm) (see Table 8). These classes are used for evaluating the influence of the tree crown areas in the detection of forest degradation patterns.

Table 8: Classification of tree crown area estimates into five classes.

Classes	Tree Crown area
Class 1	$\leq 100\text{sqm}$
Class 2	$> 100\text{sqm AND } \leq 200\text{sqm}$
Class 3	$> 200\text{sqm AND } \leq 300\text{sqm}$
Class 4	$> 300\text{sqm AND } \leq 400\text{sqm}$
Class 5	$> 400\text{sqm}$

4.6.3 Social position and dominance

Already in 1884 Kraft (1884) described a scheme for the social position of individual trees that has been used ever since. At the IUFRO congress in 1956, Leibundgut (1956) presented a similar method for tree classification based on their social position. This approach was revised in 1978 (Leibundgut, 1978) and further developed by Lamprecht (1980) in 1980. These early approaches are still applied for cultivation processes in forest management systems for forest compartments (Kennel, 1966; Pancel, 1993). Conversely, these two approaches can also be used for the individual classification of one single tree, in order to evaluate its respective social position and dominance in relation to its neighboring trees.

Figure 27 exemplary illustrates the four classes for the evaluation of tree-specific social position and dominance based on Kraft (1884).

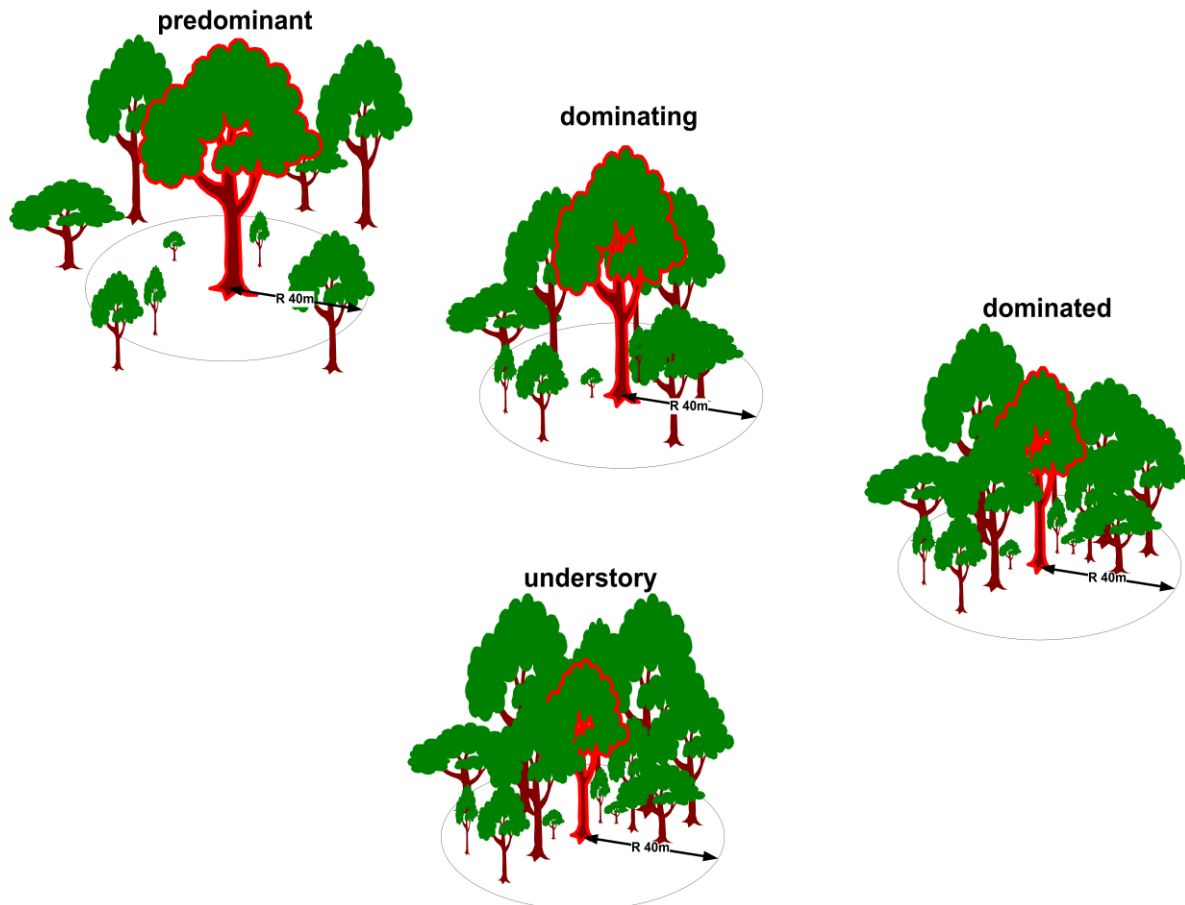


Figure 27: Classes for the evaluation of tree-specific social position and dominance; based on Kraft (1884).

These approaches by Kraft and by Leibundgut are used for the present purpose, i.e., to evaluate influences on the reliability of the detection of forest degradation using RADAR remote sensing techniques. Herein they expose information for social position and dominance on single tree basis.

Evaluation rule sets for „Kraft” (see Table 9) and for “Leibundgut” (see Table 10) are developed. These define how each individual tree is classified in respect to all surrounding trees in a distance of 40m. The two evaluation rule sets form the basis of a developed script²⁹ that ranks each tree in the classes of Kraft (1884) and Leibundgut (1956) as listed in Table 9 and Table 10.

²⁹ See Annex 9.2 on page 149

Table 9: Evaluation rule set “Kraft” with a description of the respective classes of Kraft (1884).

Evaluation rule set “Kraft”	Description	Classification (adapted from Kraft (1884))
KR_1.	There is no tree within a distance of 40m	Pre-dominant
KR_2.	The tree heights of all trees within a distance of 40m is smaller than the individual tree height	Dominating
KR_3.	The maximum tree height of all trees within a distance of 40m is larger than the individual tree height	Dominated
KR_4.	The mean tree height of all trees within a distance of 40m is larger than the individual tree height	Understory

Table 10: Evaluation rule set “Leibundgut” with a description of the respective classes of Leibundgut (1956).

Evaluation rule set “Leibundgut”	Description	Classification (adapted from Leibundgut (1956))
LG_1.	The individual tree height is larger than 2/3 of the dominant height	Upper stratum
LG_2.	The individual tree height is larger than 1/3 and lower or equal than 2/3 of the dominant height	Middle stratum
LG_3.	The individual tree height is lower than 1/3 of the dominant height	Lower stratum

Thus, single tree information by the evaluation rule sets “Kraft” consist of the classes “pre-dominant”, “dominating”, “dominated”, and “understory”. The information on the evaluation rule set “Leibundgut” entails the classes "upper stratum", "middle stratum", and "lower stratum". Both can be used for evaluating the influence of the social position and dominance of individual trees in the detection of forest degradation patterns. This developed script is based on the programming

language Python³⁰. The application of the two rule sets from Table 9 and Table 10 can provide information on the social position and dominance for all trees in the project area.

4.7 Methods to quantify influences of stand characteristics on the reliability of the detection of forest degradation

To analyze and quantify influences of stand characteristics on the reliability of the developed object-level change detection method, the three attributes aboveground tree biomass, tree crown area, and social position and dominance were evaluated and three additional accuracy assessments were conducted.

These assessments show for each of the three stand characteristics the specific producer's accuracies³¹ of the object-level change detection method in respect to the overall results. The following diagram (see Figure 28) is used as a template for the illustration of these assessments. It shows the evaluation of both the distribution of the producer's accuracies for sub-classes of the stand characteristics³², in this template i.e. sub-class 1, sub-class 2, and sub-class 3, and the distribution of the number of extracted trees in relation to the overall results of all sub-classes.

This evaluation focuses on the influences of the attributes tree biomass, tree crown area, and social position and dominance, on the accuracy of the object-level change detection. Therefore, only the producer's accuracies for the event "Change" are of interest. In other words, only the correct and incorrect detection of extracted trees must be evaluated. The template is used to show for each attribute the correct detection of the event "Change" as "detected" (blue) and the incorrect detection of the event "Change" as "not detected" (red).

³⁰ Python v2.6.5 is installed with ESRI's ArcGIS 10 ordinary installation and was used in this study. The site-package ArcPy extends Python with additional functionality for interrogating GIS data. Using the spatial analyst module and functions renders possible the necessary direct access and interaction with the used geodatabase.

³¹ See Eq. (3) on page 52

³² The respective sub-classes are described in 4.6 on pages 75ff

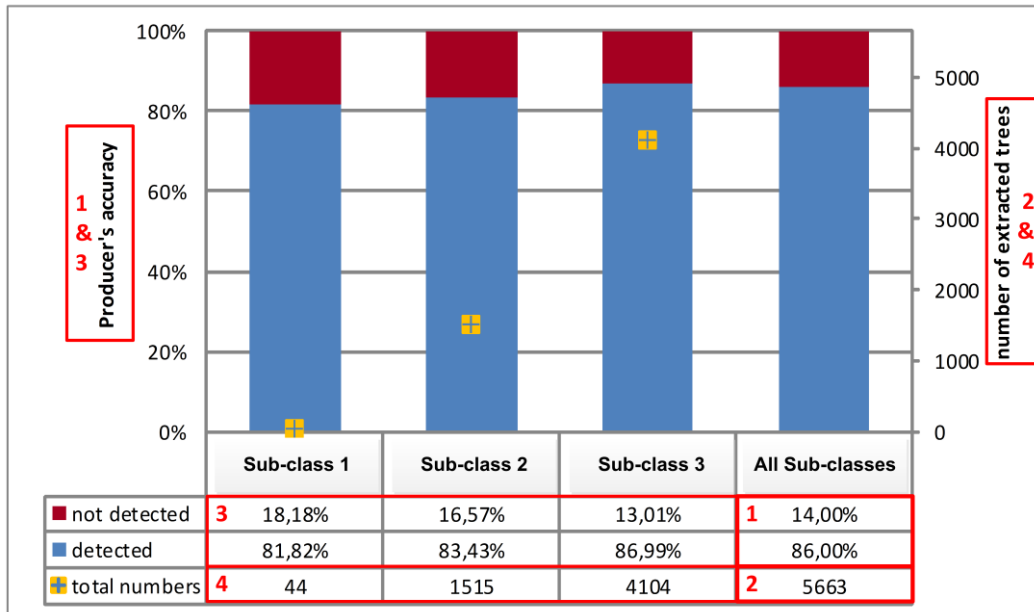


Figure 28: This diagram is used as a template for the illustration of the quantification of the influences of each of the three stand characteristics; In the red box labeled with “1” the producer’s accuracy summed for all classes is shown. In the red box labeled with “2” the number of extracted trees summed for all classes is presented. As both the numbers for “1” and “2” correspond for all three stand characteristics they are the same in all respective diagrams. In the red box “3” the producer’s accuracies of each sub-class are listed for the results “not detected” and “detected” of the event “Change”. The correct detection of the event “Change” is represented as “detected” (blue) and the incorrect detection of the event “Change” as “not detected” (red). In the red box “4” the number of the extracted trees in each sub-class is shown.

5 Results

This chapter discloses the results of the developed methods from the previous chapter. Thus, it first illustrates the results of the developed methods to detect forest degradation using RADAR. This is followed by the presentation of the results of the accuracy analysis of the object-level change detection. In a last step, the results of the analysis of the influences of the three stand characteristics on the reliability of the object-level change detection of forest degradation are revealed and explained in respective accuracy assessments.

5.1 Results of the developed methods to detect forest degradation using RADAR

5.1.1 Pre-processing stages

As stated in 4.2, the study area comprises 1,585 ha of tropical moist forests with 48,141 trees in total, whereas 5,663 trees were harvested between 2008 and 2009. Based on the results of the forest inventory and the fieldwork carried out in April 2010, all the above trees are geo-located in a GIS and stored with their respective forest inventory attributes in a geodatabase, and are used in the following evaluation as in-situ data. Table 11 shows ten exemplary datasets that are also used throughout the following chapters.

Table 11: Results of the pre-processing stages are depicted for ten exemplary datasets.

Tree_No	Latitude ³³	Longitude ³³	dbh	Tree height ³⁴
4109	725461.46	204075.93	338.7	14
5817	724774.85	204407.26	240.0	22
6233	724579.46	203882.12	180.0	20
12105	723731.31	203047.65	55.0	13
12250	723704.42	203081.33	54.3	19
12251	723700.30	203076.23	52.9	17
12253	723694.37	203079.09	97.2	20
12254	723676.35	203077.67	62.0	20
12256	723679.83	203055.77	56.0	18
12264	723700.95	203019.30	73.2	18

Figure 25³⁵ shows a subset of the bi-temporal stack of the two TerraSAR-X scenes, i.e. *TerraSAR-X 2008* and *TerraSAR-X 2009*. This stack forms the basis of remote sensing data used in the development of methods to detect forest degradation.

5.1.2 Bi-temporal segmentation

The multi-resolution, bi-temporal segmentation is performed with the aim of being able to accomplish a change detection analysis based on image objects in the study area. For this, image objects are generated that are later on used for classification. After empirical examination of the available parameters for the segmentation process, the factors in Table 12 show a strong visual correlation with the tree crowns of the in-situ data. All three parameters, i.e., “Scale parameter”, “Shape” and “Compactness” are theoretical, abstract terms that control the maximum allowed heterogeneity for the resulting image objects, and do not express direct measures.

³³ Universal Transverse Mercator (UTM), Grid Zone 20N, Northern Brazil, South American Datum 1969 (SAD_1969_UTM_Zone_20N)

³⁴ The forest inventory only gathered data on the commercial tree height.

³⁵ See 4.4.1 on page 65

Table 12: Parameters for the multi-resolution segmentation on pixel level of the used data into two “scale levels”, i.e. L25 and L50.

	Scale levels	
	L25	L50
Scale parameter:	25	50
Shape:	0.9	
Compactness:	0.9	

The two levels of this segmentation incorporate compatible image objects for the further object-level change detection. Figure 29 shows exemplary results of the segmentation process indicating the two scale levels, i.e. L25 and L50.

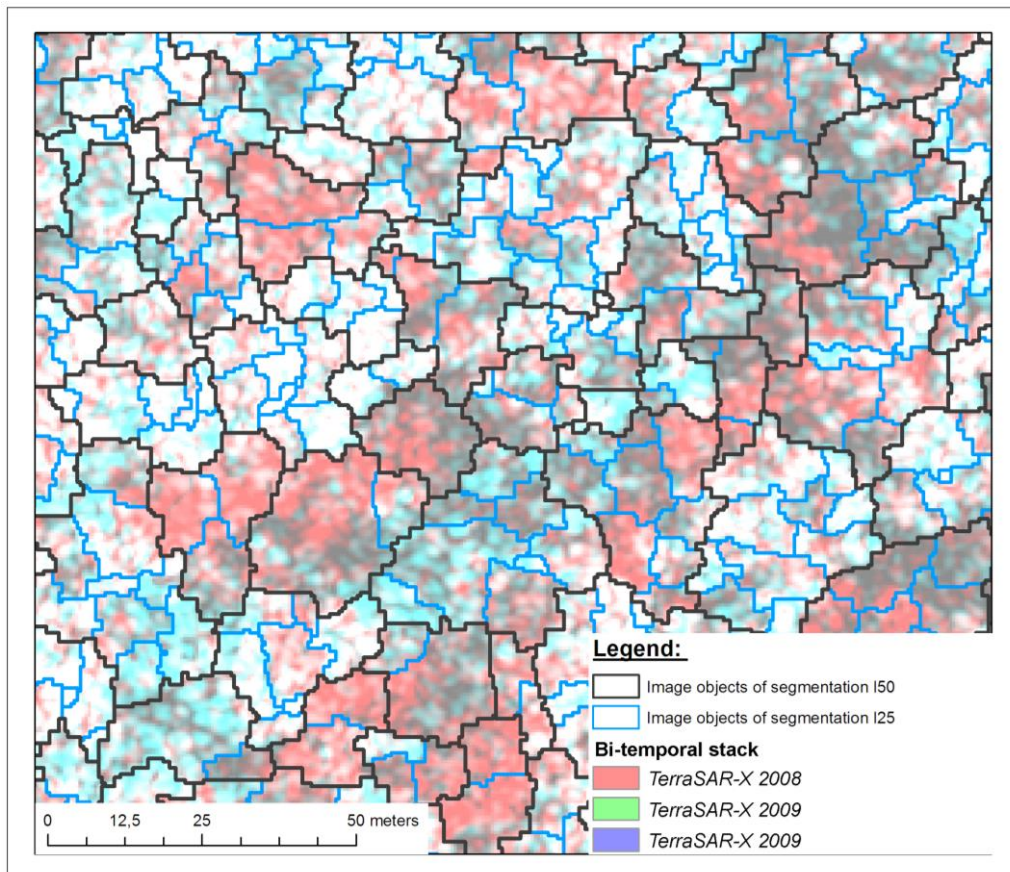


Figure 29: Image objects of the scale levels L25 and L50 derived through multi-resolution segmentation; black outlines signifies image objects of level L50, blue lines show image objects of level L25 that further subdivides the image objects of L50, in the background the bi-temporal stack of the TerraSAR-X scenes is displayed; The stack is displayed as RGB (Red = TerraSAR-X 2008, Green = TerraSAR-X 2009, Blue = TerraSAR-X 2009).

5.1.3 Image understanding and object-level change detection

The development of the object-level change detection method for the detection of patterns of selective logging uses classification algorithms that analyze image objects according to defined criteria and assign them to a class that best meets them. Preliminary image understanding identified two approaches for these classification algorithms, i.e., firstly the algebraic difference of the mean intensities for each of the image objects³⁶, and secondly the quotient of the ratios for each of the image objects³⁷. Both approaches were tested for the image objects generated by the bi-temporal segmentation. The observation stated in chapter 4.4.3 that only for Eq. (7) a decisive break for the threshold “ γ ” can be deduced, holds true, as a strong visual correlation between the extracted trees of the in-situ data and the respective image objects for $\gamma \geq 1$ exists. Thus, the development of the OLCD method for the detection of patterns of selective logging is based on Eq. (7).

Figure 30 illustrates the classification rule set for the applied object-level change detection. In the Annex³⁸ Figure 40, Figure 41 and Figure 42 show particular examples of the classification settings. Furthermore, a stepwise description of each setting is shown in the annex³⁹.

³⁶ See Eq. (6) on page 69

³⁷ See Eq. (7) on page 69

³⁸ See Annex chapter 9.5 on page 150

³⁹ See Annex chapter 9.6 on page 151

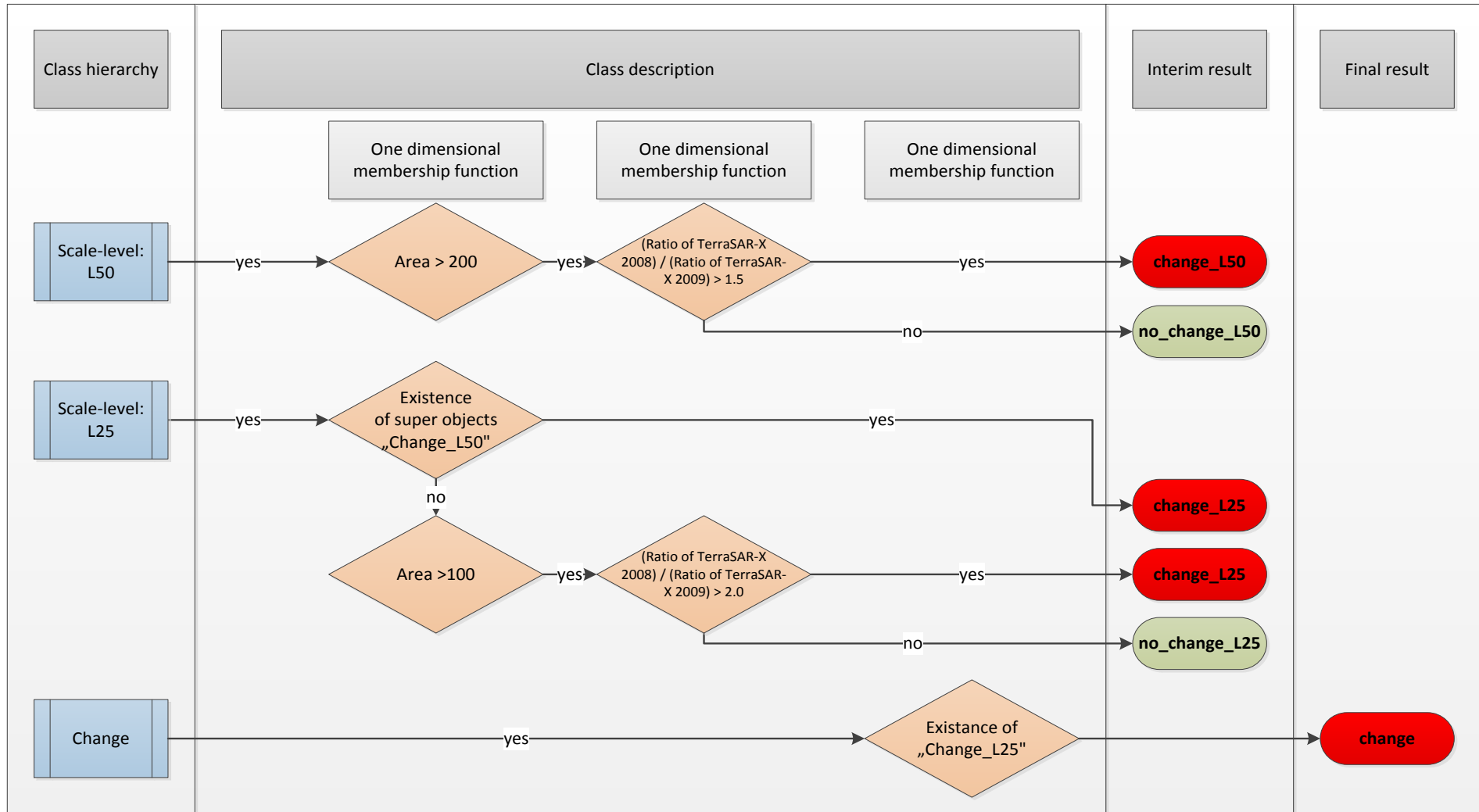


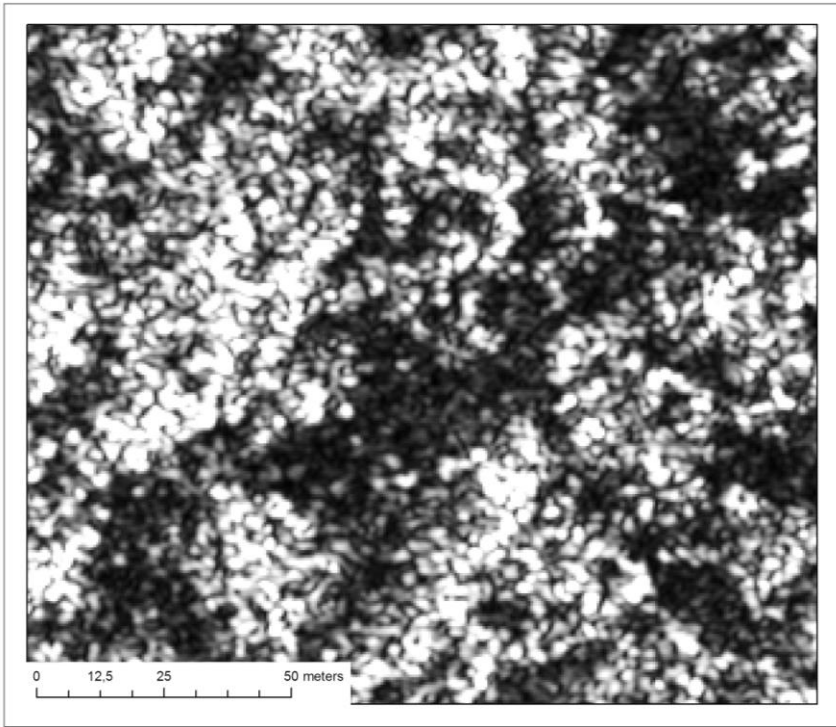
Figure 30: The classification rule set for object-level change detection shows the processing steps incorporating the class hierarchy, the class descriptions with its membership functions, the interim results and the final result.

The segmentation resulted in two “Scale levels”, i.e., L25 and L50. Both were defined as classes in the “class hierarchy”, to safeguard the detection of changes on various scales. For each class, i.e., “L50” and “L25” two sub-classes were created, incorporating areas of change, i.e. “change_L50” and “change_L25”, and areas of no change, i.e., “no_change_L50” and “no_change_L25”. The two classes incorporating areas of change were defined by one-dimensional membership functions. Firstly, an area threshold of 200sqm for image objects of the “Scale level” “L50”, respectively 100sqm for image objects of “L25”, were defined, in order to filter out small speckles. Secondly, for each subclass membership functions based on Eq. (7) were defined to detect areas of changes. For the sub-class “change_L50” the threshold was set to $y = 1.5$. The respective threshold for the sub-class “change_L25” was $y = 2.0$. The two classes for no change, i.e. “no_change_L50” and “no_change_L25”, were defined by the respective inverted functions. Additionally, the areas of change from “change_L50” were inherited by “change_L25” as super-objects.

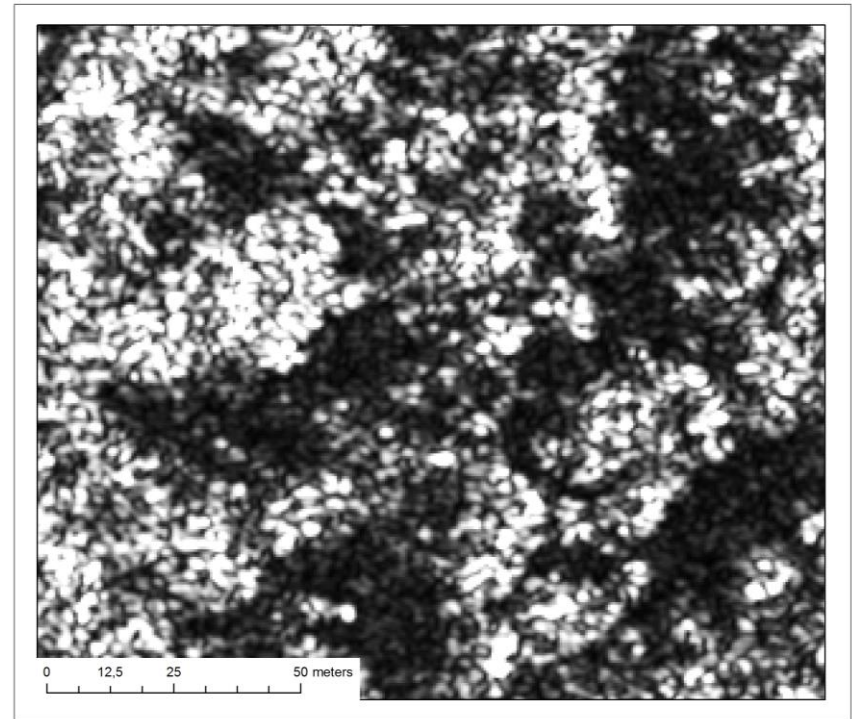
Finally, the class “change” is used to assemble the intermediate results of the two classes “change_L50” and “change_L25”. Thus, it incorporated the final classification results and, for further evaluation, is exported to the geodatabase.

Export results from eCognition to GIS

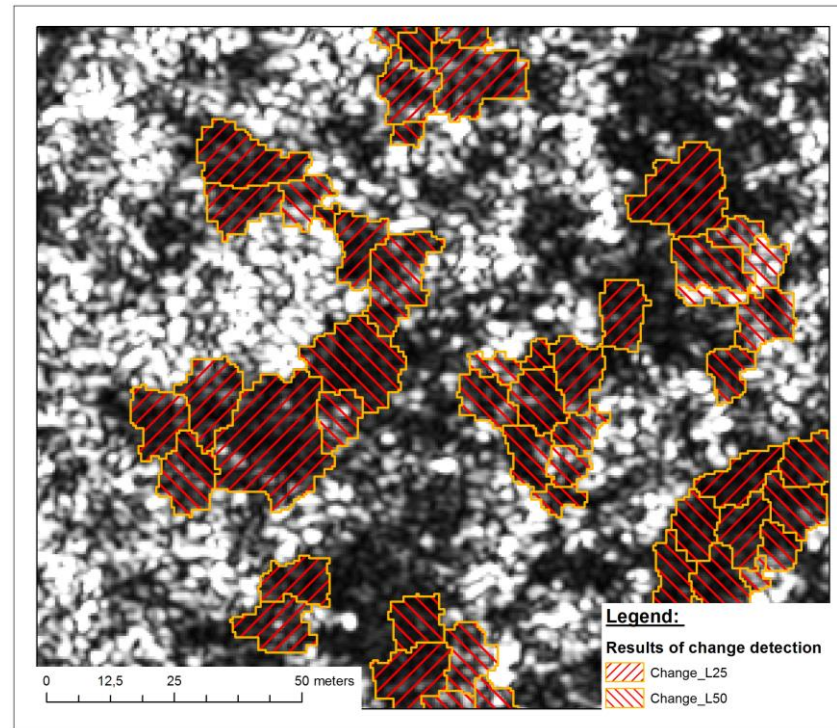
Figure 31 shows one sample location on three maps. Map (a) displays a subset of “TerraSAR-X 2008” and map (b) a subset of “TerraSAR-X 2009”. Differences between (a) and (b) in terms of areas of dissimilar patterns correspond to changes between April 20th 2008 and August 18th 2009, and originate from the extraction of trees in this specific time period and spatial location. These differences are detected as areas of change by the developed change detection algorithm. In map (c) these areas of change in the multi-temporal TerraSAR-X data are shown as polygons with lined patterns, in the background “TerraSAR-X 2009” is displayed. The specific colors of the lined areas correspond to the change detection in respective scale levels, i.e., “L50”, “L25”, and their particular classes and sub-classes, i.e., “change_L50”, and “change_L25”.



(a)



(b)



(c)

Figure 31: Screenshots exemplary showing three maps of the same location. In (a) „*TerraSAR-X 2008*“, in (b) “*TerraSAR-X 2009*” is displayed. Differences between (a) and (b) in terms of areas of dissimilar patterns are changes between April 20, 2008 and August 18, 2009, and originate from the extraction of trees in this time periode. These differences have been detected by the change detection algorithm and are displayed in (c). In (c) the background shows “*TerraSAR-X 2009*”. Polygons with lined patterns are areas of change detected in the multi-temporal TerraSAR-X data. The specific colors of the lined areas correspond to the change detection in respective scale levels, i.e. “L50”, “L25”, and their particular classes and sub-classes, i.e. “change_L50” and “change_L25”.

In order to portray different scenarios that can be found during the classification process, Figure 32 shows three example maps that oppose the results of the developed change detection algorithm as polygons with lined patterns and the in-situ data as points, whereas the optical remote sensing data is used for visualization purposes in all three maps, only. The dark green triangles correspond to tree locations, the light green circles to locations of extracted trees. Both these point layers are based on the in-situ data.

Thus, map (a) in Figure 32 shows the area of two extracted trees, which are detected whereas for the remaining trees no change is recognized. One tree has a dbh of 51cm the other one of nearly 69cm. Map (b) displays two extracted trees with a dbh of 179cm and 84cm. Their respective areas are detected by the developed algorithm. While three large extracted trees with a dbh of between 193 to 292cm in map (c) are correctly identified as change by the algorithm, one smaller tree with a dbh of 52cm is falsely classified as area of “no change”. One tree that was not extracted was standing beneath the crown of the large tree with a dbh of 292cm. Nevertheless, this area is subject to change in reality and identified as change by the algorithm.

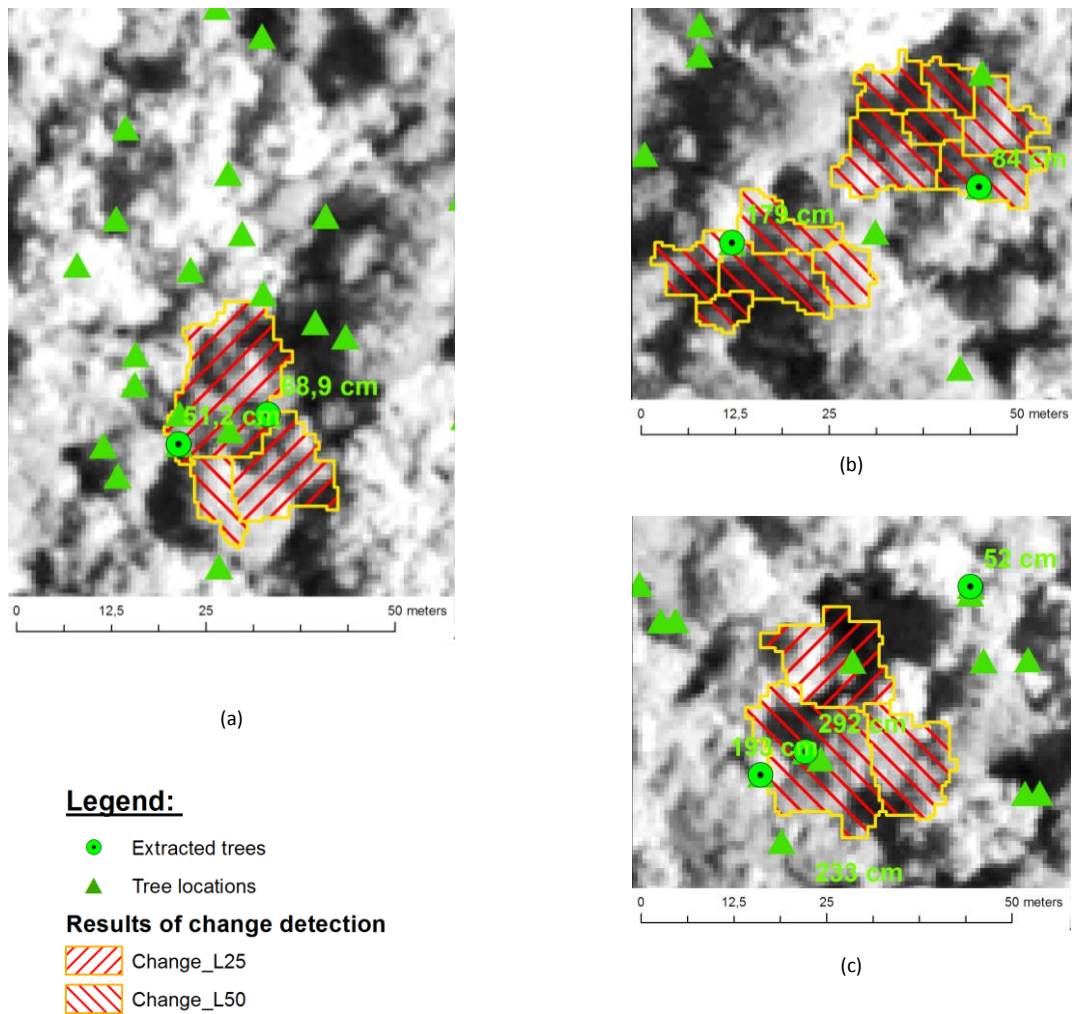


Figure 32: Screenshots showing map results of the object-level change detection for three examples, i.e., (a), (b), and (c). The legend is valid for all three maps. The background shows the optical remote sensing data that is used for visualisation. Polygons with lined patterns are areas of change detected by the classification of the multi-temporal TerraSAR-X data. According to the legend, the specific colors of the lined areas correspond to the change detection in respective scale levels. Taken from the in-situ data, the dark green triangles correspond to tree locations, light green circles to locations of extracted trees.

5.2 Results of the accuracy analysis of the object-level change detection

Although the previous chapter allows some insights, the subsequent analysis using an error matrix gives more detailed information about the applied methods and their outcomes. Hence, the results of the above classification, which is applied to detect areas of change using corresponding TerraSAR-X data of 2008 and 2009, are also presented as statistics, after comparing reference data and classification data. The reference data is taken from the in-situ data consisting of the total number of trees, i.e., **48,141** trees, and covering both all remaining trees, i.e., **42,478** individuals, and all extracted trees, i.e., **5,663** individuals, in the study area. The classification data contains all areas of change detected by the developed object-level change detection. An accuracy assessment provided the results of this one-to-one comparison. The statistics cover all scenarios. The results of the comparison are shown in an error matrix in Table 13; the specific statistics are compiled in Table 14.

Table 13: Error matrix showing the comparison of reference data and classification data. The reference data is based on the in-situ data. The classification data contains all locations of change and no change detected by the developed object-level change detection.

		Reference Data		Sum
		no_Change	Change	
Classification Data	no_Change	42,429	793	43,222
	Change	49	4,870	4,919
Sum		42,478	5,663	48,141

Table 13 shows that out of **48,141** trees in total, **42,429** trees are correctly identified as “no_Change”, whereas areas of change are incorrectly detected for only **49** trees. In-situ data shows that **5,663** trees were extracted from the study area, whereas for 4,870 individuals show areas of change and are correctly detected. However, for **793** extracted trees the developed object-level change detection identifies no change in the RADAR scenes. This figure is reconsidered in subsequent chapters.

Besides these actual numbers, estimated accuracies of the classification render higher importance. Firstly, the producer's accuracy measures how well a certain area is classified. It takes into account the error of omission, which refers to the proportion of observed features on the ground that is not classified in the map. The class "change" has the lowest producer's accuracy. This means that areas of extracted trees are classified with a probability of approximately 86%, i.e., are correctly detected. In reverse, 14% of all extracted trees will not be mapped. Again, this figure is reconsidered in subsequent chapters.

Secondly, the user's accuracy is a measure of the reliability of the map. It informs the user how well the map represents, what is really on the ground. The incorrectly identified classes in the map are referred to as errors of commission. Here, the class "no_Change" is important. Due to a user's accuracy of about 98%, in 1.9% of the visits in the field no "no_Change" will be found on the specific place marked on the map. This figure is, as well, reconsidered in subsequent chapters.

Table 14: Estimated accuracies for the classification results.

Overall accuracy	98.25%	
Kappa Index	91.07%	
	Producer's accuracy	User's accuracy
no_Change	99.88%	98.17%
Change	86.00%	99.00%

These accuracy assessments are carried out in order to estimate the imperfections of the classification performed. On the whole, the analyses show that the classification can be used to proceed with further elements of this study.

5.3 Results of the identification of influences of stand characteristics on the reliability of the detection of forest degradation

The identification of influences of stand characteristics on the reliability of the detection of forest degradation in tropical moist forests using RADAR remote sensing techniques was performed investigating the following three attributes:

- Tree biomass
- Tree crown area
- Social position and dominance

The tree specific results for these attributes are presented below. As the complete results comprise data on all 5,663 extracted trees, only a subset of ten example tree-datasets⁴⁰ are directly depicted and shown in Table 16. The complete results are shown in the Annex⁴¹.

5.3.1 Tree biomass

The tree biomass estimation is implemented by means of Eq. (8) and the dbh values taken from the in-situ data. Thus, the aboveground tree biomass can be estimated for all trees in the project area.

Subsequently, these biomass data are categorized into five equally numerous subsets, i.e., 5-quantiles or quintiles. Thus, *Quintile_1* incorporates the class with the lowest biomass values, *Quintile_5* the class with the highest biomass values. The precise tree biomass ranges for each quintile is shown in Table 15.

⁴⁰ These are the same ten datasets that have already been shown in Table 11 in chapter 5.1.1 on page 83

⁴¹ See chapter 9.7 on page 152

Table 15: The categorization of the tree biomass estimation into quintiles results in the following minimum and maximum values of tree biomass for each class.

	Tree biomass [kg]	
	Minimum	Maximum
Quintile_1	1,076	3,266
Quintile_2	3,281	4,334
Quintile_3	4,351	5,987
Quintile_4	6,008	8,674
Quintile_5	8,699	198,360

5.3.2 Tree Crown Area

Estimates on tree crown areas are calculated by means of Eq. (9) and the dbh values taken from the in-situ data. Thus, an estimation of the tree crown area for all trees in the project area is accomplished.

These estimates are further stratified into 5 classes based on their estimated tree crown area as shown in Table 8⁴².

5.3.3 Social position and dominance

The results for social position and dominance for all trees in the project area are obtained using the evaluation rule sets “Kraft” and “Leibundgut”⁴³. As a result, information on the social position and dominance for each tree is available.

The results for the three attributes aboveground tree biomass, tree crown area, and social position and dominance for the ten example tree-datasets listed in Table 16 are based on the unique identification for the individual trees in the column **Tree_No**. The aboveground tree biomass estimation in kg is shown in the column **Chave_moist_2**. The respective 5-quantiles of the biomass data are displayed in the field **Chave_moist_2_class**. Estimates on tree crown areas are depicted in

⁴² See Table 8 on page 78. The tree crown area classes are as follows: Class 1 $\leq 100\text{sqm}$; Class 2 $> 100\text{sqm}$ AND $\leq 200\text{sqm}$; Class 3 $> 200\text{sqm}$ AND $\leq 300\text{sqm}$; Class 4 $> 300\text{sqm}$ AND $\leq 400\text{sqm}$; Class 5 $> 400\text{sqm}$

⁴³ See Table 9 on page 80 and Table 10 on page 80

the column *est_Crown_Area*. The stratification of these crown area values into 5 classes is shown in column *CrownAreaClass*. In a final step, the results for social position and dominance for each tree using the classes of the evaluation rule set “Kraft” and the classes of the evaluation rule set “Leibundgut” are summarized in the columns *Kraft* and *Leibundgut*.

Table 16: Results for ten exemplary datasets are depicted for tree specific estimation of aboveground tree biomass, tree crown area, and social position and dominance; The field *Tree_No* shows the unique identification for the individual trees, *Chave_moist_2* lists the appropriate values for the single aboveground tree biomass values in kg, in *Chave_moist_2_class* these biomass data are categorized into respective quintiles. As in the field *est_Crown_Area* the results for the estimated tree crown area in square meters are given, these results are classified in *CrownAreaClass*. Lastly the fields *Kraft* and *Leibundgut* show the particular results for the social position and dominance for each depicted tree.

Tree_No	Chave _moist_2 est. tree biomass [kg]	Chave_moist _2_class Tree biomass quintile	est_Crown _Area est. tree crown area [sqm]	CrownArea Class Tree crown area class	Kraft classes of the evaluation rule set “Kraft”	Leibundgut classes of the evaluation rule set “Leibundgut”
4109	79151	Quintile_5	425	5	dominated	middle stratum
5817	42670	Quintile_5	331	4	dominating	upper stratum
6233	24308	Quintile_5	255	3	dominated	upper stratum
12105	1670	Quintile_2	51	1	understory	middle stratum
12250	1618	Quintile_1	50	1	dominated	upper stratum
12251	1518	Quintile_1	47	1	dominated	upper stratum
12253	6438	Quintile_5	127	2	dominating	upper stratum
12254	2236	Quintile_3	64	1	dominating	upper stratum
12256	1745	Quintile_2	53	1	dominated	upper stratum
12264	3330	Quintile_4	85	1	dominated	upper stratum

5.4 Results of the quantification of the influences of stand characteristics on the reliability of the detection of forest degradation

The quantification of the influences of stand characteristics are of importance as they can provide further insight, regarding under which condition the developed object-level change detection serves as an operational tool to detect forest degradation activities. Therefore, a tree specific evaluation, based on all extracted trees, of the three attributes, i.e., aboveground tree biomass, tree crown area, and social position and dominance, and their influences on the reliability of the object-level change detection of forest degradation was conducted.

Based on the findings of the preceding chapter, the influences of the three attributes are quantified for all extracted trees. In the following chapters, the quantification is visualized using the diagram template shown in Figure 28⁴⁴ with the respective producer's accuracy values for the specified classes of each attribute.

⁴⁴ See Figure 28 on page 82

5.4.1 Tree biomass

Figure 33 shows the producer's accuracy values for the quintiles for the aboveground biomass of trees. The value for all extracted trees, i.e., in column "All classes", corresponds to the final classification results presented in Table 14, however, splitting this overall value into quintiles shows different results for the producer's accuracy according to its specific tree biomass. For example, for "Quintile_1" only about 76% of the areas of extracted trees are correctly detected, whereas about 93% can be detected for "Quintile_5". In reverse, only 7% of the trees that have been extracted are missed within this quintile.

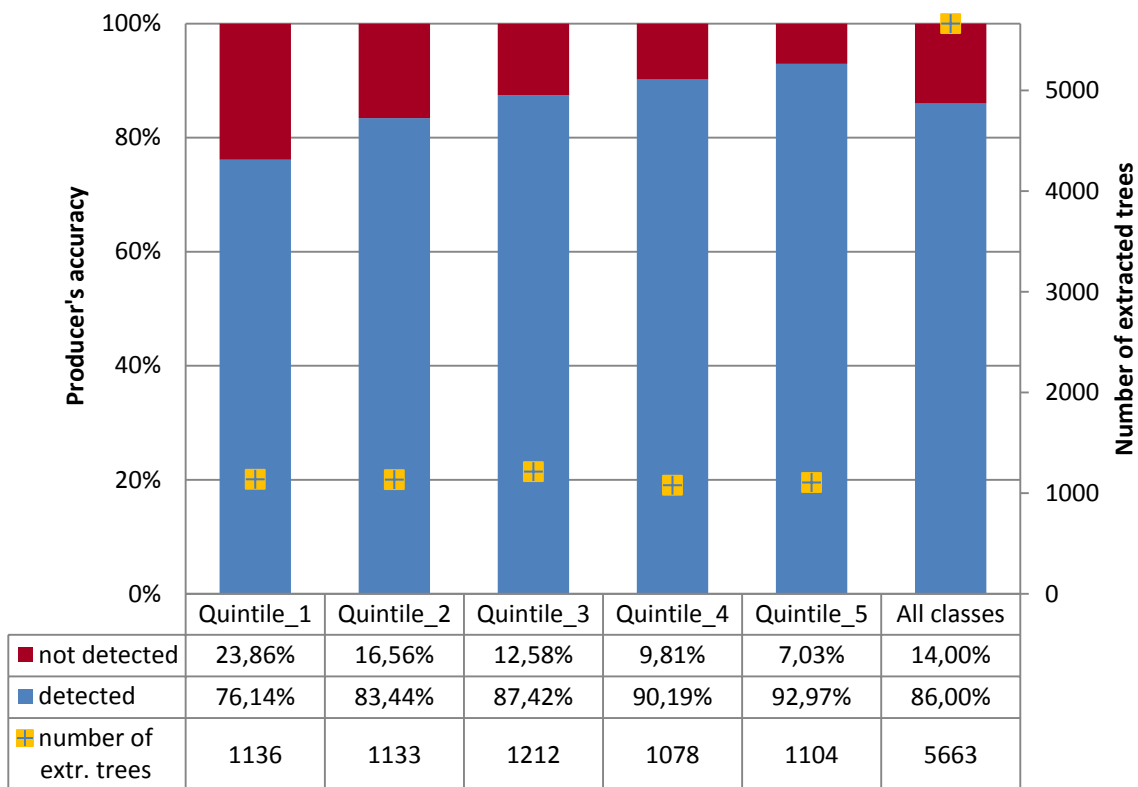


Figure 33: The diagram shows the influence of the attribute "aboveground tree biomass" on the reliability of the detection of forest degradation in quintiles. For each quintile the specific producer's accuracy values for "not detected" (red) and for "detected" (blue), and the number of trees are depicted. The rightmost column shows the respective sum of values for all quintiles.

5.4.2 Tree crown area

As for the estimation of the tree crown area, Figure 34 presents the results of the evaluation of the five classes based on the field *CrownAreaClass*⁴⁵ in respect to its specific the producer's accuracy values in combination with the total number of extracted trees in these classes. According to the natural distribution in tropical forests, the majority of trees are situated in the lower classes 1 (4,507 trees) and 2 (1,057 trees), steadily decreasing to class 5 with only five existing individuals.

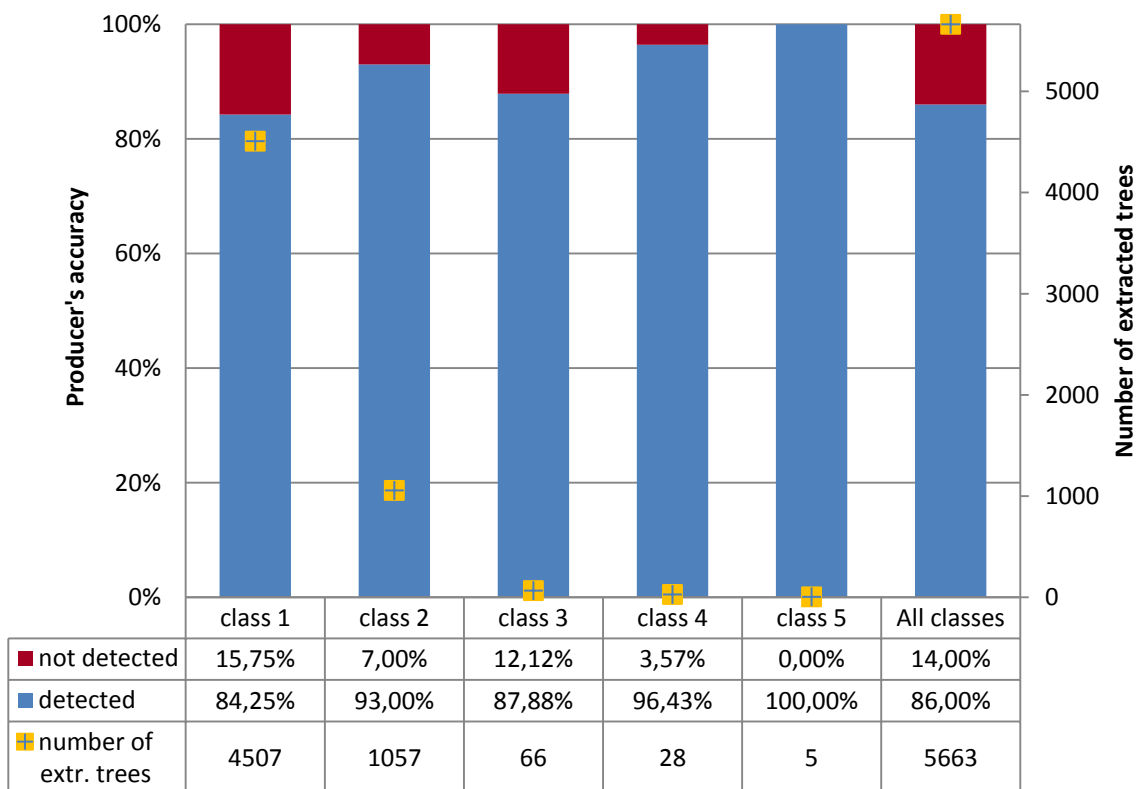


Figure 34: The diagram shows the influence of the attribute “tree crown area” on the reliability of the detection of forest degradation in five classes. For each class the specific producer’s accuracy values “not detected” (red) and “detected” (blue), and the number of trees are depicted. The rightmost column shows the respective sum of values for all classes.

Furthermore, Figure 34 presents the producer's accuracy values in relative numbers for each of the classes. Apart from class 3 the detection rates steadily ascend from about 84% to 100% corresponding to the stratification in the five classes based on the estimated tree crown area values.

⁴⁵ See Table 8 on page 78. The tree crown area classes are as follows: class 1 $\leq 100\text{sqm}$; class 2 $> 100\text{sqm}$ AND $\leq 200\text{sqm}$; class 3 $> 200\text{sqm}$ AND $\leq 300\text{sqm}$; class 4 $> 300\text{sqm}$ AND $\leq 400\text{sqm}$; class 5 $> 400\text{sqm}$.

Corresponding to the final classification results, the right column shows the above described data for all classes.

5.4.3 Social position and dominance

The evaluation of tree specific information on social position and dominance is rendered possible by the application of rule sets “Kraft” and “Leibundgut”. Hence, both rule sets are separately shown in Figure 35 and Figure 36.

In Figure 35, the results of the evaluation rule set “Kraft” in respect to its specific producer’s accuracy values are combined with the total number of extracted trees in these classes. The trees are distributed unequally in the classes “**dominating**” (KR_2), “**dominated**” (KR_3), and “**understory**” (KR_4). In respect to the results for the “Kraft” rule set, most of the 5,663 trees, i.e., 3,097, are classified “dominated”, 1,929 trees are “understory”, and only 637 are “dominating” trees. No tree is attributed to the class “**predominant**” (KR_1). While the producer’s accuracy for all trees, i.e., 86%, can again be found in the column “All classes (“Kraft”)”, this value divides into values from about 83% (KR_4) to nearly 89% (KR_2) in the respective classes.

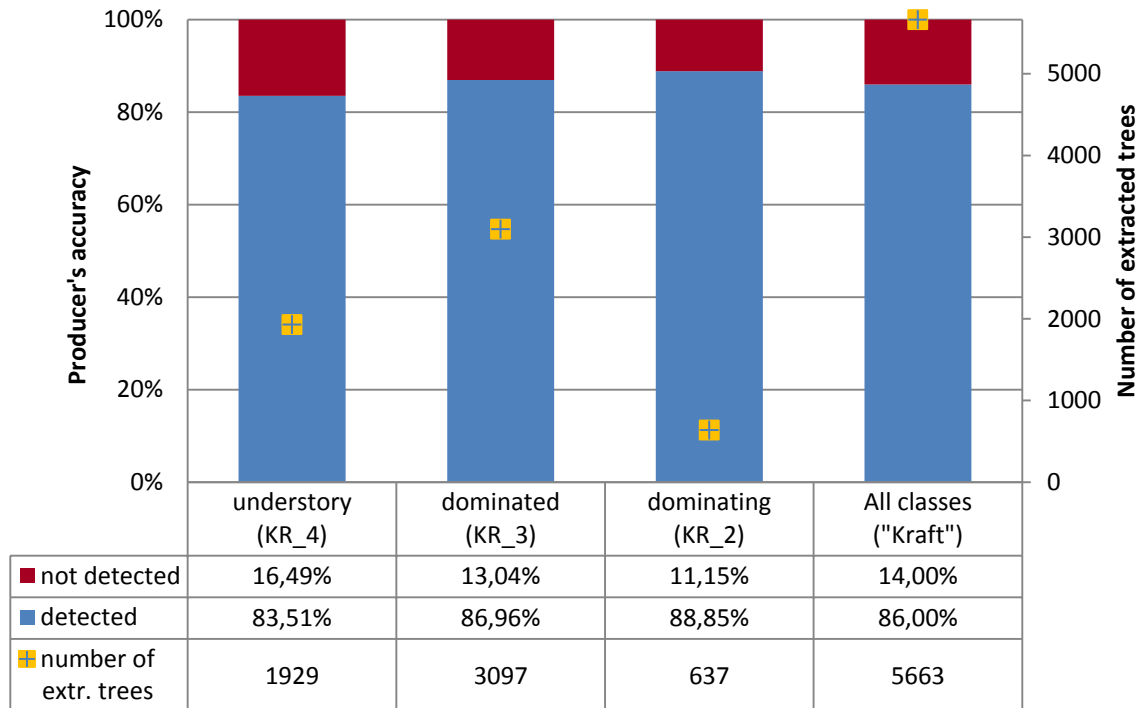


Figure 35: The diagram shows the influence of the attribute “social position and dominance” based on the evaluation rule set “Kraft” on the reliability of the detection of forest degradation in three classes. For each class the specific producer’s accuracy values “not detected” (red) and “detected” (blue), and the number of trees are depicted. The rightmost column shows the respective sum of values for all classes.

The results of the evaluation rule set “Leibundgut” are set in respect to their specific producer’s accuracy values and are depicted in Figure 36 in combination with the total number of extracted trees in these classes. Like for the rule set “Kraft” the trees are unequally distributed in the classes for “Leibundgut”, i.e. “*lower stratum*” (LG_1), “*middle stratum*” (LG_2), and “*upper stratum*” (LG_3). Due to different definitions of the classes, the total numbers for “*lower stratum*”, “*middle stratum*”, and “*upper stratum*” differ to the aforementioned results for “Kraft”. Only 44 trees are found in the “*lower stratum*”, 1,515 trees in the “*middle stratum*” and 4,104 in the “*upper stratum*”. Regarding the producer’s accuracies for each of the classes, again a trend can be seen. Starting with a detection rate of about 81% for “*lower stratum*”, this rate increases for “*middle stratum*” to 83%, and trees classified as “*upper stratum*” are detected with a producer’s accuracy of nearly 87%.

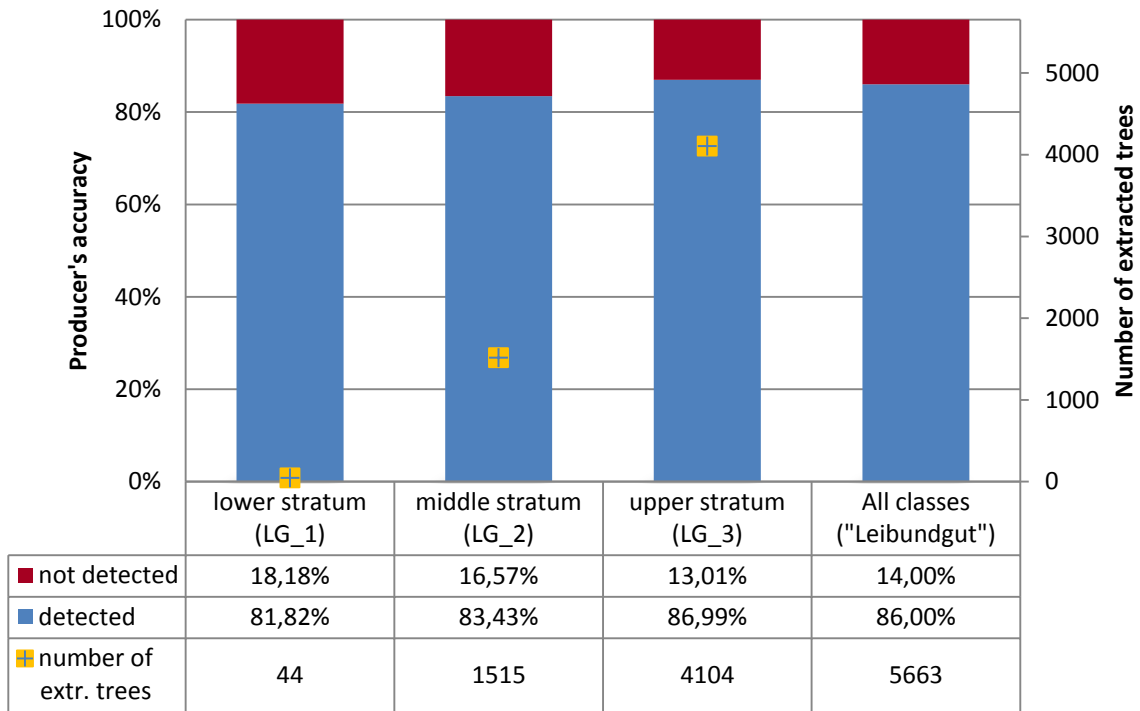


Figure 36: The diagram shows the influence of the attribute “social position and dominance” based on the evaluation rule set “Leibundgut” on the reliability of the detection of forest degradation in three classes. For each class the specific producer’s accuracy values “not detected” (red) and “detected” (blue), and the number of trees are depicted. The rightmost column shows the respective sum of values for all classes.

6 Discussion

In the following sub-chapters the elements of present study are discussed.

6.1 In-situ assessment

The in-situ data forms one of the data bases used in this research project. Not only is the accuracy of the spatial location and measurement of high importance for any forest based change detection analysis but also the additional attributes of the trees, and errors and error sources have to be carefully controlled (Carmel et al., 2001; Congalton and Green, 2007; Foody and Boyd, 1999). As stated by Köhl et al. (2006), errors in forestry surveys can be classified to two types of errors, i.e., sampling errors and non-sampling errors. Due to the fact, that in this research the in-situ data is derived from a data acquisition based on a total tally of the inventory area⁴⁶, the first type can be neglected. The second type however, has a critical meaning for this study. According to Köhl et al. (2006) non-observations and measurement errors, have to be kept under control, as they “can seriously compromise the quality and precision of a survey”. Hence, throughout the in-situ data assessment several accuracy considerations were taken in to account, with three described more in detail:

Uncertainties due to non-observations

The in-situ assessment was designed to observe all trees. Theoretically two possible scenarios can arise, (i) a tree, which is observed and planned for extraction, is not harvested, and (ii) a tree that is not observed is being harvested. The design of the in-situ assessment captures errors from both scenarios. Trees that are harvested are recognized with a UID being counterchecked when leaving the project area. If a tree was planned for harvesting, but has not been counterchecked for leaving, it has not been harvested, i.e., scenario (i). If a tree has not been inventoried, i.e. scenario (ii), it cannot leave the project without being captured at the check-out. This design renders uncertainties from non-observation of trees per-se impossible.

⁴⁶ See chapter 4.2 on page 57

Uncertainty of spatial location

The forest inventory in the project area is developed as a total tally of the inventory area and thus contains a full coverage of all trees within the respective area. Nevertheless, the spatial distribution of trees is based on measurements by several instruments, like e.g. compass or measurement tape. Errors that have a great influence on the change detection analysis can arise from these actions and processes.

A compass deviation that is not taken into account can lead to high spatial errors. This is especially true if the inventory system is designed based on the theorem of intersecting lines, as in this study. There was only one compass used for the inventory, however, this had a magnetic deviation of nearly 12° that had not been taken into account for the subsequent steps in the GIS-based planning stages. Nevertheless, this systematic error could be eliminated by the use of highly accurate GPS measurements from an intense fieldwork session that was carried out in April 2010. Counterchecks for individual trees throughout the whole project area were implemented and confirmed the elimination of the systematic error. This hardware intensive safeguarding guaranteed sufficient spatial location accuracy for this study.

Uncertainty of measurement errors for tree attributes

According to Köhl et al. (2006), this source of errors is most likely to occur, as “directly observed or compiled attribute values [...] are rarely, if ever, completely free of errors or bias”. From the tree attributes used for further calculation in this study, i.e., the tree height and dbh, the tree height was counterchecked. The measured tree height from the in-situ assessment was verified to be equivalent to the sum of length of the tree boles with one UID. No further assessment of the error for the dbh measurement was undertaken.

6.2 Detection of patterns of forest degradation using RADAR

6.2.1 Data pre-processing

Additional to the uncertainty of spatial location of the terrestrial data used, the passive remote sensing data, i.e., the QuickBird-2 scene, demanded pre-processing with regard to its spatial registration. As stated by Lunetta and Elvidge (1998), this process helps "to ensure that each pixel faithfully records the same type of measurement at the same geographic location over time". As Kennedy et al. (2009) identifies this as a main prerequisite for any change detection approach, the process of spatial co-registration was of high importance in this study and was successfully realized by the use of the 16 ground control points⁴⁷.

Although, according to, among others, Song et al. (2001), optical remote sensing data can be affected by atmospheric effects, no respective correction was carried-out. This was due to the fact that the optical data was only used for visual interpretations, which could be performed without any limitation.

Furthermore, Ortiz et al. (2012) identifies the influence of the quality of the used digital elevation model (DEM) on mapping accuracy of forests using TerraSAR-X images and proposes making use of pre-processing procedures of SAR data. However, as the present study area does not comprise any strong elevation variances, this approach was not applied.

6.2.2 Segmentation

The evaluation of the quality of the multi-resolution, bi-temporal segmentation process proves to be a complex procedure. At each single step an evaluation has to be made to determine which application is needed for the compiled objects. Up to now, the quality of this procedure can still not be directly measured. Ryherd and Woodcock (1996) report on approaches that compare different segmentations, and according to Marceau and Hay (1999) within a large-scale land use classification, objects simultaneously exist on various scale levels. These facts make the segmentation process one

⁴⁷ See chapter 4.2 on page 57

of the main steps in the whole classification strategy. Simultaneously, segmentation is the process that can be influenced the least. For this reason, the parameters used in the segmentation process have to be determined empirically. The classification rule set applied should be formulated in such a way that it can be transferred to other datasets. This has to be kept in mind early on when determining the parameters for the segmentation process.

The unique aspect of the present study is that it uses the TerraSAR-X datasets for both points in time, i.e., “*TerraSAR-X 2008*” and “*TerraSAR-X 2009*”, in the segmentation process. This bi-temporal segmentation approach guarantees the existence of objects representing changes in time. Using this approach on multiple segmentation scales allows even small scale changes for representation in the specific objects. Hence, changes between TerraSAR-X datasets for both points in time, due to the extraction of single trees and thus the absence of the respective tree crowns, can be represented in the image objects gathered by the segmentation process.

The process of segmentation is very demanding in regards of the used IT-hardware as it utilizes a huge amount of Random-Access Memory (RAM). The Workstation used was equipped with 24GB of RAM and 1.5TB of virtual memory, which both were entirely used up during the segmentation process. This circumstance limits the amount of data that can be processed in one run. Nevertheless, further solutions exist where tasks can be defined and subsequently be processed on the server side.

6.2.3 Classification

As indicated by Houhoulis and Michener (2000), the construction of the “class hierarchy” is rather a subjective process. The possibility of objects definition by diverse combinations of functions based on parameters is described, e.g. by Kok and Wever (2002). They see that they can all lead to the same final result. Thus, in order to be able to transfer the developed “class hierarchy” of the present study to another application, the functions applied are implemented by the easiest technique possible. Additionally, a compromise is made between a comprehensive knowledge base, on the one side, and a moderate performance and processing speed, on the other side..

Consistent with the statement of Hay et al. (2005) that landscape follows a definite hierarchical network, the present classification used a hierarchical approach in describing object classes in a rule base. Accordingly, Hay et al. (2005) recommend multi-scalar based methods and the use of scale levels, which were also applied in the present study.

Generally, both the segmentation and the definition of objects within a “class hierarchy” are an essential step on the way to an automated classification. These processes are the most extensive and time-consuming part of the classification. They delivered important insights in discovering the relevant objects’ properties. Conclusions in literature, however, find the need for additional empirical tasks, when working with different scale levels, since images which are too large can restrict the possibilities due to generalization. Using objects that are too small, however, will result in very tiny objects, whereas closely neighboring ones are classified differently. The results could be described as “salt’n’pepper” effect (Schiewe et al., 2001). To avoid this effect, the present study uses thresholds which take image objects into account that have a minimum area of 100sqm for scale level “L25” and 200sqm for “L50”.

Curran and Atkinson (2002) affirm that objects are not represented the same way in different scales. While a human expert concurrently works over all scale levels, object-level change detection methods have to be supplied with expert knowledge for each single scale. The method used provides this knowledge base by physical and semantic rules on diverse remote sensing data.

For this case study, the object definitions are developed in a way that makes them as simple and reproducible as possible. This technique is quite common, as even in more complex structures all steps can be followed and possible errors can be retraced. Accordingly, the expert knowledge was provided by the in-situ data assessment⁴⁸, which had to be translated into simple but stable rules for the object-level change detection method. Subsequently, this reference material was used, in order to realize the accuracy assessment, an approach that follows the methodological basis of Congalton and Green (2007).

⁴⁸ See chapter 4.2 on page 57

6.3 Results and accuracies of the object-level change detection

Generally, the results of the classification show that the study's hierarchical approach as described above performs quite well. The class hierarchies developed turn out to be stable and lead to consistent results.

The developed classification rule set produces classification results and accuracies of high level of about 86% to 99% (see Table 14). These general results, however, have to be evaluated more in detail. According to Ginevan (1979) and Köhl et al. (2006), in a typical sample based inventory the evaluation of the results and their specific accuracies incorporate the three steps: estimating the population total, determining sample size, and determining confidence intervals for sample estimates. However, to analyze the detectability of forest degradation patterns, the present study uses reference data that is compiled from a data acquisition based on a total tally of the inventory area⁴⁹. This inventory embraces all trees with a minimum dbh of 35cm and contains data on the harvested trees. Consequently, the total population, i.e., 48,141 trees, is used in both the classification and the evaluation processes superseding the application of analysis methods for typical sample based inventories.

The overall accuracy of more than 98% suggests a high-performance classification approach. Though, given the objective to analyze the detectability of patterns found for selective logging, this case study focuses on the producer's degree of accuracy for the event "change". Table 14 shows that for the detection of forest degradation in tropical moist forests, the classification leads to an accuracy value of 86%. This means that the locations of extracted trees, and thereby their extraction itself, are correctly detected with a probability of approximately 86%, and, in reverse, 14% of all extracted trees are not. The number of extracted trees per area unit could be used as an indicator of the intensity of forest degradation. In general, this is a satisfying value for a remote sensing based classification (Congalton and Green, 2007; Lillesand et al., 2004; Wulder and Franklin, 2003, 2007).

⁴⁹ See chapter 4.2 on page 57

Limiting the focus on the producer's accuracy for the event "change" is not sufficient in a binary classification system (Congalton and Green, 2007). Additionally, the producer's accuracy for "no_Change", in this case 99.88%, has to be considered. This indicates that no relevant overestimation of the event "change" takes place and consequently affirms the reliability of the developed object-level change detection method for the detection of patterns of selective logging and the accuracy level of 86%. According to Czaplewski (2003), the value of Kappa for the classification of about 0.91 is an indication of a very good consistency in forestry research.

The specific results are only valid for this case study. Technically the methods and standards used can be applied to other areas, since general transferability is one of the main characteristics of all COBIA- and OLCD-approaches (Kartikeyan et al., 1994; Leukert et al., 2004). Region specific adaptations might be necessary, but can be implemented in much shorter time as the general structure of developed "class hierarchies" can be maintained and only the parameters have to be adjusted. Nevertheless, the transferability to other projects could not be tested, and the possibility of a universal rule base is very unlikely. Consequently, the developed methods and standards can be seen as a semi-automatic workflow for object extraction with a high level of automation.

Regarding the needs of a MRV-system for REDD+, the results of the case study are of high importance. The developed object-level change detection method is able to detect patterns of forest degradation in moist tropical forests, as shown in this case study. The accuracy value of 86% promises that the developed method can be applied with appropriate accuracy in other regions, as well.

6.4 Identification and quantification of the influences of stand characteristics on the reliability of the detection of forest degradation

Identifying and quantifying the influences of the three attributes aboveground tree biomass, tree crown area, and social position and dominance on the reliability of the developed object-level change detection method, is of significant importance. Doing so can provide further insight regarding

under which condition the developed object-level change detection serves as an operational tool to detect forest degradation patterns or activities. Thus, the three tree specific results for the attributes tree biomass, tree crown area, and social position and dominance are expected to disclose information on their influences on the detectability of extracted trees. In general, the interest lies in examining how much these attributes influence the final classification results. These influences were quantified by evaluating their respective role in the accuracy assessment of the classification process⁵⁰.

6.4.1 Tree biomass

As stated in chapter 3.4.3, many previous studies showed a sensitivity of RADAR remote sensing data to forest biomass. Additionally, alterations in forest structure, e.g. by management practices, have an effect on remote sensing data (Castel et al., 2002; Hayes and Sader, 2001; Imhoff, 1995a). The present findings confirm that this effect can also be perceived by object-level change detection methods, as the final classification results show that the extraction of a single tree can be observed and verified with an accuracy of 86%, presented previously in Table 14 and in the column “All classes” in Figure 33.

In 5.4.1, the results of the tree biomass estimation based on Eq. (8) are presented and categorized into quintiles. For each of these classes Figure 33 shows the results of the accuracy assessment. Thereby, the influence of tree biomass is identified by the producer’s accuracy values for each of the quintiles. Table 15 gives an overview of the class widths of the quintiles. The accuracy values of “Quintile_1” to “Quintile_5”, indicating low to high tree biomass values, for the detection of patterns of forest degradation are continuously increasing. Although for “Quintile_1” a still reasonable accuracy level of 76% can be reached, for “Quintile_5” findings of the study show that only 7% of the trees which have been extracted are missed.

In other words, the detectability of the extraction of a tree is correlated with its specific biomass value. The planning and the extent of the applied reduced impact logging in the study area

⁵⁰ See 5.4 on page 98

concentrated on economically interesting trees with high biomass values. Under these conditions, tree biomass cannot be identified as a limiting factor in the present study. Nevertheless, tree biomass can be a limiting factor in cases with more intense forest degradation activities.

6.4.2 Tree crown area

In general, spatial scale is identified as a crucial point in understanding forest disturbances; consequently Coops et al. (2007) states that changes on single tree basis have to be respected in the selection of remotely sensed imagery. Nevertheless, the adaption of a respective accuracy assessment has to comply with these circumstances and be extended to single tree evaluation, as well.

In opposition to the tree biomass values, the tree specific estimates for crown area are not classified into quintiles but into five classes of an exact width of 100sqm. Class 5, however, is an unconfined class that comprises all values above 400sqm⁵¹. Similar to the previous evaluation of tree biomass, this classification allows for evaluating the influence of the single tree crown areas in the detection of forest degradation patterns.

Figure 34 shows that the natural distribution of tree crown area is also valid within the extracted 5,663 trees. The majority of trees are collected in the class of less than 100sqm. The extraction of trees in this class is detected with an accuracy of 84%. With the exception of class 3, the higher classes exceed the level of accuracy of 90%. As the class sizes in class 3 to class 5 are very small, spikes can intensively contribute to the levels of accuracy. Nevertheless, all but one extracted tree with tree crown areas of above 300sqm, i.e., class 4 and class 5, are correctly detected in the classification process.

On the whole, the findings of this case study show that tree crown area has an influence on the detectability of the extraction of a tree. Even so, trees belonging to the lowest class, i.e., tree crown areas of below 100sqm, are detected with an equitable accuracy level of about 84%.

⁵¹ See Table 8 on page 78

In this context, previously remote sensing based studies made use of forest canopy structures or specific elements of these (Bongers, 2001; Lefsky and Cohen, 2003; Lillesand et al., 2004). Regarding the detection of forest degradation in tropical moist forests, the evaluation of tree crown variables surely is of importance. Nonetheless, Bongers (2001) sees tree crown area, as such, as a highly dependent measure. Especially in tropical moist forests, forest canopy texture and structure, and the tree crown itself incorporate a multitude of other variables associated to it. A more detailed study of forest canopy structures that incorporates both vertical and horizontal structure parameters opposed with very high resolution 3D RADAR imagery would certainly provide a more in-depth evaluation of the inherent limitations. This requires very high resolution 3D RADAR imagery like TanDEM-X data. However, at the beginning of this case study TanDEM-X was still in planning phase and respective data was not available.

6.4.3 Social position and dominance

The study on social position and dominance of individual trees is by far the most complex and challenging approach in this case study. While the previously discussed issues on tree biomass and tree crown area are based on the attributes related to individual trees, this approach uses tree specific data in relation to neighboring trees. Information on spatial distribution of one tree and its neighborhood, both in vertical and horizontal sphere are deducted and processed, in order to oversee a more holistic view, and thereby understand the process of small scale forest disturbance and spatial pattern on a large scale.

Two schemes⁵² for the social position and dominance of individual trees are developed in the evaluation rule sets “Kraft” and “Leibundgut”. “Kraft” uses the four classes “Pre-dominant”, “Dominating”, “Dominated”, and “Understory”. “Leibundgut” works with “Upper stratum”, “Middle stratum”, and “Lower stratum”.

⁵² See chapter 4.6.3 on page 78

Kraft

In a nearly undisturbed natural forest, as it is examined in the case study, it is less surprising that the definition of the class “Pre-dominant”, however correct, result in no tree being classified as such. Having a look at the distribution of trees in total numbers between the classes in Figure 35, one would expect that the quantities of individuals would decline from “understory” to “dominating”. However, the results show that fewer trees remain in the class “understory”, i.e., only 1,929, than in the class “dominated”, i.e., 3,097. A likely explanation may be that only trees with a minimum dbh of 35cm are included in the study. In an undisturbed tropical moist forest, however, the majority of trees would to be expected to have dbh values of less than this threshold.

While Bongers (2001) raised the issue of small scale disturbance patches that “are difficult to assess using space-born optical systems”, Hoekman and Varekamp (1999) found that high-resolution RADAR data can be used to detect logging of large emergent tree individuals. The results of the case study supports Hoekman and Verkamp’s statement since these emergent trees, classified here as “*dominating*”, are detected with an accuracy of 89%. Conversely, using the developed object-level change detection method, not only the extraction of these dominating trees, but also the logging of dominated and understory individuals are detected with an accuracy of 87% and 83% respectively. Both values indicate acceptable values for the application of this method for REDD+. This unique feature is possible due to the application of object-level change detection methods including innovative multivariate alteration detection approaches in combination with very high resolution active remote sensing data. TerraSAR-X first started to provide this kind of RADAR data of 1m spatial resolution in 2007 thereby making it possible to effectively study forest canopy structures in order, for example, to monitor forest degradation processes (Baldauf and Köhl, 2009).

Leibundgut

The second scheme shows results similar to those for “Kraft”. Again, the distribution of trees between the classes differs from that which would be expected in a nearly undisturbed natural forest. The respective explanations are equivalent to those for “Kraft” in the previous chapter.

The accuracy levels for the three classes, i.e., “*lower stratum*”, “*middle stratum*”, and “*upper stratum*” increase from 81% to 87%, all being acceptable results for the developed method and its application for REDD+. Remarkable again are the accuracy values for the lower and the middle strata of Leibundgut’s classification. These confirm the results for the scheme “Kraft”.

In other words, this developed method and its application allows for the detection of changes beneath the top canopy layer, a process that has been described as stealthy degradation (Baldauf et al., 2009). This object-level change in stealthy degradation can still be detected with a sufficient accuracy level of more than 80%. This means that the developed method can be seen as a step towards overcoming the obstacles and hindrances in monitoring forest degradation.

6.5 Reporting on forest degradation within the scope of REDD+

The present study is intended to provide contributions to the development of scientifically sound and operational methods for reporting on forest degradation within the scope of REDD+. Thus, it must be feasible to implement the developed method into a MRV-system for REDD+ and at the same time keep the costs for this implementation within reasonable limits.

While the developed method could only be tested in a case study, Table 17 offers an exemplary estimate of the data costs for a national approach for the implementation of the developed method for Brazil and Madagascar. As stated by Köhl et al. (2006), scientifically sound inventory planning considers a range of methodological issues, e.g. how to select samples from the population, and thereby obtains parameters for the optimization of the inventory in this specific region, like, e.g. the best sampling design, or the optimal sample size. For this, generalities suitable for all forest inventories are not common. Nevertheless, the estimation of the expected data costs in Table 17 uses the general assumption that monitoring activities leading to forest degradation on 1% of the total forest area meets the accuracy requirements of a MRV-system for REDD+.

Table 17: Estimates of data costs for a national approach. Figures on land area and forest area in 2010 are based on data of FAO's Global Forest Resource Assessment 2010 (FAO, 2010a). With a size of 5000ha per TerraSAR-X scene the amount of scenes and the respective data costs are estimated.

	Brazil	Madagascar
Land area [1000ha]	845,651	58,154
Forest area [1000ha]	519,522	12,553
Amount of scenes for 1% coverage	1,039	25
Data costs ⁵³ for 1% coverage	7,013,547 €	169,466 €

According to MMA (2009) Brazil expends about 166 million € for monitoring and control of deforestation activities. Compared to this figure, the estimated 7 million € for TerraSAR-X data for a 1% coverage of the total forest area in Brazil, seems comparatively small. Nonetheless, the issue of costs has to be kept in mind, as the sustainability of a future REDD+ mechanism is partly founded on the simple equation that is shown in Figure 37.

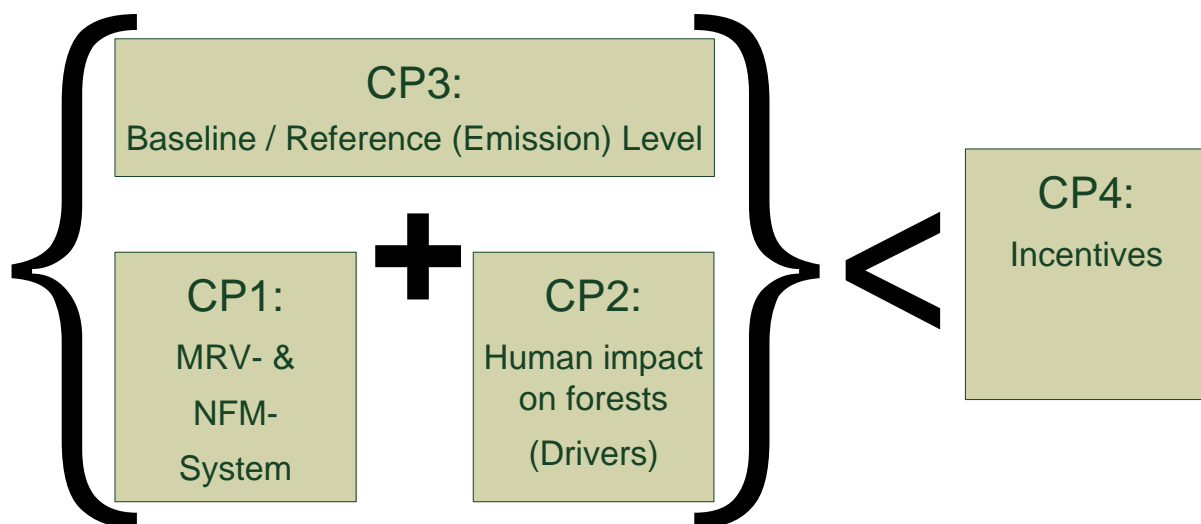


Figure 37: A simplified equation for a future REDD+ mechanism. REDD+ will only work sustainably on the ground, if the costs for the three components on the left (CP1, CP2, and CP3) are less than the benefit from the incentives component (CP4) on the right; adapted from (Baldauf and Köhl, 2012).

⁵³ Based on the Astrium International Price List for TerraSAR-X Services (Astrum, 2011).

Figure 37 illustrates that, apart from forest governance issues and general support by official development assistance, REDD+ will only work if the costs of the three essential REDD+ components⁵⁴ (i.e., a system for measuring, reporting, and verification (MRV) of carbon stocks and carbon stock changes and a national forest monitoring system (NFMS); a system to identify and quantify local and regional drivers of deforestation and forest degradation; and a forest reference (emission) level, against which the reduced emissions can be measured) are smaller than the amount that can be generated by REDD+ units, e.g. carbon credits, and delivered by adapted incentive schemes.

In return, this means that the methods applied for REDD+ for MRV, NFMs, Drivers, and Baselines need to be highly cost-efficient. The development of operational methods for REDD+ need to be based on a sound optimization process that compares different data sources and sampling designs with respect to their cost-efficiency. This helps to reduce the uncertainties related with the quantification of carbon stocks and carbon stock changes, and to increase the financial benefits from adopting a nationally applied REDD+ regime. Köhl et al. (2011) see MRV-systems “as an investment that aims to generate financial benefits” (cf. Köhl et al. (2011)), and proposes an optimization process to compare the implications of different data sources and sampling designs with respect to their cost-efficiency.

Table 17 proposes that, if monitoring activities leading to forest degradation on 1% of the total forest area are sufficient for Madagascar, it would need to use 25 TerraSAR-X scenes, each with a scene size of 5000ha, for the implementation of the developed method to detect forest degradation. Based on the price list from Astrium (2011), this would mean an investment for the data of about 170,000€ per period.

⁵⁴ See also 2.2 on page 4

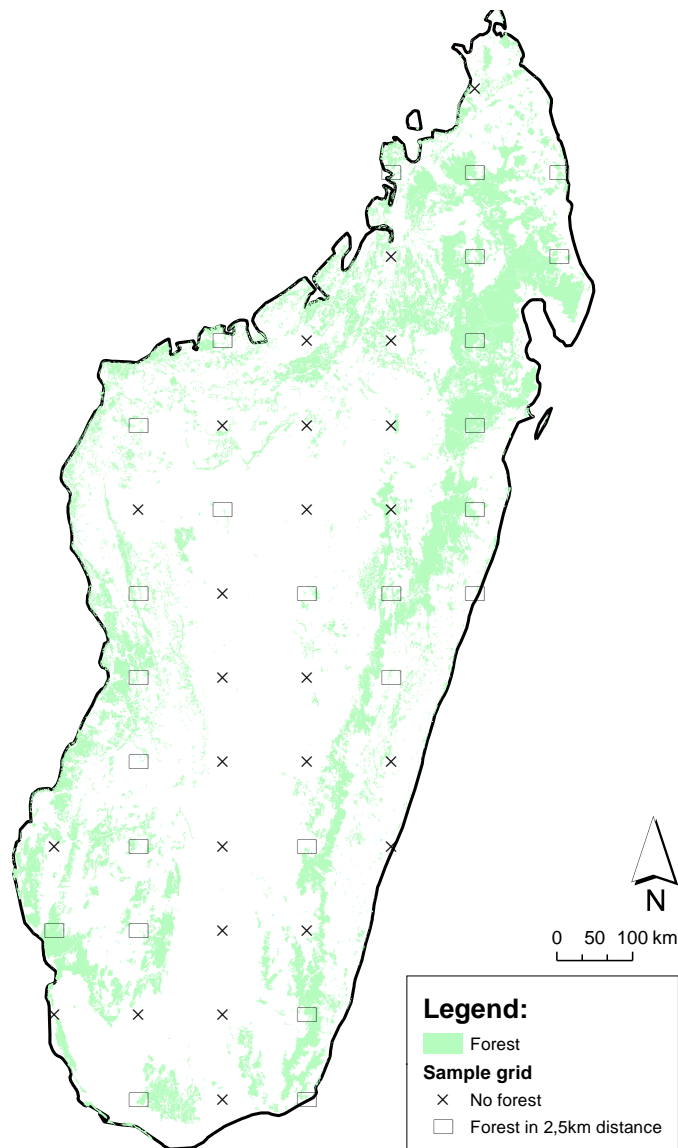


Figure 38: Map of Madagascar showing forest areas (green) and a possible systematic sample grid. The rectangular boxes show grid points, which intersect with forest areas, the crosses indicate grid points that do not contain forest areas.

Figure 38 shows a map of Madagascar with remnant forests and a grid that can be used for systematic sampling. After a pre-stratification into forested and non-forested land, e.g. by an appropriate remote sensing study, the sound distribution of the 25 TerraSAR-X scenes is conducted. In this way the developed method could be used to nationally complement, e.g. the approach for an operational REDD+ MRV-system by Plugge et al. (2010), and to provide necessary activity data for forest degradation activities within the scope of REDD+. Thereby, the developed method proves to be a suitable tool to report on forest degradation for REDD+.

7 Conclusions

REDD+ is a climate change mitigation mechanism for tropical forests presently being negotiated under the UNFCCC. It aims to attribute economic value to the carbon stored in forests, and thereby integrates forest protection into economic and political decision making processes.

In present negotiations, REDD+ embraces five activities that show a mitigating effect on climate change. One of these activities is reducing emissions from deforestation; an additional activity is reducing emissions from forest degradation. On the one hand, methods to quantify emissions from deforestation on local, national and pantropical scales exist and consensus regarding the amount of emissions caused by deforestation can be achieved (Harris et al., 2012). On the other hand, only rough estimates for the total amount of emissions from forest degradation are available (cf. Bucki et al. (2012); Houghton (2005)). Nevertheless, these estimates, ranging from 5-132% of those from deforestation, demonstrate the importance of grappling with forest degradation in REDD+, if significant emission reductions are envisaged. Currently, however, REDD+ lacks access to scientifically sound, applicable and cost-efficient methods of reporting on forest degradation on a large scale.

Existing, purely terrestrial-based methods for quantifying IPCC's two target variables, i.e., activity data and emission factors, for forest degradation can provide robust estimates on forest degradation. However, although optimization processes for these methods do improve their cost-efficiency, in the end, pure in-situ assessments turn out to be quite expensive when applied on national scale. The combination of terrestrial inventories and remote sensing based methods makes it possible to implement forest inventory designs that generally yield much higher cost-efficiencies on large scales (Köhl et al., 2009). Besides these cost-efficiency concerns, REDD+ aims to protect tropical forests, including remote forest lands, where the application of purely terrestrial based methods, especially for the estimation of accurate activity data, is highly questionable, due to the sheer restrictions of accessibility.

Forest degradation is an intrinsic part of REDD+. A multitude of causes exist that lead to forest degradation comprising small scale activities (Fearnside and Laurance, 2004; Lanly, 2003; Peres et al., 2006; Wertz-Kanounnikoff and Verchot, 2008). These small scale activities have an influence on the detection of their specific patterns or even render them technically invisible for optical remote sensing based change detection (Baldauf et al., 2009).

In the fields of active remote sensing technology, LiDAR has been reported to provide valuable information for forest biomass estimation (Clark et al., 2011; Hyde et al., 2007; Næsset et al., 2011; Sun et al., 2011). Applications of present LiDAR remote sensing sensors for the detection of forest degradation, however, fall short in cost-efficiency. Thus, suitable LiDAR systems within the scope of REDD+ do currently not exist. Regarding RADAR systems, the effect of biomass saturation makes RADAR unsuitable for the direct quantification of carbon emissions from land use changes in tropical forests (cf. Woodhouse et al. (2012)). Consequently, the development of emission factors for forest degradation activities from RADAR technologies is presently not possible.

Accurate activity data for the estimation of forest degradation is, however, of great importance within the scope of REDD+. Plugge and Köhl (2012) proved that the size of the area where forest degradation occurs has a crucial “impact on the accountable emission reductions” in any REDD+ regime (cf. Plugge and Köhl (2012)).

The present case study analyzed high-resolution active remote sensing data to determine its suitability for reporting on forest degradation within the scope of REDD+. As part of the case study a method was developed using TerraSAR-X data to detect patterns of selective logging. This object-level change detection based method identified areas undergoing forest degradation with an accuracy of 86%. While the specific results are only valid for this case study, the accuracy value of the detection promises that the developed method can be applied with appropriate accuracy to other regions as well.

Furthermore, the influences of the three attributes (aboveground tree biomass, tree crown area, and social position and dominance) on the reliability of the developed method were quantified. These influences on the results were investigated on the basis of all extracted trees in the case study. Firstly, a correlation was found between the detectability of the extraction of a tree and its specific biomass value. Secondly, tree crown area disclosed an influence on the detectability of the extraction of a tree, even if trees with tree crown areas below 100sqm are still detected with an accuracy level of about 84%. Thirdly, the investigation of social position and dominance showed that the extraction of understory tree individuals can still be detected with an accuracy of 83% by the developed method.

Finally, the implementation of the developed method into the setup of an operational, robust, and transparent MRV-system was indicated. In conclusion, the case study proved that space-born RADAR allows for monitoring patterns of forest degradation in tropical moist forests. Combined with appropriate methods, it enables the collections of unbiased activity data and thereby serves as a suitable tool for reporting on forest degradation within the scope of REDD+.

8 References

- Achard, F., DeFries, R., Eva, H.D., Hansen, M., Mayaux, P., Stibig, H.J., 2007. Pan-tropical monitoring of deforestation. *Environmental Research Letters* 2 (4), 45022.
- Achard, F., Eva, H.D., Mayaux, P., 2001. Tropical forest mapping from coarse spatial resolution satellite data: production and accuracy assessment issues. *Int. J. Remote Sens* 22 (12), 2741–2762.
- Achard, F., Eva, H.D., Mayaux, P., Stibig, H.-J., Belward, A., 2004. Improved estimates of net carbon emissions from land cover change in the tropics for the 1990s. *Global Biogeochem. Cycles* 18 (2), GB2008.
- Achard, F., Eva, H.D., Stibig, H.-J., Mayaux, P., Gallego, J., Richards, T., Malingreau, J.-P., 2002. Determination of Deforestation Rates of the World's Humid Tropical Forests. *Science* 297 (5583), 999–1002.
- Achard, F., Grassi, G., Herold, M., Teobaldelli, M., Mollicone, D., 2008. Use of Satellite Remote Sensing in LULUCF Sector: GOF-C-GOLD Report No. 33, Helsinki, Finland.
- Agrawal, A., 1995. Population pressure = forest degradation: an oversimplistic equation? *Unasylva* 46 (181).
- Anderson, J.R., 1977. Land use and land cover changes: A framework for monitoring. *Journal of Research of the U.S. Geological Survey* 5, 143–153.
- Angelsen, A. (Ed.), 2008. Moving ahead with REDD: Issues, options, and implications. Center for International Forestry Research (CIFOR), Bogor.
- Asner, G.P., Knapp, D.E., Broadbent, E.N., Oliveira, P.J.C., Keller, M., Silva, J.N., 2005. Selective Logging in the Brazilian Amazon. *Science* 310 (5747), 480–482.
- Astrium, 2011. Astrium GEO-Information Services: TerraSAR-X Services. International Price List.
- Avitabile, V., Herold, M., Henry, M., Schmillius, C., 2011. Mapping biomass with remote sensing: a comparison of methods for the case study of Uganda. *Carbon Balance and Management* 6 (1), 7.
- Baghdadi, N., Zribi, M., Loumagne, C., Ansart, P., Anguela, T.P., 2008. Analysis of TerraSAR-X data and their sensitivity to soil surface parameters over bare agricultural fields. *Remote Sensing of Environment* 112 (12), 4370–4379.

- Bähr, H.-P., Vögtle, T., 2005. *Digitale Bildverarbeitung: Anwendungen in Photogrammetrie, Fernerkundung und GIS*, 4th ed. Wichmann, Heidelberg, 325 pp.
- Baldauf, T., Köhl, M., 2009. Use of TerraSAR-X for Forest Degradation Mapping in the context of REDD: Presentation held at the World Forestry Congress in Buenos Aires on October 23rd 2009, Buenos Aires.
- Baldauf, T., Köhl, M., 2012. Working Group III: Satellite data for IPCC reporting. Thünen Institute for World Forestry. *Satellite data and monitoring systems for REDD+*, 2012, Bonn.
- Baldauf, T., Plugge, D., Rqibate, A., Köhl, M., 2009. Case studies on measuring and assessing forest degradation: Monitoring degradation in the scope of REDD. Forest Resource Assessment Working Paper 162. Forest Resource Assessment Programme, Rome.
- Baldauf, T., Plugge, D., Rqibate, A., Leischner, B., Dieter, M., Köhl, M., 2010. Development of a holistic methodology for implementing a REDD-Scheme at the example of Madagascar. Work report of the Institute for World Forestry. vTI, Hamburg.
- Beaudoin, A., Toan, T.L., Goze, S., Nezry, E., Lopes, A., Mougin, E., Hsu, C.C., Han, H.C., Kong, J.A., Shin, R.T., 1994. Retrieval of forest biomass from SAR data. *Int. J. Remote Sens* 15 (14), 2777–2796.
- Bechtold, W.A., 2003. Crown-Diameter Prediction Models for 87 Species of Stand-Grown Trees in the Eastern United States. *Southern Journal of Applied Forestry* 27 (4), 269–278.
- Bechtold, W.A., 2004. Largest-Crown-Width Prediction Models for 53 Species in the Western United States. *Western Journal of Applied Forestry* 19 (4), 245–251.
- Berberoglu, S., Akin, A., 2009. Assessing different remote sensing techniques to detect land use/cover changes in the eastern Mediterranean. *International Journal of Applied Earth Observation and Geoinformation* 11 (1), 46–53.
- Bergen, K.M., Dobson, M.C., 1999. Integration of remotely sensed radar imagery in modeling and mapping of forest biomass and net primary production. *Ecological Modelling* 122 (3), 257–274.
- Binaghi, E., Brivio, P.A., Ghezzi, P., Rampini, A., 1999. A fuzzy set-based accuracy assessment of soft classification. *Pattern Recognition Letters* 20 (9), 935–948.
- Blaschke, T., 2010. Object based image analysis for remote sensing. *ISPRS Journal of Photogrammetry and Remote Sensing* 65 (1), 2–16.

- BMZ, 2012. REDD Early Movers (REM): Rewarding pioneers in forest conservation. Financial rewards for successful climate change mitigation!, Bonn.
- Bongers, F., 2001. Methods to assess tropical rain forest canopy structure: an overview. *Plant Ecology* 153 (1), 263–277.
- Bontemps, S., Bogaert, P., Titeux, N., Defourny, P., 2008. An object-based change detection method accounting for temporal dependences in time series with medium to coarse spatial resolution. *Remote Sensing of Environment* 112 (6), 3181–3191.
- Borak, J.L.E.S.A., 2000. The use of temporal metrics for land cover change detection at coarse spatial scales. *Int. J. Remote Sens* 21, 1415-1432(18).
- Böttcher, H., Eisbrenner, K., Fritz, S., Kindermann, G., Kraxner, F., McCallum, I., Obersteiner, M., 2009. An assessment of monitoring requirements and costs of 'Reduced Emissions from Deforestation and Degradation'. *Carbon Balance and Management* 4 (1), 7.
- Bowden, C., Dixon, G., Frayer, W., Graybill, F., Jeyaratnam, S., Johnston, D., Kent, B., Labau, V., Roberts, E., 1979. Multi-level Sampling Designs for Resource Inventories. Technical report (Colorado State University. Dept. of Statistics). Colorado State University. Dept. of Forest; Wood Sciences; Rocky Mountain Forest; Range Experiment Station, USDA Forest Service. <http://books.google.de/books?id=WHj6GgAACAAJ>.
- Brown, S., 1997. Estimating biomass and biomass change of tropical forests: A Primer. A forest resources assessment publication 134. Food and Agriculture Organization of the United Nations FAO, Rome, 55 pp.
- Brown, S., Lugo, A.E., 1992. Aboveground biomass estimates for tropical moist forests of the Brazilian Amazon. *Interciencia* 17, 8–18.
- Bucha, T., Stibig, H.-J., 2008. Analysis of MODIS imagery for detection of clear cuts in the boreal forest in north-west Russia: Earth Observations for Terrestrial Biodiversity and Ecosystems Special Issue. *Remote Sensing of Environment* 112 (5), 2416–2429.
- Bucki, M., Cuypers, D., Mayaux, P., Achard, F., Estreguil, C., Grassi, G., 2012. Assessing REDD+ performance of countries with low monitoring capacities: the matrix approach. *Environmental Research Letters* 7 (1), 14031.
- Campbell, J.B., 2007. Introduction to remote sensing, 4th ed. Guilford Press, New York, 626 pp.

- Canty, M.J., 2010. Image analysis, classification, and change detection in remote sensing: With algorithms for ENVI/IDL, 2nd ed. CRC Press, Boca Raton, Fla, 8 pp.
- Carleer, A., Wolff, E., 2004. Exploitation of very high resolution satellite data for tree species identification. *PE&RS* 70 (1), 135–140.
- Carmel, Y., Dean, D.J., Flather, C.H., 2001. Combining location and classification error sources for estimating multi-temporal database accuracy. *PE&RS* 67 (7), 865–872.
- Castel, T., Guerra, F., Caraglio, Y., Houllier, F., 2002. Retrieval biomass of a large Venezuelan pine plantation using JERS-1 SAR data. Analysis of forest structure impact on radar signature. *Remote Sensing of Environment* 79, 30–41.
- Chave, J., Andalo, C., Brown, S., Cairns, M.A., Chambers, J.Q., Eamus, D., Folster, H., Fromard, F., Higuchi, N., Kira, T., Lescure, J.-P., Nelson, B.W., Ogawa, H., Puig, H., Riera, B., Yamakura, T., 2005. Tree allometry and improved estimation of carbon stocks and balance in tropical forests. *Oecologia* 145 (1), 87–99.
- Chen, C., Zhu, X., Li, F., 2008. Integrated Platform Design and Realization of Land Use Change Detection Based on ERDAS With AO and EML, in: International Society for Photogrammetry and Remote Sensing (ISPRS) (Ed.), *The International Archives of the Photogrammetry, Remote Sensing and Spatial Information Sciences (ISPRS)*. ISPRS Congress Beijing 2008, XXXVII XXXVII/B7, pp. 1575–1578.
- Clark, D., 1975. Understanding canonical correlation analysis. Concepts and techniques in modern geography 3. Geo Abstracts Ltd, Norwich, 36 pp.
- Clark, M.L., Roberts, D.A., Ewel, J.J., Clark, D.B., 2011. Estimation of tropical rain forest aboveground biomass with small-footprint lidar and hyperspectral sensors: DESDynI VEG-3D Special Issue. *Remote Sensing of Environment* 115 (11), 2931–2942.
- Congalton, R.G., 1991. A review of assessing the accuracy of classifications of remotely sensed data. *Remote Sensing of Environment* 37 (1), 35–46.
- Congalton, R.G., Green, K., 2007. Assessing the accuracy of remotely sensed data: Principles and practices, 2. ed. ed. CRC Press, Boca Raton, Fla., 183 pp.
- Coops, N.C., 2002. Eucalypt forest structure and synthetic aperture radar backscatter: a theoretical analysis. *Trees -Structure and Function* 16 (1), 28–46.

- Coops, N.C., Wulder, M.A., White, J.C., 2007. Identifying and describing forest disturbance and spatial pattern: Data selection issues and methodological implications, in: Wulder, M.A., Franklin, S.E. (Eds.), *Understanding forest disturbance and spatial pattern. Remote sensing and GIS approaches*. CRC Taylor & Francis, Boca Raton, Fla., pp. 31–61.
- Coppin, P., Jonckheere, I., Nackaerts, K., Muys, B., Lambin, E., 2004. Review Article Digital change detection methods in ecosystem monitoring: a review. *Int. J. Remote Sens* 25, 1565–1596.
- Culvenor, D.S., 2003. Extracting individual tree information: A Survey of Techniques for High Spatial Resolution Imagery, in: Wulder, M.A., Franklin, S.E. (Eds.), *Remote sensing of forest environments. Concepts and case studies*. Kluwer Acad. Publishers, Boston.
- Curran, P., Atkinson, P., 2002. Issues of scale and optimal pixel size, in: Stein, A., Meer, F., Gorte, B., Meer, F.D. (Eds.), *Spatial Statistics for Remote Sensing, vol. 1. Remote Sensing and Digital Image Processing*. Springer Netherlands, pp. 115–133.
- Czaplewski, R., 2003. Accuracy Assessment of maps of forest condition: Statistical design and methodological considerations, in: Wulder, M.A., Franklin, S.E. (Eds.), *Remote sensing of forest environments. Concepts and case studies*. Kluwer Acad. Publishers, Boston.
- Dawkins, H.C., 1957. Some results of stratified random sampling of tropical high-forest. Seventh British Commonwealth Forestry Conference Item 7 (iii), Oxford, [12] p. :
- DeFries, R., Achard, F., Brown, S., Herold, M., Murdiyarso, D., Schlamadinger, B., Souza, C. de, JR., 2007. Earth observations for estimating greenhouse gas emissions from deforestation in developing countries: Options for including agriculture and forestry activities in a post-2012 international climate agreement. *Environmental Science & Policy* 10 (4), 385–394.
- Desclée, B., Bogaert, P., Defourny, P., 2004. Object-based method for automatic forest change detection. *Geoscience and Remote Sensing Symposium, 2004. IGARSS '04. Proceedings. 2004 IEEE International* 5, 3383-3386 vol.5.
- Desclée, B., Bogaert, P., Defourny, P., 2006. Forest change detection by statistical object-based method. *Remote Sensing of Environment* 102 (1-2), 1–11.
- DLR, 2005. TerraSAR-X: Das deutsche Radar-Auge im All. Mission brochure. Deutsches Zentrum für Luft- und Raumfahrt (DLR), Bonn.
- DLR, 2010. Basic Product Specification Document: TerraSAR-X Ground Segment. TX-GS-DD-3302; Issue 1.7. DLR. <http://sss.terrasar-x.dlr.de/pdfs/TX-GS-DD-3302.pdf>. Accessed 5 April 2012.

- Eineder, M., Adam, N., Bamler, R., Yague-Martinez, N., Breit, H., 2009. Spaceborne Spotlight SAR Interferometry With TerraSAR-X. *Geoscience and Remote Sensing, IEEE Transactions on*, title=Spaceborne Spotlight SAR Interferometry With TerraSAR-X 47 (5), 1524–1535.
- Eliasch, J., 2008. Climate change: Financing global forests. the Eliasch review. Earthscan, London, 264 pp.
- Englhart, S., Keuck, V., Siegert, F., 2011. Aboveground biomass retrieval in tropical forests — The potential of combined X- and L-band SAR data use. *Remote Sensing of Environment* 115 (5), 1260–1271.
- Esch, T., Roth, A., Dech, S., 2005. Robust approach towards an automated detection of built-up areas from high resolution RADAR imagery, in: Joint Symposia URBAN - URS 2005. URBAN - URS 2005, Tempe, AZ, USA. 14.-16.03.2005.
- FAO, 1998. Terms and definitions: FRA 2000. Forest Resources Assessment Programme Working Paper 1.
- FAO (Ed.), 2003. Congress Proceedings B: XII World Forestry Congress.
- FAO, 2007. Definitional issues related to reducing emissions from deforestation in developing countries. Forests and Climate Change Working Paper 5. FAO, Rome.
- FAO, 2010a. Global forest resources assessment 2010: Global Tables. Food and Agriculture Organization of the United Nations, Rome.
- FAO, 2010b. Global forest resources assessment 2010: Key findings. Food and Agriculture Organization of the United Nations, Rome.
- FAO, 2011a. Forest degradation introduction. Assessment and monitoring of forest degradation, Rome.
- FAO, 2011b. State of the World's Forests: 2011. Food and Agriculture Organization of the United Nations, Rome, xii, 164.
- FAO, 2012a. Forestry and climate change. Food and Agriculture Organization of the United Nations (FAO). <http://www.fao.org/forestry/climatechange/53459/en/>. Accessed 15 April 2012.
- FAO, 2012b. Forestry and climate change: Roles of forests in climate change. <http://www.fao.org/forestry/climatechange/53459/en>. Accessed 4 January 2013.

- Fearnside, P.M., Laurance, W.F., 2003. Comment on "Determination of Deforestation Rates of the World's Humid Tropical Forests". *Science* 299 (5609), 1015a-.
- Fearnside, P.M., Laurance, W.F., 2004. Tropical deforestation and greenhouse gas emissions. *Ecological Applications* 14 (4), 982–986.
- Fisher, P., 1997. The pixel: A snare and a delusion. *Int. J. Remote Sens* 18 (3), 679–685.
- Flint, E., Richards J.F., 1994. Trends in carbon content of vegetation in South and Southeast Asia associated with changes in land use, in: Dale, V.H. (Ed.), *Effects of land-use change on atmospheric CO₂ concentrations. South and Southeast Asia as a case study*, 1 ed. *Ecological studies* 101. Springer, New York.
- Foody, G.M., Boyd, D., 1999. Detection of partial land cover change associated with the migration of inter-class transitional zones. *International Journal of Remote Sensing* 20 (14), 2723–2740.
- Foody, G.M., 2002. Status of land cover classification accuracy assessment. *Remote Sensing of Environment* 80 (1), 185–201.
- Foody, G.M., 2003. Remote sensing of tropical forest environments: towards the monitoring of environmental resources for sustainable development. *Int. J. Remote Sens* 24 (20), 4035–4046.
- Foody, G.M., Green, R.M., Lucas, R.M., Curran, P.J., Honzak, M., Do Amaral, I., 1997. Observations on the relationship between SIR-C radar backscatter and the biomass of regenerating tropical forests: *International Journal of Remote Sensing*. *Int. J. Remote Sens* 18 (3), 687–694.
- FSC, 2002. *FSC International Standard: FSC Principles and Criteria for Forest Stewardship*. FSC-STD-01-001 (version 4-0) EN.
- Fuller, D.O., 2006. Tropical forest monitoring and remote sensing: A new era of transparency in forest governance? *Singapore Journal of Tropical Geography* 27 (1), 15–29.
- Fuller, R.M., Smith, G.M., Devereux, B.J., 2003. The characterisation and measurement of land cover change through remote sensing: problems in operational applications? *International Journal of Applied Earth Observation and Geoinformation* 4 (3), 243–253.
- G8, 2009. *G8 Summit 2009: Responsible leadership for a sustainable future*.
- Gaston, G., Brown, S., Lorenzini, M., Singh, K.D., 1998. State and change in carbon pools in the forests of tropical Africa. *Global Change Biology* 4 (1), 97–114.

- Gibbs, H.K., Brown, S., Niles, J.O., Foley, J.A., 2007. Monitoring and estimating tropical forest carbon stocks: making REDD a reality. *Environmental Research Letters* 2 (4), 45023.
- Ginevan, M.E., 1979. Testing Land Use Accuracy: Another Look. *PE&RS* 45 (10), 1371–1377.
- GIZ, 2011. Reducing emissions from deforestation and forest degradation: Programme description. <http://www.giz.de/themen/en/34060.htm>. Accessed 25 June 2012.
- Goetz, S., Baccini, A., Laporte, N., Johns, T., Walker, W., Kellndorfer, J., Houghton, R., Sun, M., 2009. Mapping and monitoring carbon stocks with satellite observations: a comparison of methods. *Carbon Balance and Management* 4 (1), 2.
- GOFC-GOLD, 2011. A sourcebook of methods and procedures for monitoring and reporting anthropogenic greenhouse gas emissions and removals caused by deforestation, gains and losses of carbon stocks in forests remaining forests, and forestation. GOFC-GOLD Report version COP17 version 1. GOFC-GOLD Project Office, Natural Resources Canada, Alberta, Canada, Alberta, Canada.
- Grainger, A., 1993. Controlling tropical deforestation. Earthscan, London, 310 pp.
- Grassi, G., Monni, S., Federici, S., Achard, F., Mollicone, D., 2008. Applying the conservativeness principle to REDD to deal with the uncertainties of the estimates. *Environmental Research Letters* 3 (3), 35005.
- Guariguata, M.R., Nasi, R., Kanninen, M., 2009. Forest degradation: it is not a matter of new definitions. *Conservation Letters* 2.
- Guindon, B., 1997. Computer-Based Aerial Image Understanding: A Review and Assessment of its Application Very High Resolution Satellite Images. *Canadian Journal of Remote Sensing* 23 (1), 38-47.
- Haas, M., 2006. Forest Management Plan. *Madeiraira Vale Verde Ltda.*
- Haas, M., 2007. Procedimentos De Inventário Pré-Exploratório A 100% para a unidade de produção 2007/2008 na fazenda mundo novo: Versão 2.1. *Madeiraira Vale Verde Ltda.*
- Haas, M., 2009a. Plano Operacional Anual (POA) 2008: Banco de Dados 2008-2009. *Madeiraira Vale Verde Ltda.*
- Haas, M., 2009b. Plano Operacional Anual (POA) 2008: Chain of Custody (CoC). *Madeiraira Vale Verde Ltda.*

- Haas, M., 2009c. Plano Operacional Anual (POA) 2008. Madeireira Vale Verde Ltda.
- Haas, M., Glauner, R., 2005. Waldformationen, Baumartenzusammensetzung und Holzressourcen in einem Primärwald in Nordamazonien: Projektbericht N° 2, Fazenda Mundo Novo.
- Hame, T.H., 1988. Interpretation of forest changes from satellite scanner imagery, in: IUFRO Subject Group 4.02.05. Meeting (Ed.), Satellite imageries for forest inventory and monitoring. Experiences, methods, perspectives ; proceedings. Tiedinantoja. Helsingin Yliopiston. Metsänarvioimistieteen Laitoksen 21. Helsingin Yliopiston Metsäkirjasto, Helsinki.
- Hann, D., 1997. Equations for predicting the largest crown width of stand-grown trees in western Oregon. Research Contribution 17. Oregon State University, Corvallis, Oregon. http://www.cof.orst.edu/cof/fr/research/organon/pubs/FRL_RC17.pdf. Accessed 6 January 2012.
- Harris, N.L., Brown, S., Hagen, S.C., Baccini, A., Houghton, R.A., 2012. Progress toward a Consensus on Carbon Emissions from Tropical Deforestation: Policy Brief.
- Hayes, D.J., Sader, S.A., 2001. Comparison of Change-Detection Techniques for Monitoring Tropical Forest Clearing and Vegetation Regrowth in a Time Series. *PE&RS* 67 (9), 1067–1075.
- Hay, G.J., Castilla, G., Wulder, M.A., Ruiz, J.R., 2005. An automated object-based approach for the multiscale image segmentation of forest scenes: Bridging Scales and Epistemologies Linking Local Knowledge with Global Science in Multi-Scale Assessments. *International Journal of Applied Earth Observation and Geoinformation* 7 (4), 339–359.
- Healey, S.P., Cohen, W.B., Zhiqiang, Y., Kennedy, R.E., 2007. Remotely Sensed Data in the Mapping of Forest Harvest Patterns. Chapter 4, in: Wulder, M.A., Franklin, S.E. (Eds.), *Understanding forest disturbance and spatial pattern. Remote sensing and GIS approaches*. CRC Taylor & Francis, Boca Raton, Fla., pp. 85–112.
- Henderson, F.M., Lewis, A.J., 1998. Principles and applications of imaging radar. *Manual of remote sensing* 3rd ed 2. Wiley, New York, Chichester, Weinheim, 866 pp.
- Herold, M., Johns, T., 2007. Linking requirements with capabilities for deforestation monitoring in the context of the UNFCCC-REDD process. *Environmental Research Letters* 2 (4), 45025.
- Herold, M., Román-Cuesta, R.M., Heymell, V., Hirata, Y., van Laake, P., Asner, G.P., Souza, C., JR., Avitabile, V., Macdicken, K., 2011. A review of methods to measure and monitor historical carbon emissions from forest degradation. *Unasylva* 62 (238), 16–24.

- Herold, N., 2011. Resolution Vs. Minimum Mapping Unit: Size Does Matter. <http://www.csc.noaa.gov/digitalcoast/geozone/resolution-vs-minimum-mapping-unit-size-does-matter>. Accessed 13 January 2013.
- Hildebrandt, R., Iost, A., 2012. From points to numbers: a database-driven approach to convert terrestrial LiDAR point clouds to tree volumes. *European Journal of Forest Research*, 1–11.
- Hilker, T., Wulder, M.A., Coops, N.C., Linke, J., McDermid, G., Masek, J.G., Gao, F., White, J.C., 2009. A new data fusion model for high spatial- and temporal-resolution mapping of forest disturbance based on Landsat and MODIS. *Remote Sensing of Environment* 113 (8), 1613–1627.
- Hoekman, D.H., Verekamp, C., 1999. High resolution single-pass interferometric radar observation of tropical forest trees, in: *Proceedings of the workshop. 2nd International Workshop on Retrieval of Bio and Geo-physical Parameters from SAR Data for Land*, Noordwijk, The Netherlands. 21-23 October 1998, pp. 1–21.
- Holmgren, P., Thuresson, T., 1998. Satellite remote sensing for forestry planning—A review. *Scandinavian Journal of Forest Research* 13 (1-4), 90–110.
- Hotelling, H., 1936. Relations Between Two Sets of Variates. *Biometrika* 28 (3/4), 321–377.
- Houghton, R.A., 1991. Tropical deforestation and atmospheric carbon dioxide. *Climatic Change* 19 (1), 99–118.
- Houghton, R.A., 2003. Revised estimates of the annual net flux of carbon to the atmosphere from changes in land use and land management 1850-2000. *Tellus Series B Chemical And Physical Meteorology* 55 (2), 378-390.
- Houghton, R.A., 2005. Aboveground Forest Biomass and the Global Carbon Balance. *Global Change Biology* 11, 945-958(14).
- Houghton, R.A., Hackler, J.L., 1999. Emissions of carbon from forestry and land-use change in tropical Asia. *Global Change Biology* 5 (4), 481–492.
- Houhoulis, P.F., Michener, W.K., 2000. Detecting Wetland Change: A Rule-Based Approach Using NWI and SPOT-XS Data. *PE&RS* 66 (2), 205–211.
- Huang, S.Q., 2008. Change Mechanism Analysis and Integration Change Detection Method on SAR Images, in: *International Society for Photogrammetry and Remote Sensing (ISPRS) (Ed.), The International Archives of the Photogrammetry, Remote Sensing and Spatial Information Sciences (ISPRS). ISPRS Congress Beijing 2008, XXXVII XXXVII/B7*, pp. 1559–1568.

- Hudak, A.T., Morgan, P., Bobbitt, M., Lentile, L., 2007. Characterizing stand-replacing harvest and fire disturbance patches in a forested landscape: A case study from Cooney Ridge, Montana. Chapter 8, in: Wulder, M.A., Franklin, S.E. (Eds.), *Understanding forest disturbance and spatial pattern. Remote sensing and GIS approaches*. CRC Taylor & Francis, Boca Raton, Fla., pp. 209–232.
- Hyde, P., Nelson, R., Kimes, D., Levine, E., 2007. Exploring LiDAR-RaDAR synergy--predicting aboveground biomass in a southwestern ponderosa pine forest using LiDAR, SAR and InSAR. *Remote Sensing of Environment* 106 (1), 28–38.
- Hyyppä, J., Hyyppä, H., Inkinen, M., Engdahl, M., Linko, S., Zhu, Y.-H., 2000. Accuracy comparison of various remote sensing data sources in the retrieval of forest stand attributes. *Forest Ecology and Management* 128 (1–2), 109–120.
- Imhoff, M.L., 1995a. A theoretical analysis of the effect of forest structure on synthetic aperture radar backscatter and the remote sensing of biomass: *Geoscience and Remote Sensing, IEEE Transactions on*. *Geoscience and Remote Sensing, IEEE Transactions on* 33 (2), 341–352.
- Imhoff, M.L., 1995b. Radar backscatter and biomass saturation: ramifications for global biomass inventory. *IEEE Transactions on Geoscience and Remote Sensing* 33 (2), 511–518.
- Im, J., Rhee, J., Jensen, J.R., Hodgson, M.E., 2007. An automated binary change detection model using a calibration approach. *Remote Sensing of Environment* 106, 89–105.
- INPE, 2006. Metodologia para o Cálculo da Taxa Anual de Desmatamento na Amazônia Legal, São José dos Campos, Brasil. <http://www.obt.inpe.br/prodes/metodologia.pdf>. Accessed 13 April 2012.
- IPCC, 1996. Revised 1996 IPCC Guidelines for National Greenhouse Gas Inventories. Institute for Global Environmental Strategies (IGES), Japan.
- IPCC, 2000. Good Practice Guidance and Uncertainty Management in National Greenhouse Gas Inventories.
- IPCC, 2003a. Definitions and Methodological Options to Inventory Emissions from Direct Human-induced Degradation of Forests and Devegetation of Other Vegetation Types. IPCC National Greenhouse Gas Inventories Programme. Institute for Global Environmental Strategies (IGES), Hayama, Japan.

- IPCC, 2003b. Good practice guidance for land use, land-use change and forestry. IPCC National Greenhouse Gas Inventories Programme. Institute for Global Environmental Strategies (IGES), Hayama, Japan.
- IPCC, 2006. 2006 IPCC Guidelines for National Greenhouse Gas Inventories. Prepared by the National Greenhouse Gas Inventories Programme. Institute for Global Environmental Strategies (IGES), Japan.
- ITTO, 2002. ITTO guidelines for the restoration, management and rehabilitation of degraded and secondary tropical forests. International Tropical Timber Organization, Yokohama, Japan, 84 pp.
- IUFRO, 2000. Forest Terminology: Living Expert Knowledge: How to Get Society to Understand Forest Terminology. Proceedings of the 6.03.02/SilvaVoc Group Session at the IUFRO World Congress 2000, and Selected Contributions on Forest Terminology. IUFRO Occasional Paper (14).
- Iverson, L.R., Brown, S., Prasad, A., Mitasova, H., Gillespie, A.J.R., Lugo, A.E., 1994. Use of GIS for estimating potential and actual forest biomass for continental South and Southeast Asia, in: Dale, V.H. (Ed.), Effects of land-use change on atmospheric CO₂ concentrations. South and Southeast Asia as a case study, 1 ed. Ecological studies 101. Springer, New York.
- JAXA, 2012. Advanced Land Observing Satellite "DAICHI" (ALOS). JAXA. http://www.jaxa.jp/projects/sat/alos/index_e.html. Accessed 13 January 2013.
- Jones, S.D., Richards, G., Lowell, K., Woodgate, P., Buxton, L., 2004. Towards An Understanding of Uncertainty In Greenhouse Forest Assessments, in: International Society for Photogrammetry and Remote Sensing (ISPRS) (Ed.), The International Archives of the Photogrammetry, Remote Sensing and Spatial Information Sciences (IAPRS). ISPRS Congress Istanbul 2004 XXXV/B7, pp. 747–752.
- JRC, 2010. Global Land Cover 2000. <http://bioval.jrc.ec.europa.eu/products/glc2000/glc2000.php>. Accessed 13 January 2013.
- Kartikeyan, B., Gopolkrishna, B., Kalumbarme, M.H., Majumder, K.L., 1994. Contextual techniques for classification of high and low resolution remote sensing data. International Journal of Remote Sensing 15 (5), 1037–1051.
- Kasischke, E.S., BOURGEOU-CHAVEZ, L.L., Christensen, N.L., HANEY, E., 1994. Observations on the sensitivity of ERS-1 SAR image intensity to changes in aboveground biomass in young loblolly pine forests: International Journal of Remote Sensing. International Journal of Remote Sensing 15 (1), 3–16.

- Kasischke, E.S., Melack, J.M., Craig Dobson, M., 1997. The use of imaging radars for ecological applications--A review: Spaceborne Imaging Radar Mission. *Remote Sensing of Environment* 59 (2), 141–156.
- Kennedy, R.E., Townsend, P.A., Gross, J.E., Cohen, W.B., Bolstad, P., Wang, Y.Q., Adams, P., 2009. Remote sensing change detection tools for natural resource managers: Understanding concepts and tradeoffs in the design of landscape monitoring projects: Monitoring Protected Areas. *Remote Sensing of Environment* 113 (7), 1382–1396.
- Kennel, R., 1966. Soziale Stellung, Nachbarschaft und Zuwachs. *Forstwissenschaftliches Centralblatt* 85, 193–204.
- Köhl, M., 1993. Forest Inventory: Chapter 5, in: Pancel, L. (Ed.), *Tropical forestry handbook*, vol. 1. Springer, Berlin, pp. 243–332.
- Köhl, M., Baldauf, T., 2012. Resource Assessment Techniques for Continuous Cover Forestry, in: Pukkala, T., Gadaw, K. von (Eds.), *Continuous Cover Forestry*, 2nd ed. *Managing Forest Ecosystems* 23. Springer Verlag; Springer, Dordrecht, London, pp. 273–291.
- Köhl, M., Baldauf, T., Plugge, D., Krug, J., 2009. Reduced emissions from deforestation and forest degradation (REDD): a climate change mitigation strategy on a critical track. *Carbon Balance and Management* 4, 10.
- Köhl, M., Lister, A., Scott, C., Baldauf, T., Plugge, D., 2011. Implications of Sampling Design and Sample Size for National Carbon Accounting Systems. *Carbon Balance and Management* 6 (1), 10.
- Köhl, M., Magnussen, S., Marchetti, M., 2006. *Sampling Methods, Remote Sensing and GIS Multiresource Forest Inventory*. Springer-11642 /Dig. Serial]. Springer, Berlin, Heidelberg.
- Köhl, M., Traub, B., Päivinen, R., 2000. Harmonisation and Standardisation in Multi-National Environmental Statistics: Mission Impossible? *Environmental Monitoring and Assessment* 63 (2), 361–380.
- Kok, R. de, Wever, T., 2002. Automatische Informationsgewinnung aus einheitlichen Megadatensätzen am Beispiel des IRS-1C / IRS-1D-Mosaiks von Deutschland, in: *Tagungsband 19. DFD Nutzerseminar*, pp. 105–112.
- Kraft, G., 1884. *Beiträge zur Lehre von den Durchforstungen, Schlagstellungen und Lichtungshieben*. Kessinger Pub Co, 150 pp.

- Kugler, F., Papathanassiou, K., Hajnsek, I., Hoekman, D. (Eds.), 2006. INDREX-II - Tropical Forest Height Estimation with L- and P-Band Polarimetric Interferometric SAR: European Conference on Synthetic Aperture Radar (EUSAR). VDE Verlag GmbH, Dresden, Germany, 1-4.
- Kuntz, S., 2010. Potential of spaceborne SAR for monitoring the tropical environments. *Tropical Ecology* 51 (1), 3–10.
- Kuplich, T.M., Curran, P.J., Atkinson, P.M., 2005. Relating SAR image texture to the biomass of regenerating tropical forests. *International Journal of Remote Sensing* 26 (21), 4829–4854.
- Kuplich, T.M., Salvatori, V., Curran, P.J., 2000. JERS-1/SAR backscatter and its relationship with biomass of regenerating forests. *Int. J. Remote Sens* 21 (12), 2513–2518.
- Laestadius, L., Potapov, P., Yaroshenko, A., Turubanova S., 2011. Global forest alteration, from space. *Unasylva* 62 (238), 8–13.
- Lambin, E.F., 1999. Monitoring forest degradation in tropical regions by remote sensing: some methodological issues. *Global Ecology & Biogeography* 8, 191–198.
- Lamprecht, H., 1980. Zur Methodik waldkundlicher Untersuchungen in Naturwaldreservaten. *Natur und Landschaft* 55 (4), 146–147.
- Lanly, J.-P., 2003. Deforestation and forest degradation factors, in: Congress Proceedings B. XII World Forestry Congress. XII World Forestry Congress, Quebec City, Canada. 21.-28.09.2003, pp. 75–83.
- Le Toan, T., Beaudoin, A., Riom, J., Guyon, D., 1992. Relating forest biomass to SAR data. *IEEE Transactions on Geoscience and Remote Sensing* 30 (2), 403–411.
- Le Toan, T., Quegan, S., Woodward, I., Lomas, M., Delbart, N., Picard, G., 2004. Relating Radar Remote Sensing of Biomass to Modelling of Forest Carbon Budgets. *Climatic Change* 67, 379-402(24).
- Leckie, D.G., Walsworth, N., Dechka, J., Wulder, M., 2002. An investigation of two date unsupervised classification in the context of a national program for Landsat based forest change mapping, in: *Geoscience and Remote Sensing Symposium, 2002. IGARSS '02. 2002 IEEE International*, pp. 1307–1311.
- Lefsky, M.A., Cohen, W.B., 2003. Selection of remotely sensed data, in: Wulder, M.A., Franklin, S.E. (Eds.), *Remote sensing of forest environments. Concepts and case studies*. Kluwer Acad. Publishers, Boston, pp. 13–46.

- Leibundgut, H., 1956. Empfehlungen für die Baumklassenbildung und Methodik bei Versuchen über die Wirkung von Waldpflegemaßnahmen: 12. IUFRO-Congress Bd.2: 92-94, Oxford, England.
- Leibundgut, H., 1978. Die Waldpflege, 2nd ed. Haupt, Bern, 204 pp.
- Leukert, K., Darwish, A., Reinhardt, W., 2004. Transferability of Knowledge-Based Classification Rules, in: Geo-Imagery Bridging Continents. Proceedings and Presentation of Congresses: ISPRS Congress Istanbul 2004. IAPRS, Vol. XXXV Part 4. XXth ISPRS Congress Istanbul 2004, Turbey. 12.-23. July 2004, pp. 1059–1064.
- Leyk, S., Köhl, M., Poncet, F. von, 2002. Application of Future TerraSAR Data for Improvement of Forest Resource Assessments, in: ForestSAT 2002. Operational tools in forestry using remote sensing techniques. Conference Proceedings. Heriot Watt University, Edinburgh, Scotland, Heriot Watt University, Edinburgh, Scotland. 5.-9. AUGUST 2002.
- Lillesand, T.M., Kiefer, R.W., Chipman, J.W., 2004. Remote sensing and image interpretation, 5. ed. ed. Wiley, Hoboken, NJ, 763 pp.
- Linke, J., Betts, M.G., Lavigne, M.B., Franklin, S.E., 2007. Introduction: Structure, Function, and Change of Forest Landscapes, in: Wulder, M.A., Franklin, S.E. (Eds.), Understanding forest disturbance and spatial pattern. Remote sensing and GIS approaches. CRC Taylor & Francis, Boca Raton, Fla.
- Luckman, A., Baker, J., Honzák, M., Lucas, R., 1998. Tropical Forest Biomass Density Estimation Using JERS-1 SAR: Seasonal Variation, Confidence Limits, and Application to Image Mosaics. Remote Sensing of Environment 63 (2), 126–139.
- Luckman, A., Baker, J., Kuplich, T.M., da Costa Freitas Yanasse, C., Frery, A.C., 1997. A study of the relationship between radar backscatter and regenerating tropical forest biomass for spaceborne SAR instruments. Remote Sensing of Environment 60 (1), 1–13.
- Lu, D., Mausel, P., Brondizio, E., Moran, E., 2004. Change detection techniques. Int. J. Remote Sens 25 (12), 2365-2401.
- Lund, H.G., 1999. A 'forest' by any other name... Environmental Science & Policy 2 (2), 125–133.
- Lunetta, R.S., Elvidge, C., 1998. Remote sensing change detection: Environmental monitoring methods and applications. Ann Arbor Press, Chelsea, Mich, xviii, 318.
- Magnussen, S., 2009. A Bayesian approach to classification accuracy inference. Forestry 82 (2), 211–226.

- Malingreau, J.-P., 1993. Satellite monitoring of the world's forests: A review. *Unasylva* 44 (174), 21–38.
- Mandallaz, D., 1993. Geostatistical methods for double sampling schemes: application to combined forest inventories. *Habilitationsschrift*, Zürich.
- Marceau, D.J., Hay, G.J., 1999. Remote sensing contributions to the scale issue. *Canadian Journal of Remote Sensing* 25 (4), 357-366.
- Mas, J.-F., 1999. Monitoring land-cover changes: A comparison of change detection techniques: *International Journal of Remote Sensing*. *Int. J. Remote Sens* 20 (1), 139–152.
- Mayaux, P., Holmgren, P., Achard, F., Eva, H.D., Stibig, H.-J., Branthomme, A., 2005. Tropical forest cover change in the 1990s and options for future monitoring. *Philosophical Transactions of the Royal Society B: Biological Sciences* 360 (1454), 373–384.
- Meneses-Tovar, C., 2011. NDVI as indicator of degradation. *Unasylva* 62 (238), 39–46.
- Meridian Institute, 2009. Reducing Emissions from Deforestation and Forest Degradation (REDD): An Options Assessment Report. Prepared for the Government of Norway, Norway.
- Mesquita Jr., H.N., Dupas, C., Silva, M., Valeriano, D., 2008. Amazon deforestation monitoring system with ALOS SAR complementary data, in: *International Society for Photogrammetry and Remote Sensing (ISPRS) (Ed.), The International Archives of the Photogrammetry, Remote Sensing and Spatial Information Sciences (ISPRS). ISPRS Congress Beijing 2008 XXXVII/B7*.
- Mitchard, E.T.A., Saatchi, S.S., Lewis, S.L., Feldpausch, T.R., Woodhouse, I.H., Sonké, B., Rowland, C., Meir, P., 2011. Measuring biomass changes due to woody encroachment and deforestation/degradation in a forest-savanna boundary region of central Africa using multi-temporal L-band radar backscatter. *Remote Sensing of Environment* 115 (11), 2861–2873.
- Mitchard, E.T.A., Saatchi, S.S., Woodhouse, I.H., Nangendo, G., Ribeiro, N.S., Williams, M., Ryan, C.M., Lewis, S.L., Feldpausch, T.R., Meir, P., 2009. Using satellite radar backscatter to predict above-ground woody biomass: A consistent relationship across four different African landscapes. *Geophys. Res. Lett* 36 (23), L23401.
- MMA, 2009. Plano de ação para a prevenção e o controle do desmatamento na Amazônia legal (PPCDAM): 2ª Fase (2009 - 2011), Brasília, Brazil.

- Mollicone, D., Achard, F., Federici, S., Eva, H.D., Grassi, G., Belward, A., Raes, F., Seufert, G., Stibig, H.-J., Matteucci, G., Schulze, E.-D., 2007. An incentive mechanism for reducing emissions from conversion of intact and non-intact forests. *Climatic Change* 83, 477–493.
- Morisette, J.T., Khorram, S., Mace, T., 1999. Land-cover change detection enhanced with generalized linear models. *Int. J. Remote Sens* 20 (14), 2703–2721.
- Mugo, J., Njunge, J., Malimbwi, R., Kigomo, B., Mwasi B.N., Muchiri, M., 2011. Models for Predicting Stem Diameter from Crown Diameter of Open Grown Trees in Sondu-Nyando River Catchment, Kenya. *Asian Journal of Agricultural Sciences* 3 (2), 119–126.
- Murdiyarsa, D., Skutsch, M., Guariguata, M.R., Kanninen, M., Luttrell, C., Verweij, P., Martins, O.S., 2008. How do we measure and monitor forest degradation?, in: Angelsen, A. (Ed.), *Moving ahead with REDD: Issues, options, and implications*. Center for International Forestry Research (CIFOR), Bogor, pp. 99–106.
- Nackaerts, K., Vaesen, K., Muys, B., Coppin, P., 2005. Comparative performance of a modified change vector analysis in forest change detection: *International Journal of Remote Sensing*. *Int. J. Remote Sens* 26 (5), 839–852.
- Næsset, E., Gobakken, T., Solberg, S., Gregoire, T.G., Nelson, R., Ståhl, G., Weydahl, D., 2011. Model-assisted regional forest biomass estimation using LiDAR and InSAR as auxiliary data: A case study from a boreal forest area. *Remote Sensing of Environment* 115 (12), 3599–3614.
- NASA, 2009. World of Change: Amazon Deforestation: Deforestation on the frontier in the northwestern part of Rondônia in western Brazil. Image courtesy of the Image Science & Analysis Laboratory, NASA Johnson Space Center. http://earthobservatory.nasa.gov/Features/WorldOfChange/images/amazon/amazon_deforestation_20000730_lrg.jpg.
- NASA, 2010. The Gateway to Astronaut Photography of Earth: Astronaut Photography of Earth - Display Record; ISS024-E-11941. Image courtesy of the Image Science & Analysis Laboratory, NASA Johnson Space Center. <http://eol.jsc.nasa.gov/scripts/sseop/photo.pl?mission=ISS024&roll=E&frame=11941>.
- NASA, 2012. The Enhanced Thematic Mapper Plus. <http://landsat.gsfc.nasa.gov/about/etm+.html>. Accessed 4 January 2013.

- Neeff, T., Alencastro Graça, P.M. de, Dutra, L.V., da Costa Freitas, C., 2005. Carbon budget estimation in Central Amazonia: Successional forest modeling from remote sensing data. *Remote Sensing of Environment* 94 (4), 508–522.
- Neeff, T., Vieira Dutra, L., dos Santos, J.R., Freitas, C.d.C., Araujo, L.S., 2003. Tropical forest stand table modelling from SAR data. *Forest Ecology and Management* 186 (1–3), 159–170.
- Nielsen, A.A., Conradsen, K., Simpson, J.J., 1998. Multivariate Alteration Detection (MAD) and MAF Postprocessing in Multispectral, Bitemporal Image Data: New Approaches to Change Detection Studies. *Remote Sensing of Environment* 64 (1), 1–19.
- NSIDC, 2013. ICESat/GLAS Data: Overview. The National Snow and Ice Data Center (NSIDC). <http://nsidc.org/data/icesat/index.html>. Accessed 3 January 2013.
- Ortiz, S.M., Breidenbach, J., Knuth, R., Kändler, G., 2012. The Influence of DEM Quality on Mapping Accuracy of Coniferous- and Deciduous-Dominated Forest Using TerraSAR-X Images. *Remote Sensing* 4 (3), 661–681.
- Pancel, L. (Ed.), 1993. *Tropical forestry handbook*. Springer, Berlin.
- Parker, G.G., Harding, D.J., Berger, M.L., 2004. A portable LIDAR system for rapid determination of forest canopy structure. *Journal of applied ecology* 41 (4), 755–767.
- Patenaude, G., Milne, R., Dawson, T.P., 2005. Synthesis of remote sensing approaches for forest carbon estimation: reporting to the Kyoto Protocol. *Environmental Science & Policy* 8 (2), 161–178.
- Pawlowicz, L., 2007. Determining Local GPS Satellite Geometry Effects On Position Accuracy. <http://freegeographytools.com/2007/determining-local-gps-satellite-geometry-effects-on-position-accuracy>.
- Penman, J., 2008. Informal Meeting of Experts on Methodological Issues relating to Reducing Emissions from Forest Degradation in Developing Countries: An exploration by the EU. European Union (EU), Bonn.
- Peres, C.A., Barlow, J., Laurance, W.F., 2006. Detecting anthropogenic disturbance in tropical forests. *Trends in Ecology & Evolution* 21 (5), 227–229.
- Pitz, W., Miller, D., 2010. The TerraSAR-X Satellite: Geoscience and Remote Sensing, *IEEE Transactions on Geoscience and Remote Sensing*, IEEE Transactions on DOI - 10.1109/TGRS.2009.2037432 48 (2), 615–622.

- Plugge, D., Baldauf, T., Köhl, M., 2011. Reduced Emissions from Deforestation and Forest Degradation (REDD): Why a Robust and Transparent Monitoring, Reporting and Verification (MRV) System is Mandatory, in: Blanco, J., Kheradmand, H. (Eds.), *Climate Change - Research and Technology for Adaptation and Mitigation*. InTech, Rijeka, Croatia, pp. 155–170.
- Plugge, D., Baldauf, T., Köhl, M., 2012. The global climate change mitigation strategy REDD: monitoring costs and uncertainties jeopardize economic benefits. *Climatic Change*.
- Plugge, D., Baldauf, T., Rakoto Ratsimba, H., Rajoelison, G., Köhl, M., 2010. Combined biomass inventory in the scope of REDD (Reducing Emissions from Deforestation and Forest Degradation). *Madagascar Conservation & Development* 5 (1), 23–34.
- Plugge, D., Köhl, M., 2012. Estimating carbon emissions from forest degradation: implications of uncertainties and area sizes for a REDD+ MRV system: *Canadian Journal of Forest Research*. *Can. J. For. Res.* 42 (11), 1996–2010.
- Pulliainen, J., Engdahl, M., Hallikainen, M., 2003. Feasibility of multi-temporal interferometric SAR data for stand-level estimation of boreal forest stem volume. *Remote Sensing of Environment* 85, 397–409.
- Ranson, K.J., Sun, G., Weishampel, J.F., Knox, R.G., 1997. Forest biomass from combined ecosystem and radar backscatter modeling. *Remote Sensing of Environment* 59 (1), 118–133.
- Richards, J.A., 2009. *Remote Sensing with Imaging Radar*. Signals and Communication Technology. Springer-Verlag Berlin Heidelberg, Berlin, Heidelberg.
- Romshoo, S., Shimada, M., 2001. Employing SAR for biomass retrieval from tropical forests in Southeast Asia, in: *Asian Conference on Remote Sensing (ACRS) 2001. Conference Proceedings*. Asian Conference on Remote Sensing, Singapore. 5.-9. November 2001.
- Rosenqvist, A., Milne, A., Lucas, R., Imhoff, M.L., Dobson, C., 2003. A review of remote sensing technology in support of the Kyoto Protocol. *Environmental Science & Policy* 6 (5), 441–455.
- Roth, A., Hoffmann, J., Esch, T., 2005. TerraSAR-X: how can high-resolution SAR data support the observation of urban areas?, in: *Joint Symposia URBAN - URS 2005*. URBAN - URS 2005, Tempe, AZ, USA. 14.-16.03.2005.
- Ryherd, S., Woodcock, C.E., 1996. Combining Spectral and Texture Data in the Segmentation of Remotely Sensed Images. *PE&RS* 62 (2), 181–194.

- Saatchi, S., Marlier, M., Chazdon, R.L., Clark, D.B., Russell, A.E., 2011. Impact of spatial variability of tropical forest structure on radar estimation of aboveground biomass. *Remote Sensing of Environment* 115 (11), 2836–2849.
- Sader, S.A., Bertrand, M., Hoffhine-Wilson, E., 2003. Satellite Change Detection of Forest Harvest Patterns on an Industrial Forest Landscape. *Forest Science* 49 (3), 341–353.
- Santos, J.R. dos, Freitas, C.d.C., Araujo, L.S., Dutra, L.V., Mura, J.C., Gama, F.F., Soler, L.S., Sant'Anna, S.J., 2003. Airborne P-band SAR applied to the aboveground biomass studies in the Brazilian tropical rainforest. *Remote Sensing of Environment* 87, 482–493.
- Santos, J.R. dos, Maldonado, F.D., Lopes, A., Disperati, A., Servello, E., Lisboa, G., 2008. Change detection in the mixed ombrophilous forest using multispectral radiometric rotation approach, in: *Silk Road for Information from Imagery. Proceedings and Presentation of Congresses: XXI ISPRS Congress, Commission I-VIII. XXXVII-A,B1-B8. XXI ISPRS Congress, Commission I-VIII, Beijing. 3-11. July 2008.*
- Santos, J.R. dos, Spinelli Araujo, L. de, Mora Kuplich, T., da Costa Freitas, C., Vieira Dutra, L., Siqueira Sant'Anna, S.J., Furlan Gama, F., 2006. Tropical forest biomass and its relationship with P-band SAR data. *Revista Brasileira de Cartografia* 58 (01), 37–42.
- Saura, S., 2002. Effects of minimum mapping unit on land cover data spatial configuration and composition. *International Journal of Remote Sensing* 23 (22), 4853–4880.
- Schiewe, J., Tufte, L., Ehlers, M., 2001. Potential and problems of multi-scale segmentation methods in remote sensing. *Scientist* 49 (0), 34-39.
- Schimel, D.S., 1995. Terrestrial ecosystems and the carbon cycle. *Global Change Biology* 1 (1), 77–91.
- Schroeder, P., Brown, S., Mo, J., Birdsey, R., Cieszewski, C., 1997. Biomass Estimation for Temperate Broadleaf Forests of the United States Using Inventory Data. *Forest Science* 43 (3), 424–434.
- Scott, C., Köhl, M., 1993. A method for comparing sampling design alternatives for extensive inventories. *Mitteilungen der Eidgenössischen Forschungsanstalt für Wald, Schnee und Landschaft* 68. Eidg. Forschungsanstalt für Wald, Schnee und Landschaft, Birmensdorf.
- Scott, C.T., Köhl, M., 1994. Sampling with Partial Replacement and Stratification. *Forest Science* 40, 30–46.
- Segura, M., Kanninen, M., 2005. Allometric Models for Tree Volume and Total Aboveground Biomass in a Tropical Humid Forest in Costa Rica. *Biotropica* 37 (1), 2–8.

- Simard, M., Rivera-Monroy, V.H., Mancera-Pineda, J.E., Castañeda-Moya, E., Twilley, R.R., 2008. A systematic method for 3D mapping of mangrove forests based on Shuttle Radar Topography Mission elevation data, ICESat/GLAS waveforms and field data: Application to Ciénaga Grande de Santa Marta, Colombia: Earth Observations for Terrestrial Biodiversity and Ecosystems Special Issue. *Remote Sensing of Environment* 112 (5), 2131–2144.
- Simmon, R., 2011. Global Land Cover Classification: Map of Land Cover Classification from the MODIS instrument aboard Terra. NASA; MODIS Land Cover Group, Boston University. <http://visibleearth.nasa.gov/view.php?id=76695>. Accessed 4 January 2013.
- Simula, M., 2009. Towards Defining Forest Degradation: Comparative Analysis of Existing Definitions. Forest Resource Assessment Working Paper 154. Forest Resource Assessment Programme, Rome.
- Simula, M., Mansur, E., 2011. A global challenge needing local response. *Unasyuva* 62 (238), 3–7.
- Singh, A., 1989. Digital change detection techniques using remotely-sensed data. *Int. J. Remote Sens* 10 (6), 989–1003.
- Song, C., Woodcock, C.E., Seto, K.C., Lenney, M.P., Macomber, S.A., 2001. Classification and Change Detection Using Landsat TM Data: When and How to Correct Atmospheric Effects? *Remote Sensing of Environment* 75 (2), 230–244.
- Stehman, S.V., Czaplewski, R.L., 1998. Design and analysis for thematic map accuracy assessment: Fundamental principles. *Remote Sensing of Environment* 64 (3), 331–344.
- Stern, N., 2007. *The economics of climate change: The Stern review*. Cambridge Univ. Press, Cambridge, 692 pp.
- Stibig, H.-J., Bucha, T., 2005. Feasibility study on the use of medium resolution satellite data for the detection of forest cover change caused by clear cutting of coniferous forests in the northwest of Russia. Institute for Environment and Sustainability, Joint Research Centre of the European Commission.
- St-Onge, B., Hu, Y., Vega, C., 2008. Mapping the height and above-ground biomass of a mixed forest using lidar and stereo Ikonos images. *Int. J. Remote Sens* 29 (5), 1277–1294.
- Stuckens, J., Coppin, P.R., Bauer, M.E., 2000. Integrating Contextual Information with per-Pixel Classification for Improved Land Cover Classification. *Remote Sensing of Environment* 71 (3), 282–296.

- Sun, G., Ranson, K.J., Guo, Z., Zhang, Z., Montesano, P., Kimes, D., 2011. Forest biomass mapping from lidar and radar synergies. *Remote Sensing of Environment* 115 (11), 2906–2916.
- Sun, G., Simonett, D.S., Strahler, A.H., 1991. A radar backscatter model for discontinuous coniferous forests. *IEEE Transactions on Geoscience and Remote Sensing* 29 (4), 639–650.
- Thiel, C., Weise, C., Riedel, T., Schmullius, C., 2006. Object based classification of L-band SAR data for the delineation of forest cover maps and the detection of deforestation, in: *Proceedings of the 1st International Conference on Object based Image Analysis OBIA (2006)*. 1st International Conference on Object based Image Analysis, Salzburg. 4.-5. July 2006.
- Tomppo, E., Olsson, H., Ståhl, G., Nilsson, M., Hagner, O., Katila, M., 2008. Combining national forest inventory field plots and remote sensing data for forest databases: Earth Observations for Terrestrial Biodiversity and Ecosystems Special Issue. *Remote Sensing of Environment* 112 (5), 1982–1999.
- Trimble, 2011. *Trimble Documentation: eCognition Developer 8.7. User Guide*. Trimble, München.
- UN, 1997. *The Earth Summit: United Nations Conference on Environment and Development (UNCED)*, Rio de Janeiro, 3-14 June 1992. <http://www.un.org/geninfo/bp/enviro.html>. Accessed 15 April 2012.
- UN, 2012. 20 years after their birth, three sister Rio Conventions reaffirm their collective responsibility for sustainable development, Rio de Janeiro, Brazil.
- UNEP-WCMC, 2008. *Carbon and biodiversity: a demonstration atlas*, Cambridge, UK.
- UNFCCC, 2005. *Reducing emissions from deforestation in developing countries: approaches to stimulate action: United Nations Framework Convention on Climate Change; Conference of the Parties; Eleventh session; Montreal. Submissions from Parties FCCC/CP/2005/MISC.1*. <http://unfccc.int/resource/docs/2005/cop11/eng/misc01.pdf>.
- UNFCCC, 2006. *Background paper for the workshop on reducing emissions from deforestation in developing countries: Part I: Scientific, socioeconomic, technical and methodological issues related to deforestation in developing countries. Workshop on reducing emissions from deforestation in developing countries. 30 August - 1 September 2006, Rome, Italy. United Nations Framework Convention on Climate Change*.

- UNFCCC, 2008. Report of the Conference of the Parties on its thirteenth session, held in Bali from 3 to 15 December 2007: Addendum. Part Two: Action taken by the Conference of the Parties at its thirteenth session.
- UNFCCC, 2009. Cost of implementing methodologies and monitoring systems relating to estimates of emissions from deforestation and forest degradation, the assessment of carbon stocks and greenhouse gas emissions from changes in forest cover, and the enhancement of forest carbon stocks: Technical paper. FCCC/TP/2009/1.
- UNFCCC, 2010. Report of the Conference of the Parties on its fifteenth session, held in Copenhagen from 7 to 19 December 2009: Addendum. Part Two: Action taken by the Conference of the Parties at its fifteenth session. Accessed 27 April 2011.
- UNFCCC, 2011a. Kyoto Protocol Intro. United Nations Framework Convention on Climate Change. http://unfccc.int/essential_background/kyoto_protocol/items/6034.php. Accessed 15 April 2012.
- UNFCCC, 2011b. Report of the Conference of the Parties on its sixteenth session, held in Cancun from 29 November to 10 December 2010: Addendum. Part Two: Action taken by the Conference of the Parties at its sixteenth session. <http://unfccc.int/resource/docs/2010/cop16/eng/07a01.pdf>. Accessed 27 April 2011.
- UNFCCC, 2012a. Report of the Conference of the Parties on its seventeenth session, held in Durban from 28 November to 11 December 2011: FCCC/CP/2011/9/Add.2. Part Two: Action taken by the Conference of the Parties at its seventeenth session.
- UNFCCC, 2012b. Subsidiary Body for Scientific and Technological Advice (SBSTA); Thirty-seventh session; Doha, 26 November to 1 December 2012;: FCCC/SBSTA/2012/L.31 Agenda item 5: Methodological guidance for activities relating to reducing emissions from deforestation and forest degradation and the role of conservation, sustainable management of forests and enhancement of forest carbon stocks in developing countries. Draft conclusions proposed by the Chair.
- UNFCCC, 2012c. List of Non-Annex I Parties to the Convention. http://unfccc.int/parties_and_observers/parties/non_annex_i/items/2833.php. Accessed 12 January 2013.
- UNFCCC, 2012d. List of Annex I Parties to the Convention. http://unfccc.int/parties_and_observers/parties/annex_i/items/2774.php. Accessed 12 January 2013.

- UNFF, 2009. Means of implementation for sustainable forest management: Special session of the ninth session. E/CN.18/SS/2009/L.1. United Nations (UN); United Nations Forum on Forests (UNFF), New York. <http://daccess-dds-ny.un.org/doc/UNDOC/GEN/N09/563/82/PDF/N0956382.pdf>. Accessed 3 August 2010.
- van der Werf, G.R., Morton, D.C., DeFries, R.S., Olivier, J.G.J., Kasibhatla, P.S., Jackson, R.B., Collatz, G.J., Randerson, J.T., 2009. CO₂ emissions from forest loss. *Nature Geoscience* 2 (11), 737–738.
- van Oort, P.A.J., 2007. Interpreting the change detection error matrix. *Remote Sensing of Environment* 108 (1), 1–8.
- Vanclay, J.K., 2001. Modelling forest growth and yield: Applications to mixed tropical forests. CAB International, Wallingford, 312 pp.
- Vermote, E., Elsaleous, N., Kaufman, Y.J., Dutton, E., 1994. Data pre-processing: Stratospheric aerosol perturbing effect on the remote sensing of vegetation: Correction method for the composite NDVI after the Pinatubo eruption. *Remote Sensing Reviews* 15, 7-22.
- Vieilledent, G., Vaudry, R., Andriamanohisoa, S.F.D., Rakotonarivo, O.S., Randrianasolo, H.Z., Razafindrabe, H.N., Rakotoarivony, C.B., Ebeling, J., Rasamoelina, M., 2011. A universal approach to estimate biomass and carbon stock in tropical forests using generic allometric models: Ecological Applications. *Ecological Applications* 22 (2), 572–583.
- Wang, Y., Davis, F.W., Melack, J.M., Kasischke, E.S., Christensen, N.L., 1995. The effects of changes in forest biomass on radar backscatter from tree canopies. *Int. J. Remote Sens* 16 (3), 503–513.
- Wang, Y., Dong, D., 1997. Retrieving forest stand parameters from SAR backscatter data using a neural network trained by a canopy backscatter model. *Int. J. Remote Sens* 18 (4), 981–989.
- Wertz-Kanounnikoff, S., Verchot, L.V., 2008. How can we monitor, report and verify carbon emissions from forests?: Chapter 9, in: Angelsen, A. (Ed.), *Moving ahead with REDD: Issues, options, and implications*. Center for International Forestry Research (CIFOR), Bogor.
- WMO (Ed.), 1979. *Proceedings of the World Climate Conference: A conference of experts on climate and mankind* ; Geneva, 12-23 February 1979. WMO 537. World Meteorological Org, Geneva, 791 pp.
- Woodcock, C.E., Strahler, A.H., 1987. The factor of scale in remote sensing. *Remote Sensing of Environment* 21 (3), 311–332.

- Woodhouse, I.H., Mitchard, E.T.A., Brolly, M., Maniatis, D., Ryan, C.M., 2012. Radar backscatter is not a 'direct measure' of forest biomass. *Nature Clim. Change* 2 (8), 556–557.
- Wulder, M.A., Franklin, S.E. (Eds.), 2003. *Remote sensing of forest environments: Concepts and case studies*. Kluwer Acad. Publishers, Boston, 519 pp.
- Wulder, M.A., Franklin, S.E. (Eds.), 2007. *Understanding forest disturbance and spatial pattern: Remote sensing and GIS approaches*. CRC Taylor & Francis, Boca Raton, Fla., 8 pp.
- Wulder, M.A., White, J.C., Coops, N.C., Butson, C.R., 2008. Multi-temporal analysis of high spatial resolution imagery for disturbance monitoring. *Remote Sensing of Environment* 112 (6), 2729–2740.
- Zhang, Z., et al., 2008. Estimation of forest Structural parameters from LiDAR and SAR data, in: *International Society for Photogrammetry and Remote Sensing (ISPRS) (Ed.), The International Archives of the Photogrammetry, Remote Sensing and Spatial Information Sciences (ISPRS). ISPRS Congress Beijing 2008 XXXVII/B7*.
- Zhan, X., Sohlberg, R.A., Townshend, J.R.G., DiMiceli, C., Carroll, M.L., Eastman, J.C., Hansen, M.C., DeFries, R.S., 2002. Detection of land cover changes using MODIS 250m data. *Remote Sensing of Environment* 83 (1-2), 336–350.

9 Annex

9.1 Processes of the four objectives to verify the hypothesis

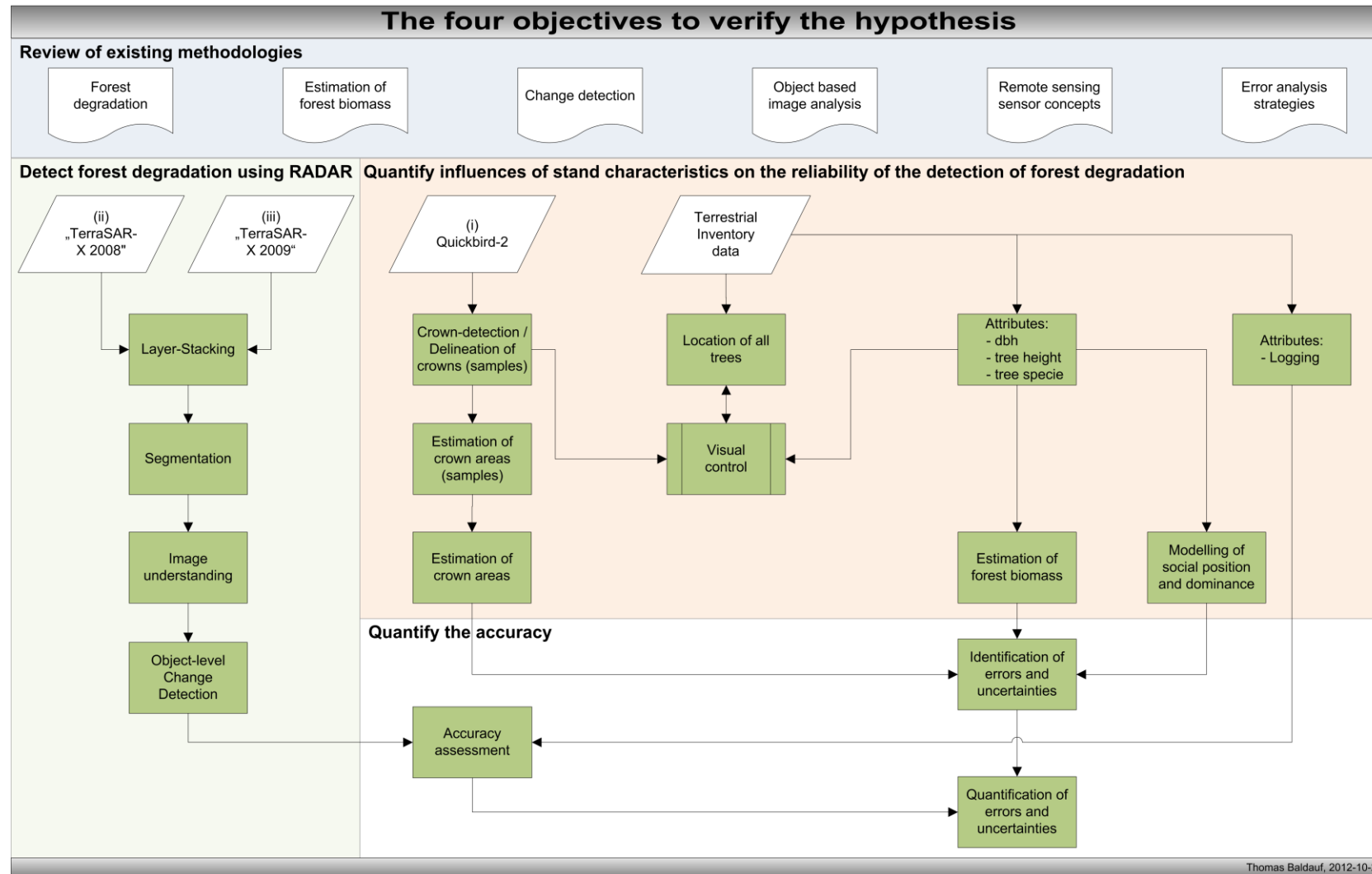


Figure 39: A flowchart shows the single processes of the four objectives to verify the hypothesis.

9.2 Metadata for „TerraSAR-X 2008“

Metadata is available on enclosed DVD:

```
\metadata\TSX1_SAR__EEC_SE__HS_S_SRA_20080420T094840_20080420T094841.xml
```

9.3 Metadata for „TerraSAR-X 2009“

Metadata is available on enclosed DVD:

```
\metadata\TSX1_SAR__EEC_SE__HS_S_SRA_20090817T094851_20090817T094852.xml
```

9.4 Script for social position and dominance

Script text is available on enclosed DVD:

```
\Script\Script.py
```

9.5 Class hierarchy, class descriptions and membership functions of the applied object-level change detection

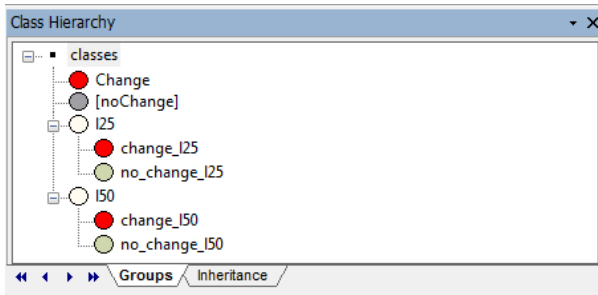
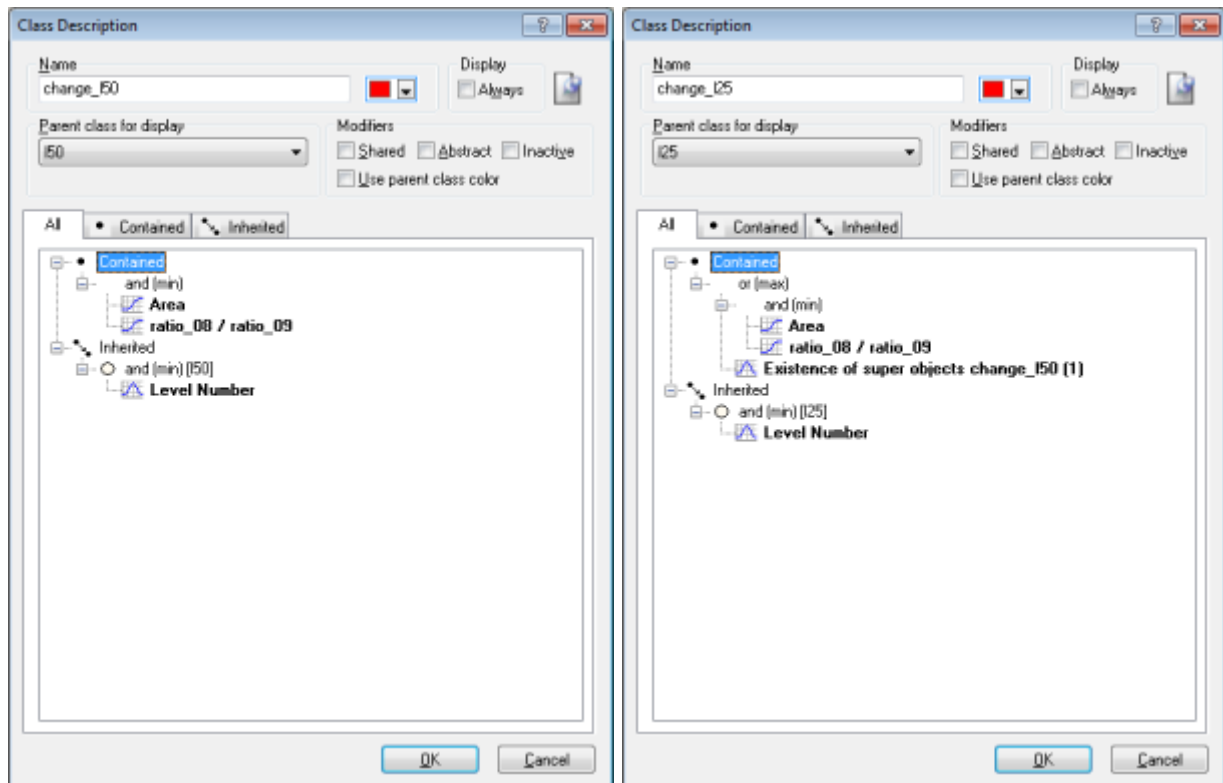


Figure 40: Screenshot showing the “Class Hierarchy” of the used classification.



(a)

(b)

Figure 41: Screenshots showing the “Class Description” for (a) the class "change_L50" in scale “L50” and (b) the class "change_L25" in scale “L25”.

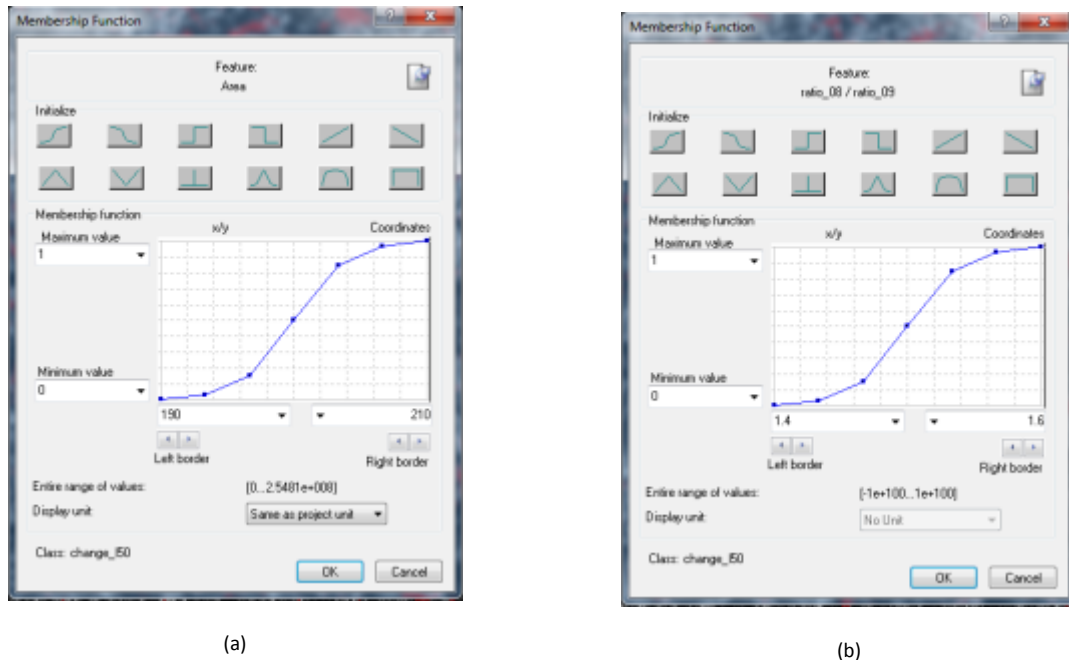


Figure 42: Screenshots exemplary showing the “Membership Functions” for (a) the feature “Area” in scale “L50”, and for (b) the feature “ratio_08/ratio_09” in scale “L25”.

9.6 Stepwise description of settings for the classification rule set

- Class description “L50” [Class active]:
 - o Sub-Class “change_L50” [Class active]:
 - Member ship Function “Area” [Function active]: “AND” Expression
 - Function form: “larger than”
 - Left border: 190
 - Right border: 210
 - Member ship Function “ratio_08/ratio_09” [Function active]: “AND” Expression
 - Function form: “larger than”
 - Left border: 1.4
 - Right border: 1.6
- Class description “L25” [Class active]:
 - o Sub-Class “change_L25” [Class active]:
 - Member ship Function “Area” [Function active]: “AND” Expression
 - Function form: “larger than”
 - Left border: 90

- Right border: 110
 - Member ship Function “ratio_08/ratio_09” [Function active]: “AND” Expression
 - Function form: “larger than”
 - Left border: 1.9
 - Right border: 2.1
 - Member ship Function “Existence of super objects ‘change_L50’” [Function active]: “AND” Expression
 - Function form: “Singleton”
 - Left border: 0
 - Right border: 2
- Sub-Class “no_change_L25” [Class active]:
 - Member ship Function “” [Function active]:
 - Function form: “Invert Expression”
 - Sub-Class “change_L25”
- Class description “change” [Class active]:
 - Member ship Function “Classified as change_L25” [Function active]:
 - Function form: “Singleton”
 - Left border: 0
 - Right border: 2

9.7 Results for all extracted trees for the estimation of aboveground biomass, the crown area, and the social position and dominance

Table is available on enclosed DVD:

\\Tables\\All_extracted_trees_AGB-CrownArea-SocPositionDom.xls